# University of Naples Federico II

Department of Chemical, Materials and Industrial
Production Engineering

XXXV° Ph.D. Programme in
Industrial Products and Processes Engineering

Ph.D. Thesis

## Optimization of hybrid composite structures for applications under dynamic loading conditions

**Ph.D Course Coordinator**
Ch.mo Prof. Andrea D'Anna

**Ph.D. Candidate**
Donadio Federica

**Ph.D. Supervisors**
Prof.ssa Valentina Lopresto

# Contents

# List of figures

# List of tables

# Abstract

Fiber reinforced composites play a significant role in several structural and no-structural applications. This work wants to investigate on the hybrid composite structures. In particular it is focused on the possibility to optimize the composite structures under dynamic loading.

Composites provide several advantages compared to traditional metallic counterparts for high-performance products that need to be lightweight but strong enough for tough loading conditions. These are often subjected to dynamic loading conditions under low and high velocity impacts. The impact energy involved in these dynamic loading events can cause damage modes such as matrix cracking, matrix splitting, delamination, fiber-matrix debonding, fiber micro-buckling and fiber pull-out. Interaction of these damages can severely reduce the load carrying capacity of such structures. In this scenario fibre hybridisation have been extensively acknowledged as a strategy that can lead to improved composite properties and performance, because it changes the material properties but also changes the damage propagation mechanisms leading to failure. Hybrid composites are laminates obtained by combining two or more different types of fibers within a matrix, so the behaviour of these materials results a balancing act between disadvantages and advantages of each single fiber.

The growing awareness about environmental problems and the environmental legislations induce the industry and society to focus on environmentally friendly materials. Reinforcements and matrices obtained from renewable resources, such as natural fibres and biopolymers, are the main players of this green transition.

Moreover, hybridization of natural and synthetic fibers represents an important way to reduce the carbon footprint of traditional composite materials, while maintaining good mechanical performance. The scientific community is really interested in all possible kinds of hybridization by varying matrix, thermoset and thermoplastic, and fibers, natural and synthetic.

The materials considered in this project include the traditional synthetic fibers normally used for hybrid composites as carbon and glass fibers but also new organic materials that are getting through in many industries. We are interested in studying the impact behaviour at both low and high speed because laminated composite structures are more exposed to impact damage, for example during maintenance or manufacturing operations tools might be dropped on the structure but also they are susceptible to dynamic accidents during life service. Moreover driven by the necessity to assess damage tolerance and durability of composites, required above all by military and aerospace industry, ballistic impacts and an analysis of multi-hit impact are performed.

On composite structures, common visual inspections cannot be useful to investigate the internal impact damages that could develop under load and could cause critical strength decreases. For this reason, different non-destructive and destructive testing methods were taken into account for the evaluation of composite damages. The confocal laser microscopy is used for the identification of damages like the indentation, the plastic deformation impressed on the surface of the material during the loading phase at the contact point. Ultrasonic spectroscopy, an analysis based on absorption phenomenon clearly related to the material structure and periodicity and advantage, is utilized to investigate the internal damage and to identify the presence of defects like delamination and porosities. Another very interesting non-destructive testing used within this research on the composite laminates is the Holographic Interferometry, that can accurately track delamination

growth and can also provide information on the through-the-thickness distribution of delamination.

## Thesis objectives

Fibre reinforced composites play a fundamental role in structural applications, however the optimization of their use is still
in progress. In particular although the hybridization of composite materials was a large field of study since the 80s, in the last years, hybridization has become a field of interest mainly due to the possibility of delaying and achieving a more gradual failure of composite materials by controlling the damage mechanisms.

The final purpose of this work is to develop the knowledge on the mechanical behaviour of hybrid composites under dynamic loadings, especially the effects that including fibres of different types has in the impact behaviour. The main focus of hybridization in this work is the improvement of impact response in composite materials and understanding the fibre and matrix properties required to achieve this goal.

The ultimate goal is to design a composite material able to adsorb the impact energy and a good damage tolerance without damaging the main composite properties such as resistance, attractive for several industrial applications. The first step of this research project has been to investigate the impact behaviour of conventional (carbon, glass, basalt) composite materials.

Then, hybrid composite laminates were tested at low velocity impact at penetration and high-speed tests at different impact velocity were carried out at room and low temperatures. Another goal of this thesis is the development of totally bio hybrid composite material with good mechanical properties.

The effect of repeated low velocity impacts at different energy levels on vinyl ester composite laminates was, then, investigated.

## Thesis layout

This thesis is organized by chapters that address different topics that are connected to the main goal of analyze hybrid composites under dynamic loads.

The overall structure of the thesis have... chapters, which can be summarised as follows:

Section I, STATE OF THE ART. In this chapter the background and state of the art are revised. A literature review regarding composites is presented, focussed in hybrid composites and in hybrid green composites for structural application.

Section II, STANDARD MATERIAL, presents the investigation on hybrid composite laminates made of materials, such as carbon and glass, typically used in this field. The basalt is introduced as a good impact resistant material.

Section III, BIO HYBRID COMPOSITE, explore the possibility to propose a new totally bio-based composite material.

Section IV, MULTIHITS, is focused on the development of one more realistic impact test, the repeated impact test.

Section V, SUMMERY OF RESULTS, this chapter gives a brief summary of the understandings gained from this research.

Section VI explains the FUTURE DEVELOPMENTS.

# Section I: State of the art

Fiber reinforced plastics could be considered innovative materials, but their commercialization and the efforts spent to improve the components, made them conventional in some applications. Fiber reinforced plastics are irreplaceable in the aerospace and naval sectors, and also for other applications such as motorsport and biomedical [1]. Nevertheless, the possibility to create new configurations are very much, due to the opportunity to combine different stacking sequence or new materials, resins or fiber, that become day by day available for researches [2]. By considering the industrial applications of the composite materials, like structural engineering, fiber reinforced composites made by continuous fibers show excellent possibility to reduce both, the weight and also lifetime maintenance costs owing to their corrosion and fatigue resistance. In the sectors mentioned before, carbon and glass fiber reinforced polymer composites represent the most employed, with very large production quantities if compared to other type of fibers (Figure 1) [3]. Among the other composites, in the last few years, there was an important expansion in the natural fiber study and development (Figure 2)[4]. This is principally due to the ecological needed, as a matter of fact, the natural fibers allow to obtain a renewable source and to produce biocompatible wastes. Despite the progress done in natural fiber development, the use of carbon and glass fibers remains unavoidable, in particular in marine, aerospace, and civil engineering industries, the sectors which are focused to take advantage of their attractive properties [5]. These applications are also the most challenging for the particular operational environment, so the fiber reinforced composites in aircraft, naval or structural applications need damage tolerance and damage resistance under impact loading which have to be assessed during the manufacturing process and in service[6].

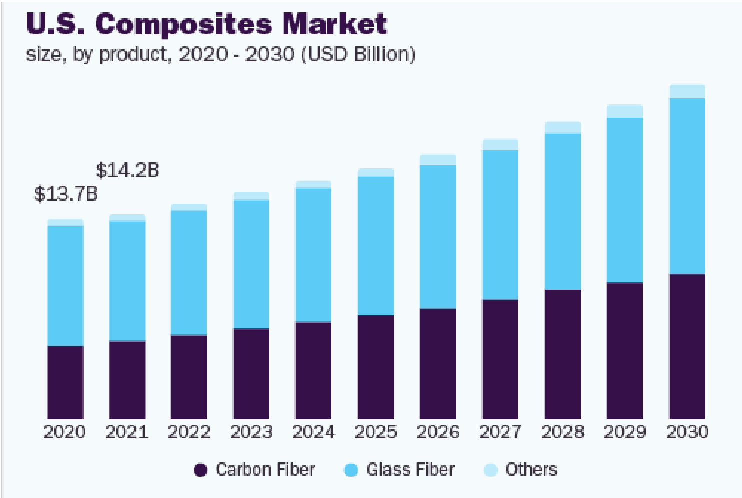


**Figure 1** - United States composites market, size by products *[3]*

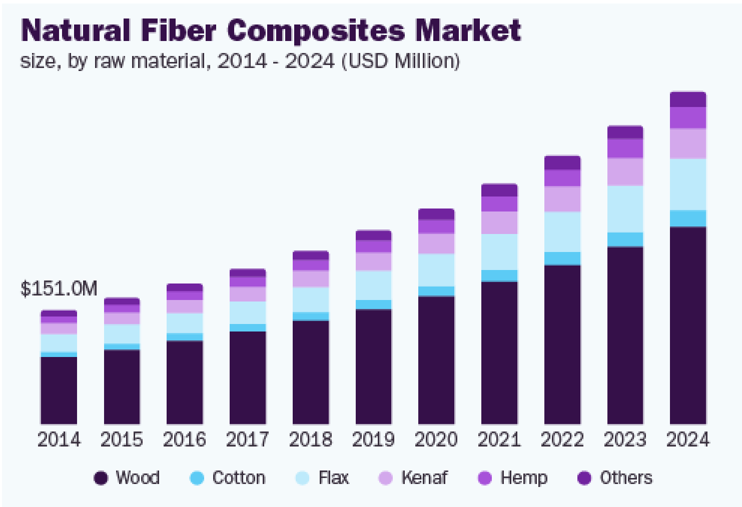


**Figure 2** - Natural fiber composites market [4].

Then, by considering the impact properties, the use of natural fiber reinforced composites is in development, but they cannot still compete with traditional synthetic fiber, this is the motivation to study an hybridization. The hybrid design could reduce the weakest aspects from both natural and synthetic fibers, it can assure more sustainability by reducing the synthetic fiber contents, and an increase in impact energy absorption and in load carrying capacity given by the presence of traditional and most performative fibers [7]. Hybridization is, therefore, mainly used to combine the advantages of two or more types of fibers, or to do the same by combining different matrices, or both unions, different matrices and different fibers. At the same time it is aimed to mitigate their less desirable properties, for instance low mechanical properties, high costs or high environmental impact [8]. Hybrid composite materials have been developed and applied to larger applications over the last decade in structural and engineering industries because hybrid composites fulfil the need to reduce cost in terms of operation, maintenance, and construction, and enhance the performance requirements with respect to applicability range, strength, payload and stability. In the aerospace industry, hybrid composites have been attaining more acceptability for their capability of meeting the demand of the high stiffness requirement for their applications as composite structural parts in airplanes.

The unlimited opportunities, given by the numerous combinations, that can be realized with all the fibers and matrices, produce an increase of recent study about the possible combinations of fiber in hybrid composites, natural/synthetic fibres, natural/natural fibres, or synthetic/ synthetic fibres, in thermoplastic or thermosetting matrix [9].

There are two types of fibers: natural and synthetic fibers. The second ones are more expensive, but they are the most commonly used in industries. Natural fibers, obtained from animals, plants or stones, have good mechanical properties, but not excellent and comparable to the best synthetic fibers (Table 1), with the additional benefit of being slightly lightweight, and this is not enough to make them the primary choice for structural applications as composite reinforcement [10]. Natural fibers show various advantages over their synthetic counterparts, such as low cost (Figure 3) [11], acceptable specific strength properties, low density, and biodegradability [11,12]. There has been increasing interest in the replacement of synthetic fibers with natural ones in engineering applications because of their eco-friendly and bio-renewable [13–15]. An important challenge of the last years is evaluating the impact resistance of natural fiber-reinforced composites.

**Table 1** - Fibers characteristics comparison

| Fiber | Density ($g/cm^3$) | Elongation at Break (%) | Elastic (Young) Modulus (GPa) | Tensile Strength (MPa) |
|---|---|---|---|---|
| Aramid | 1.4 | 3.3–3.7 | 63–67 | 3000–3150 |
| Carbon | 1.4 | 1.4–1.8 | 230–240 | 4000 |
| E-glass | 2.5 | 0.5 | 70 | 2000–3000 |
| S-glass | 2.5 | 2.8 | 86 | 4570 |
| Polyester | 1.2–1.5 | 2.0–4.5 | 2 | 40–90 |
| Polyhydroxyalkanoates | 1.1–1.4 | 1–6 | 3–6 | 35–100 |
| Cotton | 1.2–1.6 | 7.0–8.0 | 5.5–12.6 | 250–500 |
| Coir | 1.2 | 24–51 | 6 (40) | 140–593 |
| Flax | 1.2–2.4 | 2.3–3.2 | 27.6–80.0 | 500–1500 |
| Hemp | 1.3 | 2–40 | 45 (70) | 690 (530–1100) |
| Jute | 1.2–1.8 | 1.5–2.5 | 10–55 | 325–800 |
| Kenaf | 1.2–1.6 | 1.6 | 41 (53) | 745–930 |
| Sisal | 1.2-1.5 | 2.0–3.2 (8) | 9.4–22.0 | 310–855 |
| Abaca | 1.5 | 3.4 | 41 | 410–810 |
| Henequen | 1.4 | 4.8 | 13.2 | 500 |
| Pineapple | 1.5 | 0.8–3.2 | 82 | 1020–1600 |
| Banana | 1.3 | 2.0–3.7 | 27–32 | 720–910 |
| Nettle | 1.5 | 1.7 | 38 | 650 |
| Ramie | 1.4 | 1.2–3.7 | 23–44 | 500–915 |

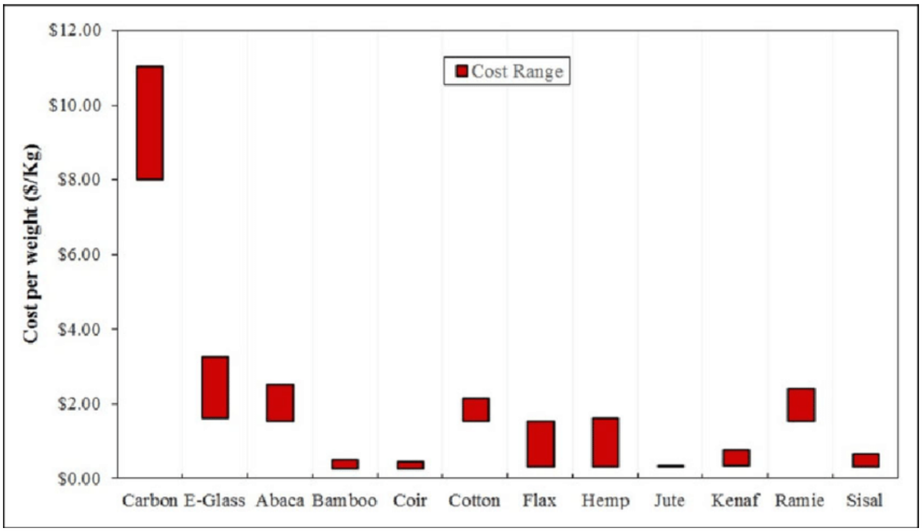


**Figure 3** - Cost per weight of current available fibers [11]

It has to be preface that composites are costly and difficult to repair when exposed to impact damage, so the main objective is to obtain the less damage, after impact, in operative conditions. All the structures are subjected to risk of experiencing structural failure and damages, so composite structures must maintain structural integrity with respect to damage and degradation under both low and high velocity impact. Voids in the material, design errors and corrosion of the material lead to failures of the structures that does not resist the stress applied to it [16].

It is important to understand how dynamic loads affect the failure and damage of composite structures during an impact event, because the characteristics of the hit influence the failure mode in different manner. There are different types of impact loading such as low velocity, intermediate velocity, high/ballistic velocity and hyper velocity impact that produce extreme changes in energy transfer, energy dissipation and damage propagation mechanisms [17–19]. The polymeric constituent in the material, the matrix, adsorbs the energy inside it and makes the composite capable of absorbing impact energy. Under low velocity impact, the composite material is damaged but is still able to however operate; for high velocity impact events, the composite is normally perforated or penetrated by the impactor. There are different factors which affect the behavior of composite materials under impact loads, for example type of matrix, laminate thickness, type of fiber, boundary conditions, fiber arrangement and stacking sequence [20,21]. In the ballistic impact cannot be neglected also the kinetic energy, shape, and size of the impactor [19]. Moreover the temperature variation dramatically affects the properties of polymer interlayer material and its suitability especially in terms of the impact performance of the whole laminated structure [22,23].

The impacts should be distinguished into two categories, low velocity and high velocity. The first ones do not produce perforation but create decohesion between the layers (delaminations) that could not visibly appear on the surface[24]. The second ones can occur during some flight operations, for instance bird strikes [25], and could produce instant damage and failure in composite structures, in the laboratory scale test the objective is to replicate the immediate failure of the material [26]. The manufacturing procedure, the composite design and the operating conditions can influence the impact behavior. In particular is crucial to consider the temperature variations in order to preserve the performance of the whole laminated structures [27,28].

Since many years, the hybridization design involves the most employed fibers, glass and carbon. As a matter of fact, in literature, there a lot of studies focused on the mechanical properties characterization for hybrid composite made of these two type of fibers in continuous and unidirectional configuration. In 2014 Swolfs et al. in a review, which consider different researches on hybrid composites, they start to consider crucial the new trends as natural fibers hybrids, specifically by considering their impact properties

[29]. Hybridisation guarantees similar or better properties respect to the single elements, by taking advantages from the different properties of different used fibres, obtaining a composite with the more personalized performance [30–34].

As mentioned before the most important requirement for aircraft and land-based vehicles is the resistance to high-speed impacts because it can generate critical failures [35].

In this regard, glass fibers are the best option from the costs point of view, accessibility and simplicity of treating, and hybrid carbon/glass fiber composites have shown to better tolerate the damage respect to fiber matching part [25,26]. At the same time, basalt fiber laminates have gain attention of many researchers, since the increasing interest in the environment impact reduction that had promoted the use of natural fibers from renewable sources as reinforcement in polymer matrices [36,37]. Sarasini et al. studied the impact performance of hybrid flax-carbon using the drop weight test. The experimental results demonstrate that a flax-carbon-flax hybrid composite has better impact performance than carbon-flax-carbon hybrid composites [38]. In 2013, Mansor [27,39] studied the compatibility of natural fibers when hybridized with glass fibers to produce new composite materials for brake levers.

Another usual occurrence, in composite structures, regards the repeated impacts that they could be subjected to. Several researches investigated this aspect and its effects on the mechanical properties degradation [5]. Sugun and Rao[28] reported a numerical relationship between the impact energy and the impact numbers to failure in glass, carbon and Kevlar composites. Shah et al.[40] compared the performance of thermoplastic and thermoset 3D composites under recurrent low speed impacts at an energy of 50 J. Both composites show a reduction in peak force and an increase in contact duration as the number of impacts increased. Hosur et al.[41] performed an experimental investigation on the response of woven glass/epoxy laminates subjected to single and repeated low-speed impacts. The study shows the results in terms of the damaged area, peak force and absorbed energy for samples subjected up to 40 repeated impacts at different energy levels from 10 to 50 J. Significant changes in the peak force were observed only at high energy levels, 40 and 50 J, where a sudden drop in peak force was found. Furthermore, the tests showed a growth of the damaged area with the number of impacts, but after a certain number of events, depending on the energy, it does not increase significantly. Sevkat et al. [42] studied the multi-impacts effect on the responses of different hybrid composite laminates made by S2 glass fibre and IM7 graphite fibre toughened epoxy varying the lay-up sequence. The results show a significant effect of the lay-up sequence on the repeated impact performance, indeed the hybrid glass/graphite/glass laminate withstood twice the number of impacts compared to the graphite/glass/graphite one.

Also the influence of operating temperature was taken into account for studying the mechanical characteristics decrease after repeated impacts. Ferrante et al.[43] set three temperature levels, -40 °C, room temperature and 80 °C, and studied the number of repeated impacts on the damage response of polypropylene laminates reinforced with intraply flax/basalt hybrid fabric layers in the impact energy range 5-30J.

**Lack of knowledge**

After the literature survey, it was retained that, as regards the hybrid composite materials, there a research gap in the comparison between the effects of low velocity and high velocity impact behavior. Furthermore, considering the important efforts in engineering ecological improvement, and since the natural-synthetic composites have proven their excellent structural properties; further researches are necessary to deeply evaluate the effect of the materials, the design and the configuration on the performance of natural-synthetic fiber composite materials in impact tests. Finally, for a comprehensive assessment of these hybrid structures, because the response of the material depends on a multitude of variables including nature, architecture, content of the reinforcements and due to the scarcity of experimental evidence available, further investigations on repeated impacts are deemed necessary.

Extremely summarizing, this Ph.D. thesis want to investigate several hybrid composites, from traditional ones to natural and innovative ones, with the purpose to evaluate and to optimize the behavior under dynamic loading.

# Section II: The hybridization and its effect on the impact resistance

## 1. Framework

The weakest part of a composite structure is the polymeric gap between the fiber layers. This is the reason why fiber composites are subject to delamination due to their low intralaminar strength. A low velocity impact state does not produce perforation but creates delaminations between the layers with no visible damage on surfaces [24]. During the industrial process, delamination can also occur in the material because of contaminated reinforcing fibers, insufficient wetting of fibers, machining and mechanical loading and the lack of reinforcement in the thickness direction[44].

During flight, take-off and landing, aircraft structures and equipment, such as radome, radar antenna, landing lights, canopy, windshield, lateral section or intake of the engine nacelle, turbine blades, wing or tail empennage leading edges, are open to high velocity impact loading. One of the major causes is bird strikes, because of their high probability of occurrence and their consequences [45]. When a bird strikes an aircraft, the relative velocities between the two objects are so high that the material of the airplane could suffer instant damage and failure. This situation can be simulated by high velocity impact testing. High velocity impact testing provides more severe damages which could lead to the immediate failure of the material [46]. Various applications require structural survivability against impact by high speed projectiles. In aircraft and land-based vehicles, composites are used and designed to survive high speed impact from wrecking engine parts, turbine blades and other debris [35]. It is important for these materials to be highly resistant against penetration by high velocity projectiles.

The impact behaviour of composite materials is influenced by many factors as thickness, architecture, laminate lay-up [47–50], and so on. However, also the service temperature can influence their mechanical and impact beheaviour. This temperature variation dramatically affects the properties of polymer interlayer material and its suitability especially in terms of the impact performance of the whole laminated structure [22,23].

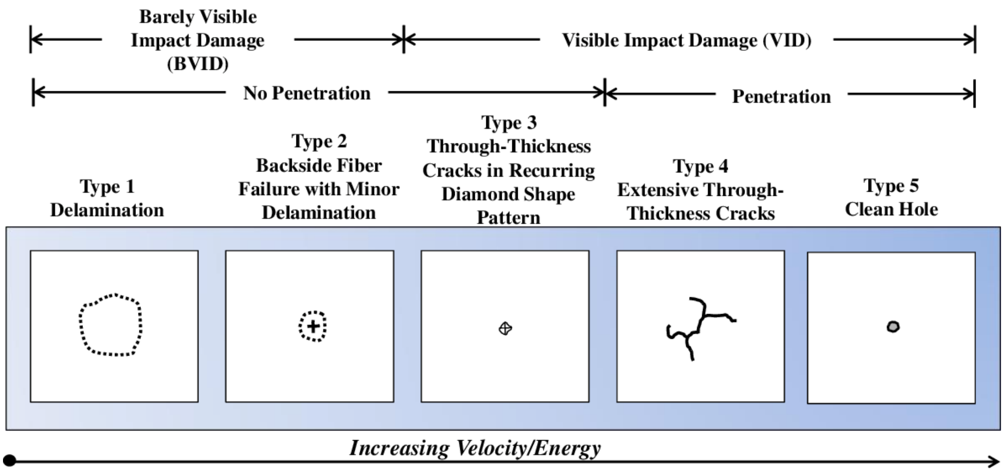


**Figure 4** - Different kinds of damage

In this scenario, several approaches have been positively exploited to improve the impact damage resistance of composite laminates in different conditions. Among these, the development of composite laminates stacking different fibres in the same matrix results very interesting [51,52].

Hybridisation guarantees similar or better properties respect to the principal elements, by taking advantages from the different properties of different used fibres, obtaining a composite with the more personalized performance [41]. In this regard, glass fibres are the best option from the viewpoint of cost, accessibility and simplicity of treating, and hybrid carbon/glass fibre composites have shown to better tolerate the damage respect to fibre matching part [8,53,54]. Also basalt fibre laminates have gain attention of many researchers since the increasing interest in the environment that had promoted the use of natural fibres as reinforcement in polymer matrices [52,55]. The low cost, easy availability and the simple manufacturing process, very similar to that of glass fibres but without any precursor nor additives, lead to choosing basalt fibres, thus obtaining an economic gain and a reduction of the environmental impact [23,56–59].

In this section, basalt composites, hybrid basalt/glass and basalt/carbon was made with vinylester resin. Low velocity impact at penetration and high speed tests at different impact velocity were carried out at room and low temperatures. The goodness of the hybridisations in terms of load, penetration energy and the ballistic limit was evaluated. The influence of the temperature on the mechanism and damage creation was analysed.

## 2. Materials and experimental setup

Basalt woven 200g/m$^2$ reinforced vinyl ester CRYSTIC® VE 679PA, composed by 36 layers of basalt woven fabric(0,90) (BB) were used to compare the results obtained by impacting no mixed hybrid basalt/glass (BG) and no mixed hybrid basalt/carbon (BC) reinforced vinylester. BG are made of 18 layers of basalt woven fabric and 20 layers of glass woven fabric and BC ones are made of 18 layers of basalt woven fabric and 10 layers of carbon woven fabric The different number of carbon layers is due to obtain the same thickness (Figure 5). The manufactured composite panels showed a nominal thickness of t=5.5 ± 0.25 mm and a fibre volume fraction of $V_f$=58%.

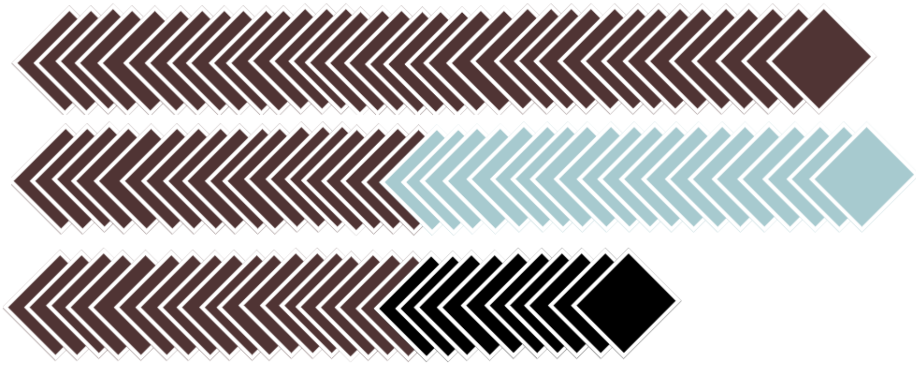


**Figure 5** - Stacking configurations of the hybrid manufactured composites

The specimens were impacted at low velocity and high velocity impact at room and at low temperature -50°C.

The instrumented drop weight apparatus (Figure 6) for low velocity impact tests, Instron/Ceast, equipped with a digital acquisition system allows impact velocity in the range 2-20 m/s, with impactor masses 3.6-10 kg, updating with a thermal chamber for tests at temperatures from +150°C to -70°C was used for the experimental tests. The square specimens, 100x100mm$^2$ cut from the original panels, were centrally impacted by an instrumented impactor, cylindrical with a hemispherical nose 19.8 mm in diameter. The total minimum mass is 3.6 kg. The maximum falling height of the testing machine is 1 m, which corresponds to maximum impact energy of 35.7J with the minimum mass of the impactor. Different impact energy values can be obtained adding masses up to 10.6 kg and varying the drop height, whereas the maximum velocity of 20 m/s can be reached as a result of the updating of the machine with a preloaded spring. The impact velocity of about 4.0 m/s was measured for only complete penetration tests (impact energy U=280J) carried out in the present research. The updating of the test machines by a thermal chamber allowed the tests at low temperature. Liquid Nitrogen was used to lower the temperature. For testing at temperatures lower than room one, the samples were soaked at that temperature for a minimum of 45 minutes. After the sample reached a uniform temperature throughout its length, testing was performed in the climatic chamber as for standard.

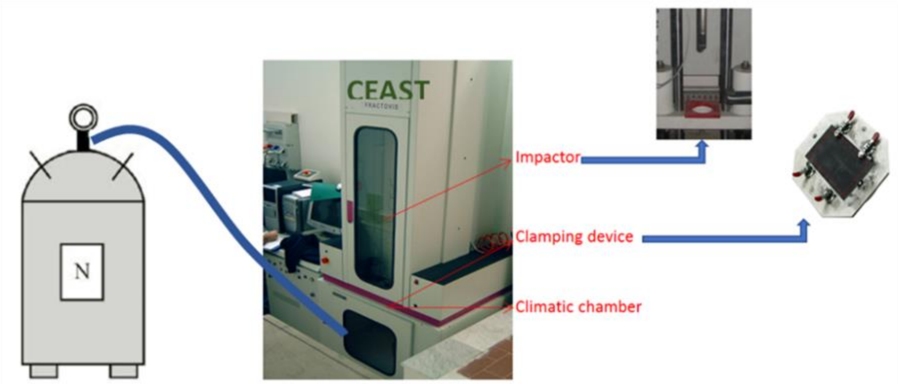


**Figure 6** - Low velocity impact tests set up

A batch of 5 samples was tested at each temperature to determine the effect of temperature on the impact behavior for each type of sample. The equipment for high speed impact tests (Figure 7) consists of a compressed gas cannon equipped with a chamber inside which a projectile is placed (d = 6.49mm) inside the sabot (d = 7.62mm) to stabilize the flight of the projectile, helium cylinders to reach the desired speed (V = 300-700 m / s). In addition, an infrared camera of 80000fps to measure the impact speed connected to a computer with Phantom 675.2 software, is used. For these types of tests 9 samples were tested for each condition.

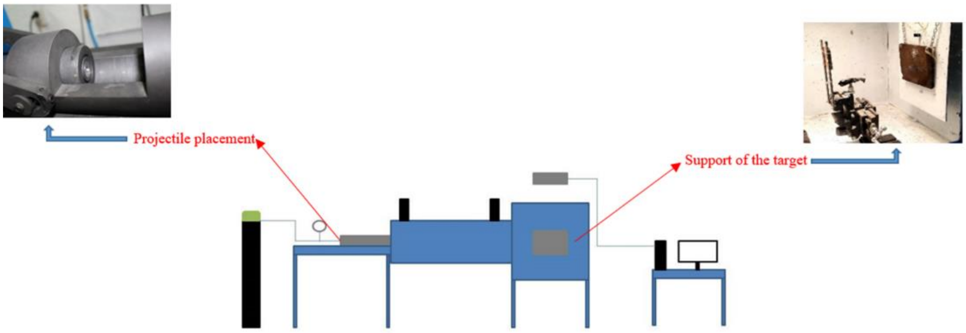


**Figure 7** - High velocity impact setup

The machine is equipped with software that allows us to measure the distance in terms of pixels and the time taken to travel this distance. In order to identify the ballistic limit and, therefore, the impact speed so that the projectile crosses the specimen 50% of the time, the Navy criterion has been used Figure 8. Also for the high speed tests the samples were tested at room temperature and at low T = -50 ° C.

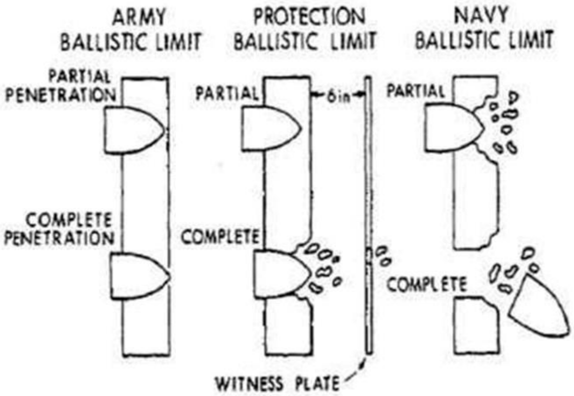


**Figure 8** - Ballistic limit [34]

In order to reach the temperature of -50 ° C, the specimens were housed in a box with ice bucket pellets, adjusting the temperature with a thermocouple. The samples to be tested were housed on the support equipped with a dry ice box to maintain the operating temperature.

# 3. Basalt/carbon - basalt/glass hybrid laminates. Room and extreme temperature.

## *3.1 Low velocity impact*

Specimens in pure basalt fibers (labelled as BB) as well as hybrids in basalt/carbon (BC) and basalt/glass (BG) fibers were impacted at penetration using the high impact energy $U_i$=280J to be sure to obtain penetration. All the specimens were dynamically loaded by the basalt side.

In the following

Table 2, maximum load, $F_{max}$, and penetration energy, $U_p$, measured in the described tests, are listed. Penetration energies are always lower than the impact energy, for BC laminates the impactor rebound on the surface without causing penetration, this is shown in the Figure 9 where the shape of the BC curve is different and the area enclosed in the loop of the load curve corresponds to the absorbed energy by the surface.

Interestingly, BC laminates don't reach the complete penetration. This behavior is highlighted in Figure 10- 12 the hybrid systems impacted on the basalt side at room temperature. In particular, in Figure 11 it is evident that BC laminate resists to the penetration showing only a curling of the specimens.

**Table 2** -Impact parameters

| | $U_i$ [J] | $F_{max}$ [N] | $U_p$ [J] |
|---|---|---|---|
| BB | 280 | 28745,2±125 | 220±5 |
| BC | 280 | 31880,3±155 | 250±2 |
| BG | 280 | 24728,3±200 | 251±4 |

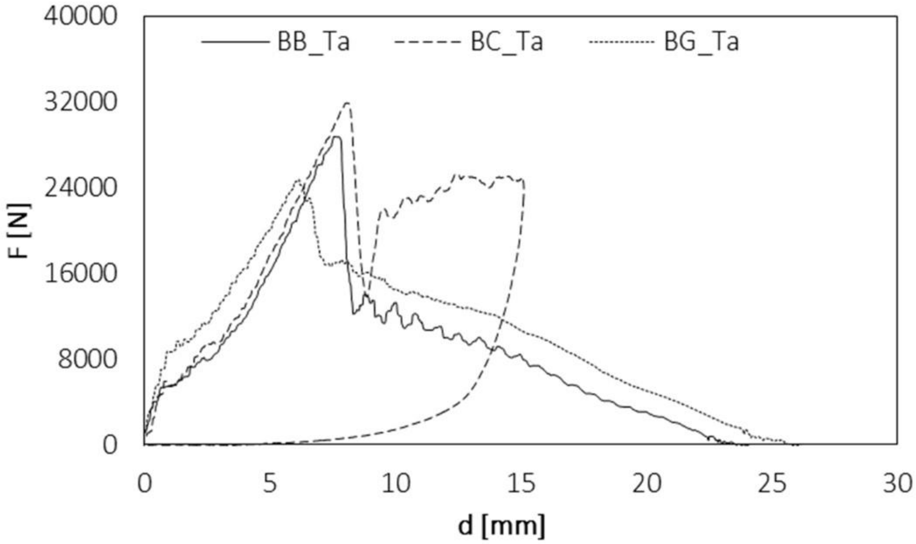


**Figure 9** - Load curves at penetration on basalt pure (BB) and hybrid laminates (BC and BG)

What asserted is clear also from the images of the impacted laminates in the following.

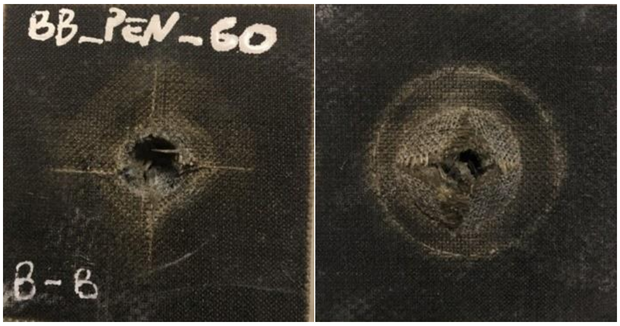


**Figure 10** - Front side (left) and back side (right) of pure basalt laminate

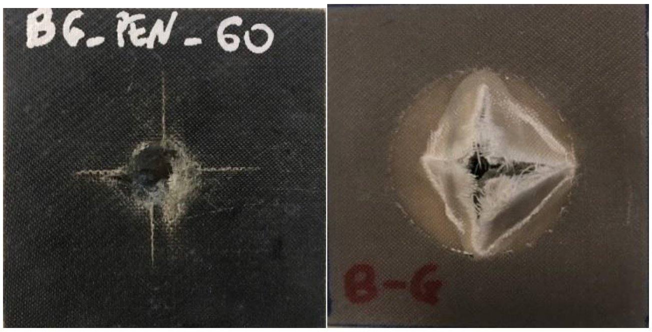


**Figure 11** - Front side (left) and back side (right) of basalt/glass hybrid laminate


**Figure 12** - Front side (left) and back side (right) of basalt/carbon hybrid laminate

According with the model used by Papa et al. [35] it was possible to predict the penetration energy of a laminate in pure carbon with the same number of layers of the laminate consider in this work. The model showed the complete penetration at an impact energy of about 220J, this is an interesting result since well beyond the value of 280J that did not cause penetration of the basalt/carbon hybrid laminate. The advantages are twice: first, a high impact resistance then, an economic gain since some carbon layers are replaced by basalt fibres and the latter are less expensive than the carbon ones with costs comparable to glass fibres.

The same specimens above discussed were tested at the low temperature T=-50°C. In the following Table 3, maximum load, $F_{max}$, and penetration energy, $U_p$, are listed. Penetration energies are always lower than the impact energy even if in Figure 13, where the load curves at -50°C are plotted, it is clear by the shape of the curve that the impactor rebounds on the surface of BG and BC samples without causing penetration.

**Table 3** - Impact parameters at T=-50°C

| | **T=-50°C** | | |
|---|---|---|---|
| | **Ui [J]** | **Fmax [N]** | **Up [J]** |
| BB | 280 | 13223,8±100 | 259±1 |
| BC | 280 | 14264,2±150 | 260±3 |
| BG | 280 | 20451,5±125 | 254±3 |

By overlapping on the same graph, Figure 14Figure **16**, the load displacement curves at room and low temperatures at fixed impact energy value, U, it is clear the influence of the temperature denoting the worse behaviour of all configurations at T=-50°C [22]. This is due to the presence of the styrene, which forms cross-links, and therefore the shear deformation is homogeneous [32,33]. The curing times of the matrix and the temperature influence the presence of styrene in the resin. It could act as a plasticizer and reduce the stiffness of the composite by increasing the strain to failure. It is also possible that the fabrics surface chemistry, during the samples conditioning phase, reacted in such a way as to produce an isothermal reaction with the different resin for the various fabrics [32,33]. Therefore the results of the three configurations are different.

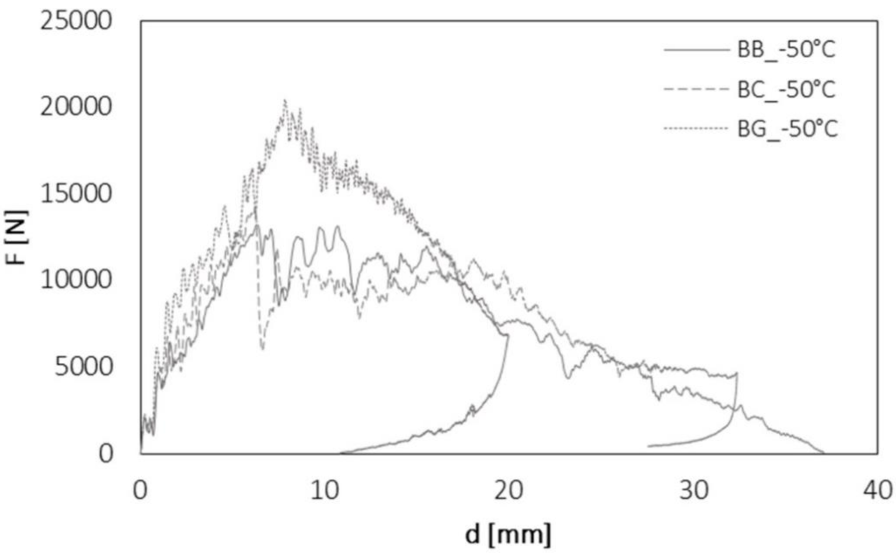


**Figure 13** - Load curves of hybrid laminates at T=-50°C.

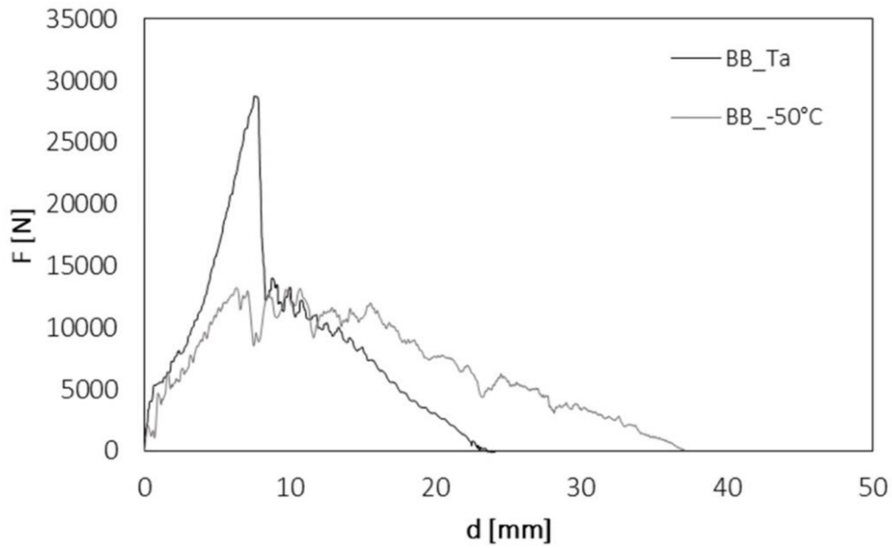


**Figure 14** - Load curves of BB laminates: influence of the temperature

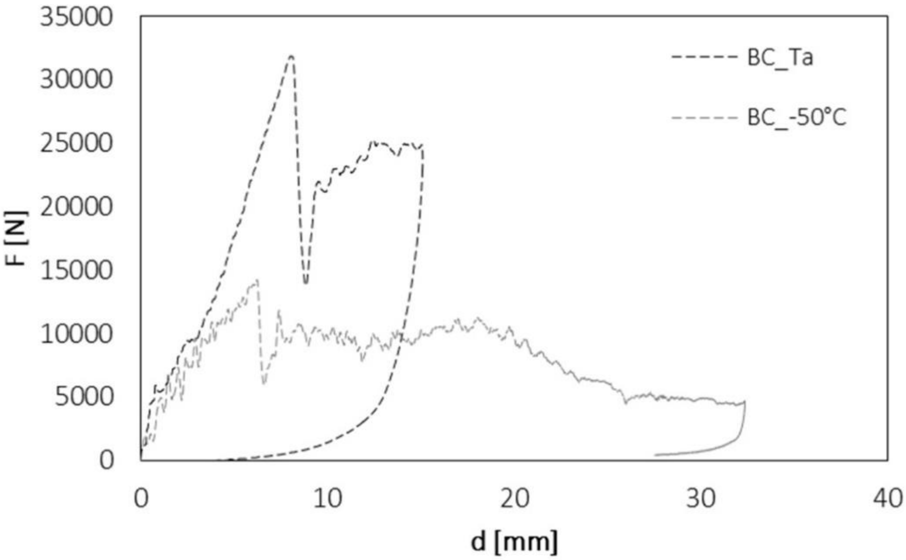


**Figure 15** - Load curves of BC laminates: influence of the temperature

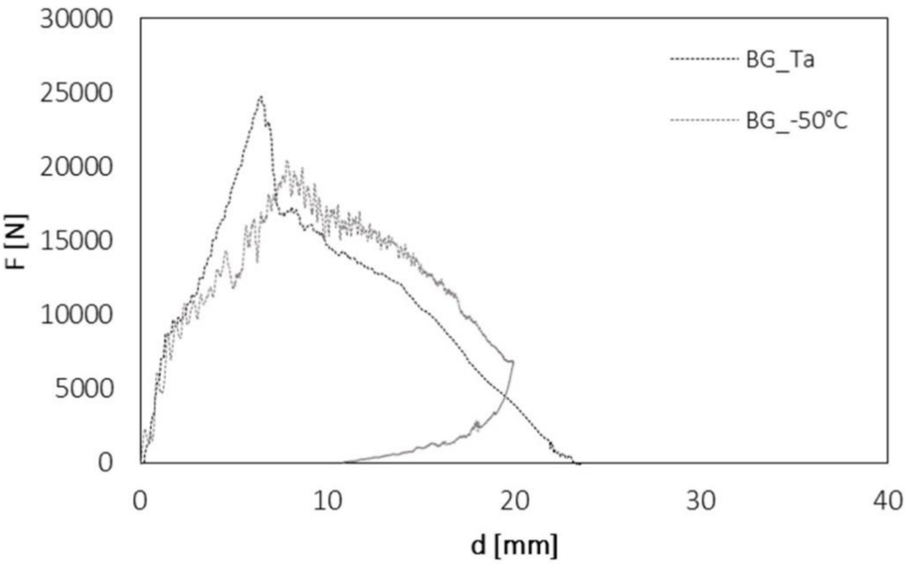


**Figure 16** - Load curves of BG laminates: influence of the temperature

In particular, unlike what happens in the penetration tests at room temperature, at low temperature the BG laminate shows a higher maximum resistance even if the stiffness ratio between the materials remains the same and the higher value of penetration energy is always shown by the hybrid BC. The maximum force decreases even if higher penetration energies are required. The energy is more involved in breaking the matrix as can be seen from the greater jaggedness of the force-displacement curve and a greater value of the deflection. This behavior requires less energy than is needed to break the fibers at room temperature. Basically there are easy breakages but many that involve a high amount of energy.

In the following Figure 17 , the data obtained at room and lower extreme temperature in terms of maximum load and penetration energy, were compared in bar graphs highlighting the differences.

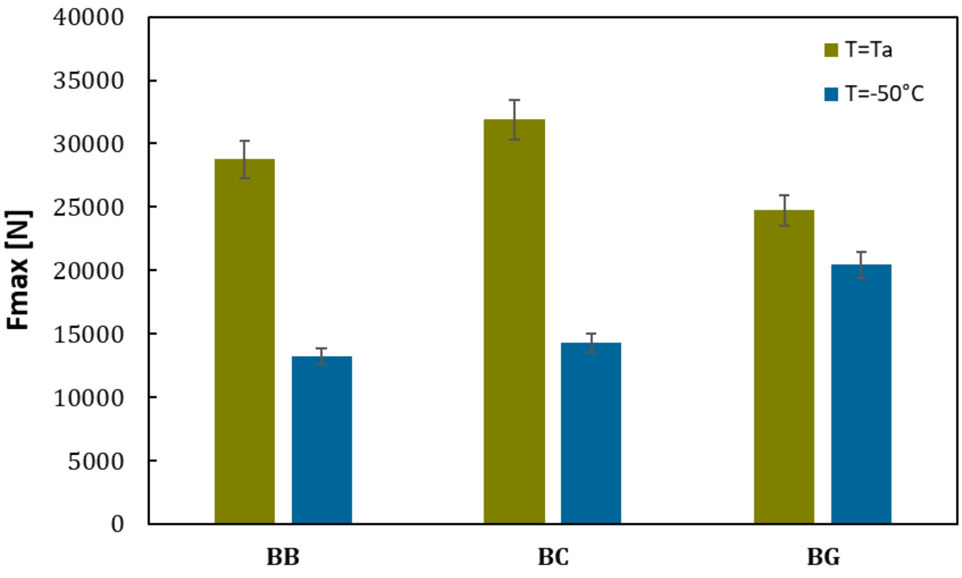


a)

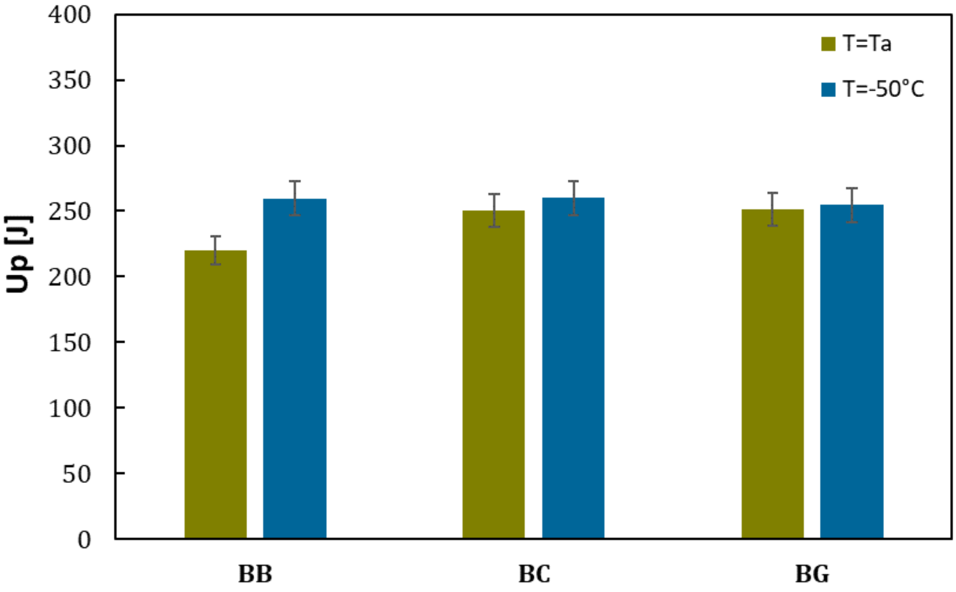


b)

**Figure 17** - Comparison between Ta and T=-50°C: a) Maximum load, Fmax; b) Penetration energy,Up

### *3.2 High velocity impct tests*

The objective of the high speed tests is to identify the ballistic limits at room and low temperature T = -50 ° C. The ballistic limit is the impact velocity required for a particular projectile to reliably (at least 50% of the time) penetrate the material.

In the tests, ballistic limit was found in this way: first, an high velocity impact was chosen, setting a very high pressure; afterwards, the pressure was set till the switch "projectile no stop" - "projectile stop". The average value between the impact velocity that corresponds to the lower residual velocity and the higher impact velocity with residual velocity equal to 0, was chosen as ballistic limit.

Obviously, the higher is the ballistic limit of a material, the more is the resistance to ballistic impact.

By comparing the experimental ballistic limits at different temperatures, in Figure 18. It can be observed that the temperatures at which normally navy ship is exposed in the Arctic ocean do not affect the ballistic limit of the composite materials under attention. In fact, considering an error of measurement of $\pm 10\ \frac{m}{s}$ the experimental results of ballistic limits are more or less the same for the two temperature conditions. For this reason the conclusion is that the temperatures observed does not influence the ballistic limit of the materials under attention.

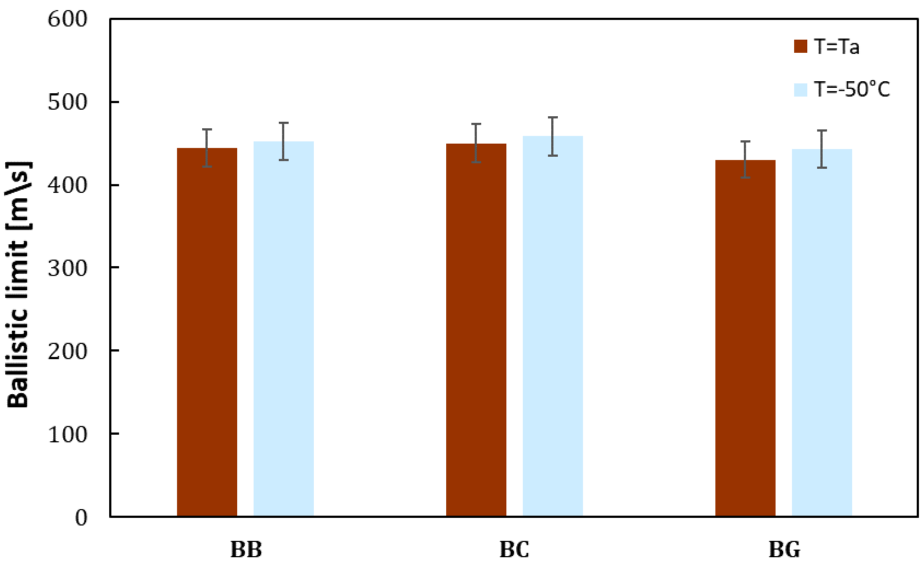


**Figure 18** - Ballistic limit histogram

Furthermore, an important parameter to evaluate the impact ballistic performances, is the value of the residual velocity ($v_r$) that is the projectile velocity after perforation of all impacted layers. In fact, in the same experimental conditions, if the impact velocity is the same but the residual velocity of the projectile is lower, the resistance of the material is higher. As indicated in the Table 4 and Table 5, the BC samples show a lower residual velocity for both the temperatures tested.

**Table 4** - High velocity impact parameters, T=Ta

| | **Impact velocity** $\mathbf{V_0}\,[\frac{m}{s}]$ | **Residual velocity** $\mathbf{V_r}\,[\frac{m}{s}]$ | **Perforation results** |
|---|---|---|---|
| BB | 444 | 86 | Perforation |
| BG | 450 | 109 | Perforation |
| BC | 430 | 60 | Perforation |

**Table 5** - High velocity impact parameters, T=-50°C

| **T=-50°C** | | | |
|---|---|---|---|
| | **Impact velocity** $\mathbf{V_0}\,[\frac{m}{s}]$ | **Residual velocity** $\mathbf{V_r}\,[\frac{m}{s}]$ | **Perforation results** |
| BB | 452 | 83 | Perforation |
| BG | 458 | 87 | Perforation |
| BC | 443 | 79 | Perforation |

In the following images, the frames of the nearest shot at ballistic limit at room temperature, $T_a$ (Table 4), and low temperature, T=-50°C (Table 5), are reported.

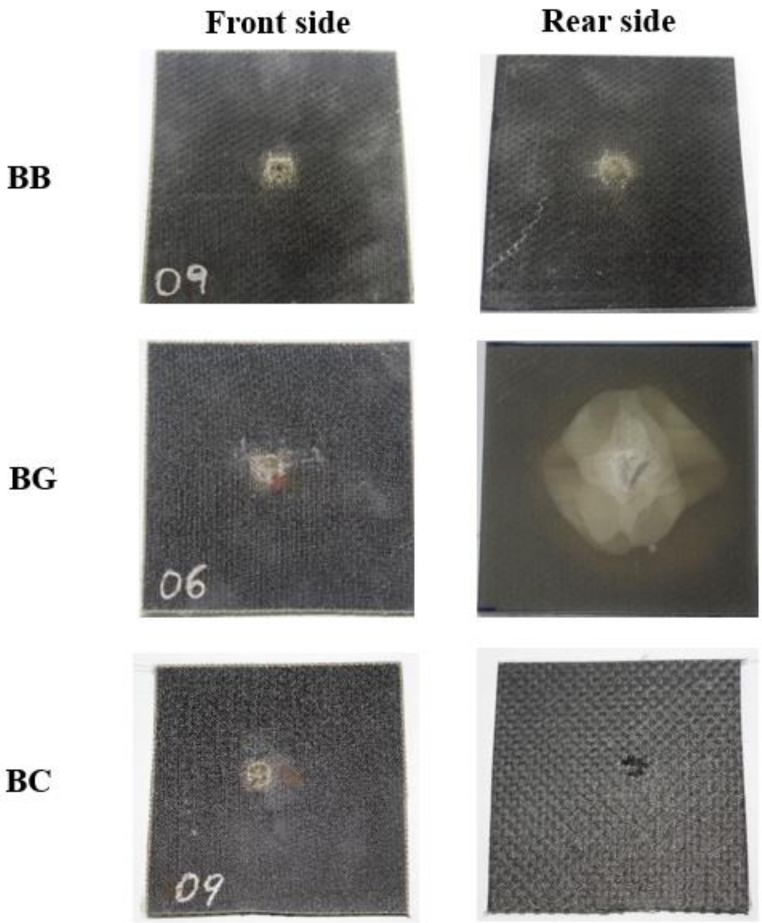


a)

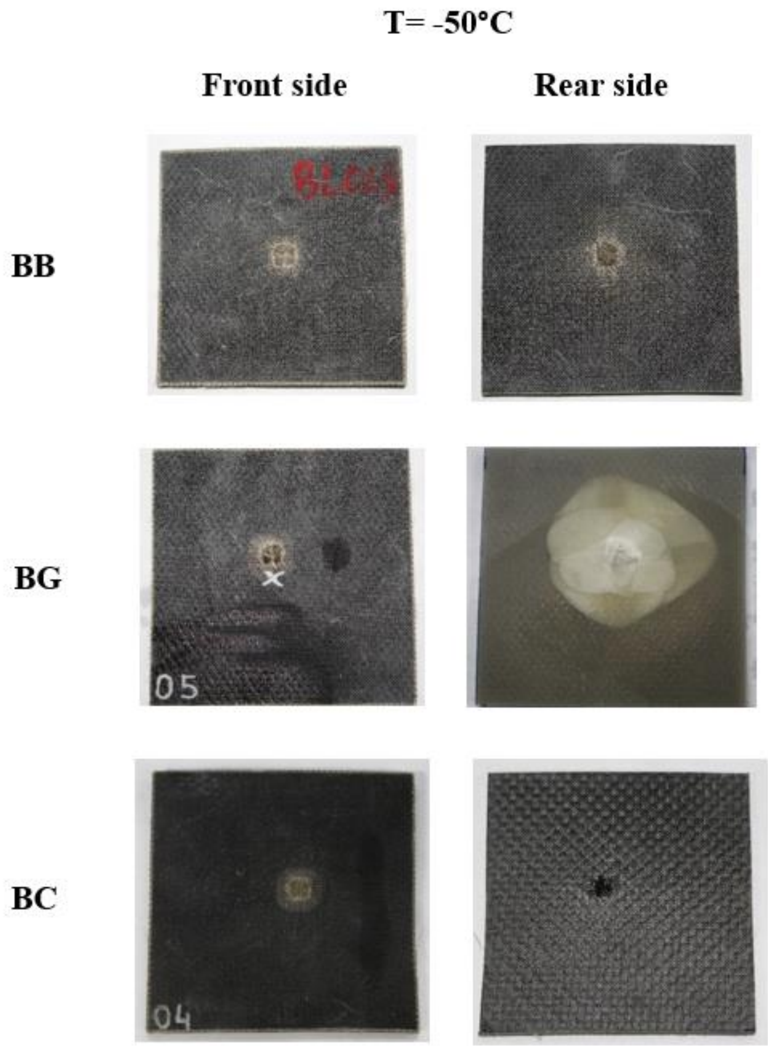


b)

**Figure 19** - Pictures of samples impacted at T=-50°C, a)front side; b) rear side

The energy dissipation in hybrid composite materials is due to synergistic sequence of failure mechanisms, the delamination first of all.

By the results obtained is possible to conclude that when the impact velocity is near to the ballistic limit, each laminate tested shows a very large delamination area, as can be seen in Figure 20.

The extent of the damage is lower when the impact velocity is higher than the ballistic limit of composite. This happens because when the impact velocity is high, the load is more concentrated and the material has not the necessary time to delaminate, while when the velocity is lower, near to the ballistic limit, the materials have all the time to absorb the deformation energy and so to delaminate.

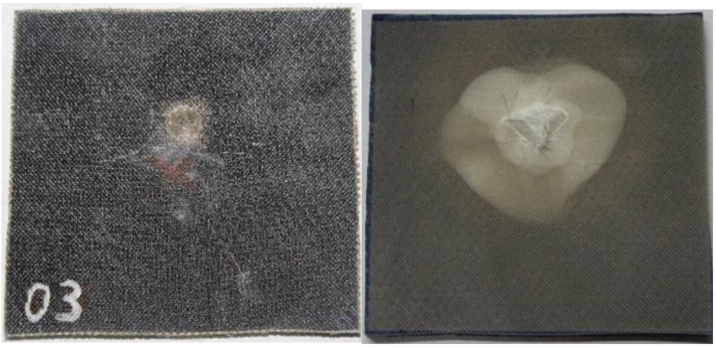


a)

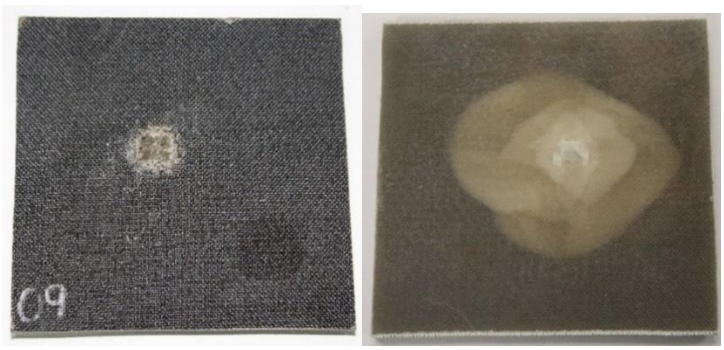

b)

**Figure 20** - The difference of the delamination at different impact velocities. a) high velocity b) lower velocity

The energy dissipation in hybrid composite materials is due to the synergistic sequence of failure mechanisms, first of all, the delamination. By the results obtained is possible to conclude that when the impact velocity is near to the ballistic limit, each laminate tested shows an extensive delamination area. The extent of the damage is lower when the impact velocity is higher than the ballistic limit of the composite. This happens because when the impact velocity is high, the load is more concentrated and the material has not the necessary time to delaminate. In contrast, when the speed is lower, near to the ballistic limit, the materials have time to absorb the deformation energy and so to delaminate.

# Section III: The bio-based hybrid composite materials

## 1. Framework

Basalt is considered natural fiber due to its origin, as a matter of fact it is produced by magma deposits generated during the volcanoes eruptions. The development of the manufacturing process, for this fiber type, and the improvement of research studies about its mechanical properties, lead to an increase for its applications in each manufacturing sector (Figure 21). If basalt is compared with other traditional fibers for composite reinforcement, it can be seen that its employment is increasing and is absolutely comparable to Carbon fibers use (Figure 22) [60].

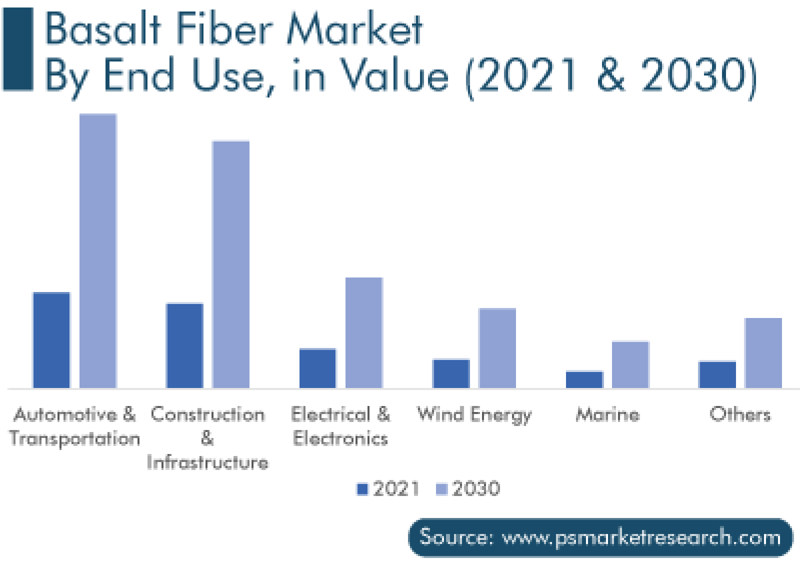


**Figure 21** - https://www.psmarketresearch.com/market-analysis/basalt-fiber-market

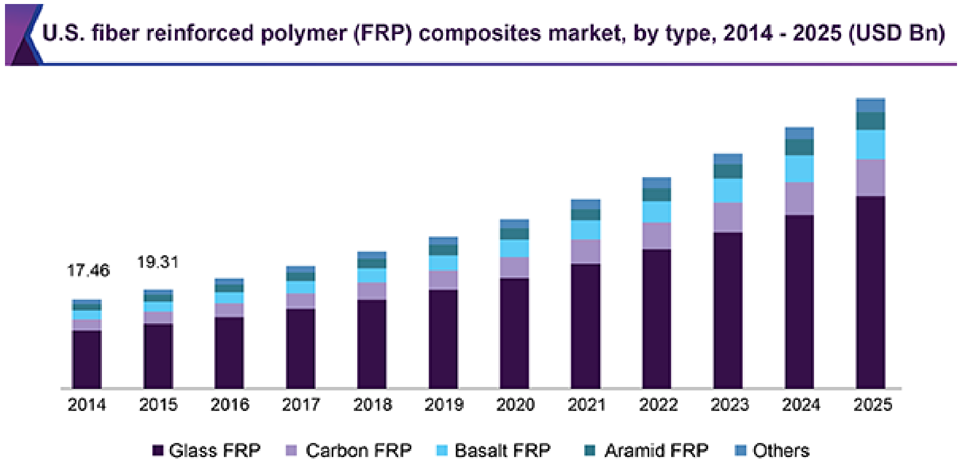


**Figure 22** - Composite market[60]

Even tough basalt should be considered renewable, the speed of renewal is unaccountable, moreover its costs and the fibers processing time make it difficult to include in a really sustainable production system. So current trend is to improve the use of natural materials which could be found already in a fibrous state, and whose growth could be managed through traditional harvesting process. The growing interest in natural fibers is mainly due to their low specific density, which is typically 1.25–1.50 g/cm3 , compared to glass fibers at about 2.6 g/cm3 , allowing natural fibers to provide s higher specific strength and stiffness in plastic materials [61]. The other key driver for substituting natural fibers for glass is the lower price of natural fibers (200–1000 US$/tonnes) compared to glass (1200–1800 US$/tonnes) [62]. Natural fibers are also are recyclable, biodegradable, abundant, exhibit good mechanical properties, provide better working conditions and are less abrasive to equipment when compared to common synthetic fibers, which can contribute to significant cost reductions [63]. The key differences between natural fibers and glass fibers are shown in Table 6 .

**Table 6** - Comparison between natural and glass fibres *[64]*

| Properties | Natural fibers | Glass fibers |
|---|---|---|
| Density | Low | Twice that of natural fibers |
| Cost | Low | Low, but higher than NF |
| Renewability | Yes | No |
| Recyclability | Yes | No |
| Energy consumption | Low | High |
| Distribution | Wide | Wide |
| $CO_2$ neutral | Yes | No |
| Abrasion to machines | No | Yes |
| Health risk when inhaled | No | Yes |
| Disposal | Biodegradable | Non-biodegradable |

All these characteristics make their use very attractive for the manufacture of polymer matrix composites.

The natural fiber reinforced composited are already successfully employed in various production sectors, for instance building and construction or automotive, where they have replaced other traditional and less sustainable materials. In particular, previously, the majority of studies employed no-biodegradable petroleum-based polymers as matrix. Currently, more researches have been conducted to study the use of natural fiber fabric reinforced with biodegradable matrix in automotive applications [65].The study shows as biocomposites had an average strength higher than the threshold strength required for car instrument or dashboard panels.

However, their use in aerospace, which is the most environmental impacting sector, is discouraged due the low mechanical properties (Figure 23) [66].

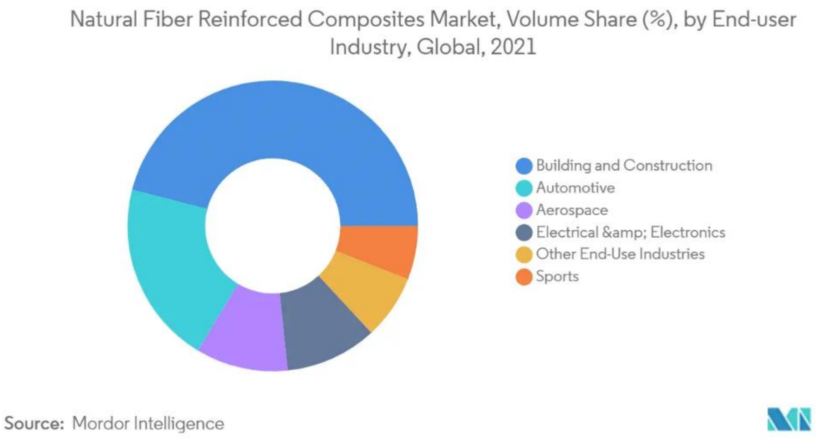


**Figure 23** - Natural Fiber Reinforced Composite Market[61]

Within many automotive and aerospace companies including Ford, Mercedes-Benz, Audi, Toyota, BMW, Mitsubishi motors, Airbus and Boeing there is a shift towards application natural fiber-based composites for their automobile and aircraft parts to address high energy and safety requirements[13,67]. Furthermore, automobile door liners have been produced with hemp fibre and cabin doors of aeroplanes are fabricated with fibre based composites [68].

These reasons lead to enhance the efforts in a natural fibers integration in hybrid structures, where they should take advantage from the mechanical characteristics of traditional fibers, by giving less environmental impact.

The novelty introduced by this section is the use of fully bio-based materials.

One of the main reasons that flax is increasingly considered for use in composites is the growing emphasis on using more sustainable and environmentally-friendly materials in industrial applications.

Hybridization of flax fibres with stronger and more corrosion resistant fibres improves the stiffness, strength, as well as moisture resistant behaviour of the composite. In the last ten years, hybrid composites with flax fibers have been the subject of much research [69–73]. However, there aren't many investigations on the hybridization of flax fibers with mineral fibers such basalt fibers [74,75].

Flax fibre requires less times and less energy to produce per unit weight than glass fibre, and because the carbon capture during its growth the carbon emissions from its production are often considered null. Flax fibre as a composite reinforcement is not without its compromises. Compared to conventional reinforcements such as glass or carbon fibre, flax does have lower mechanical performance. For this reason the hybridization with basalt, that shown a good impact behaviour, has been selected.

## 2. Materials and experimental setup

The fabrication of composites was realized by using the vacuum bag infusion. As reinforcement, basalt and flax twill 2/2 wave fabrics with areal densities of 235 g/m2 and 220 g/m2 respectively, were used. The basalt was provided by Timeout Composite oHG and Amplitex flax was provided by CTM GmbH - Composite Technologie & Material. These three materials were chosen because they are natural materials suitable for the vacuum infusion process [76]. In addition to standard natural fabrics, another innovative fabric has been studied in this work. The intraply woven fabric twill 2/2 made of Filava and flax with nominal surface weight 250 gsm is provided by ISOMATEX. The texture construction is 50% FILAVA and 50% flax. FILAVA is made of enhanced basalt enriched with various mineral additives and manufactured in the melt spinning process with the aim to increase and guarantee its original mechanical and chemical properties. As a result of especially engineered project that provides high tensile strength, elongation and high thermal resistance, the composite reinforced by this material delivers an outstanding resistance to impact stress and turns out suitable to high-end applications. The aim of this investigation was to propose a composite, as much as possible, bio-based. It has not been simple to find in the market a thermosetting resins completely biobased. No vinyl ester resins were found, as in the previous study, and an epoxy resin was chosen. The partially biobased epoxy resin, GreenPoxy 56, was supplied by Sicomin Composites. This resin contents up to 56% of its molecular structure coming from plant origin. The final percentage of the mix bio-based carbon content will depend on the hardener choice. The SD 8824 hardener by Sicomin. The epoxy and hardener, were mixed with a stoichiometric weight ratio of 100/21 and the final bio content was 46%. The processing method used for the fabrication of the laminates has been the Vacuum Bag Infusion, dry materials are laid into the beg and the vacuum is applied before resin is introduced. Once a complete vacuum is achieved, resin is carried into the laminate via carefully placed tubing.

Seven laminates have been investigated:

- Basalt woven reinforced epoxy, composed by 12 layers of woven fabric;
- Flax woven reinforced epoxy, composed by 12 layers of woven fabric;
- Intraply filava-flax woven reinforced epoxy, composed by 12 layers of woven fabric;
- Four different hybrid basalt/flax reinforced epoxy, composed by 6 layers of basalt woven fabric and 6 layers of flax woven fabric;

The hybrid composite laminates were symmetrical and balanced and were fabricated by ordering six basalt and six basalt fabric layers in different stacking sequence. The stacking sequences and the abbreviations of prepared laminate configurations are shown in Figure 24. The thickness and fiber volume fraction values of the prepared composite laminates are summarized in Table 7.

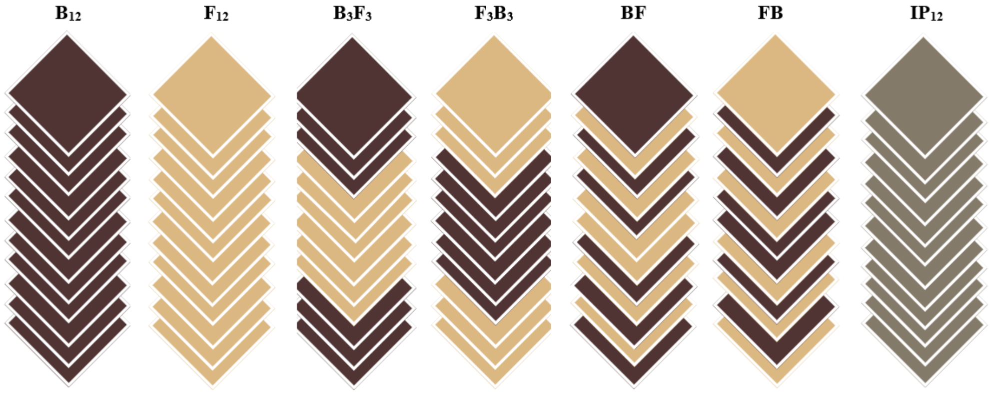


**Figure 24** - Stacking sequences of basalt (B), flax (F) and intraply B-F(IP) fabric layers

**Table 7** - Laminates design

| | STACKING SEQUENCE | Th [mm] | TEXTURE [g/m2] | VOLUME FIBER | LAYERS | | | RESIN [g] | |
|---|---|---|---|---|---|---|---|---|---|
| | | | | | Basalt | Flax | Intraply | R | H |
| B | $[B_{12}]$ | 2.10 ±0.05 | 235 | 0,52 | 12 | | | 300 | 63 |
| F | $[F_{12}]$ | 4.80±0.05 | 200 | 0,52 | | 12 | | 400 | 84 |
| $B_3F_3$ | $[B_3/F_3]_S$ | 3.50±0.05 | 235/200 | 0,52 | 6 | 6 | | 350 | 73,3 |
| $F_3B_3$ | $[F_3/B_3]_S$ | 3.60±0.05 | 235/200 | 0,52 | 6 | 6 | | 350 | 73,3 |
| BF | $[B/F]_{3S}$ | 3.60±0.05 | 235/200 | 0,52 | 6 | 6 | | 350 | 73,3 |
| FB | $[F/B]_{3S}$ | 3.60±0.05 | 235/200 | 0,52 | 6 | 6 | | 350 | 73,3 |
| IP | $[IP_{12}]$ | 4.80±0.05 | 250 | 0,52 | | | 12 | 550 | 115,5 |

Low velocity impact tests were performed using an Instron/Ceast Drop Tower Impact System equipped with a digital acquisition system. The specimens (100mmx100mm) cut from the original panels, were clamped between two metal fixtures, according to the ASTM D7137 standard, and centrally impacted by an impactor with a hemispherical nose 19.8 mm in diameter. This work aims to investigate bio based composite materials by insights on the damage due to the dynamic behaviour and the influence of the stacking sequence.  Low velocity impact response has been studied, in particular drop indentation tests with an impact energy of U=15J, 30J and 40J, and penetration tests at Up=150J. The penetration energy was chosen from literature and was applied for all types of specimens in order to have comparable data Three identical samples for each composite laminates configuration were tested at each different energy levels.

Key parameters such as maximum force, deflection, and absorbed energy were systematically recording and the averages of results were utilized to study the laminates impact behaviour and the hybridization effect on the last. The damage in terms of indentation depth and delamination extension were evaluated and compared with those for basalt fiber reinforced composite laminates BFRP and FFRP (Flax) to investigate the hybridization effect. The damage was analysed by Electronic Speckle Pattern Interferometry (ESPI) technique and by Confocal microscope to evaluate the evolution of the damaged area.

## 3. Impact tests

In this paragraph the results of the impact tests are presented. Figure 25 shows the impact response of the seven investigated different composite laminates. Each graph includes the force-displacement curve at 15J, 30J, 40J and at 150J, this last is the energy deemed necessary for the complete penetration of the specimen. Basalt adds stiffness whereas flax contributes with high renewable content

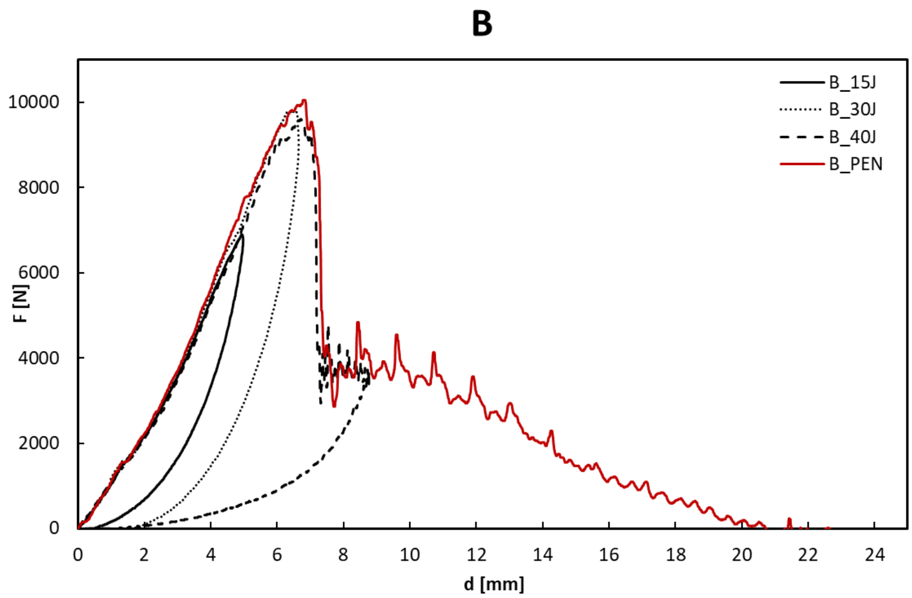
B
B_15J
B_30J
B_40J
B_PEN
F [N]
d [mm]
0
2000
4000
6000
8000
10000
0
2
4
6
8
10
12
14
16
18
20
22
24

a)

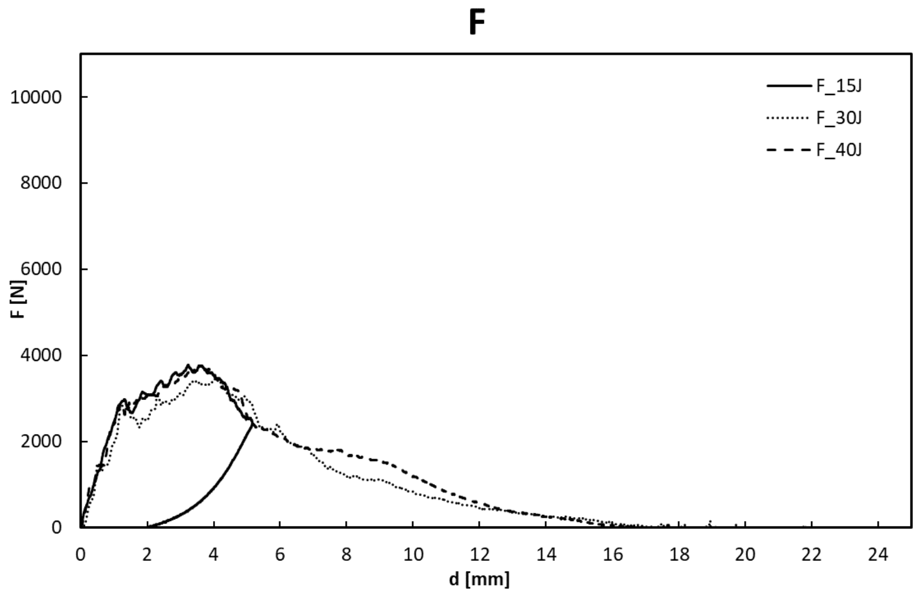
F
F_15J
F_30J
F_40J
F [N]
d [mm]
0
2000
4000
6000
8000
10000
0
2
4
6
8
10
12
14
16
18
20
22
24

b)

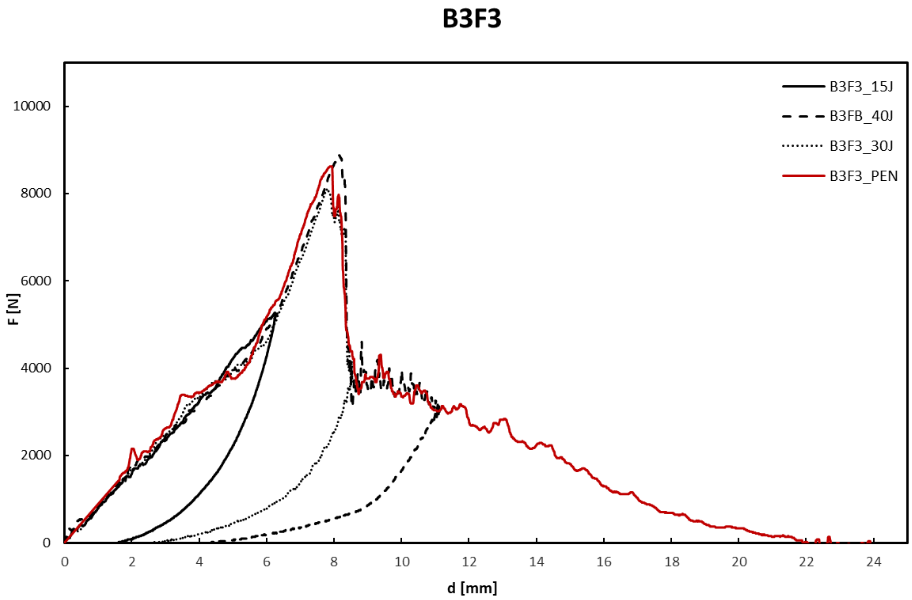
B3F3
B3F3_15J
B3FB_40J
B3F3_30J
B3F3_PEN
10000
8000
6000
4000
2000
0
F [N]
0
2
4
6
8
10
12
14
16
18
20
22
24
d [mm]

c)

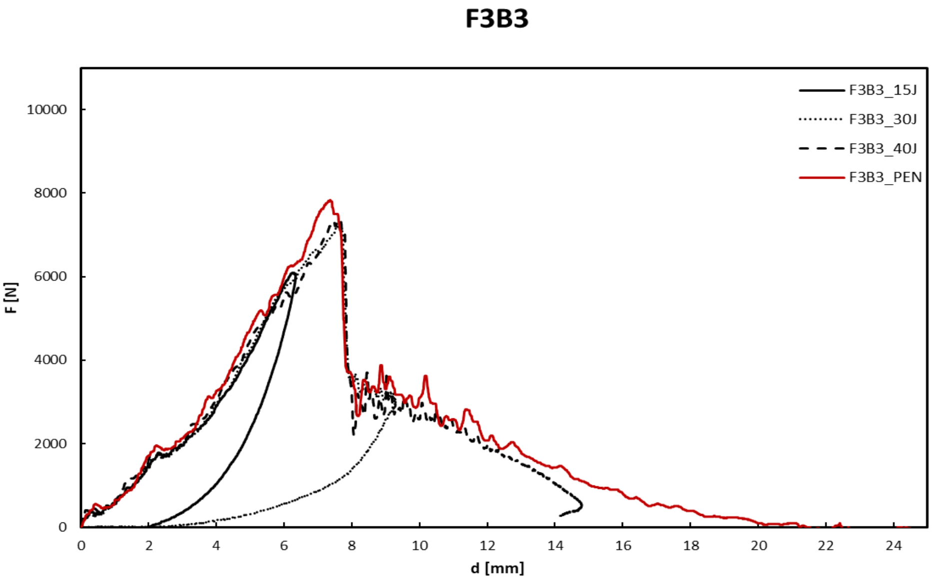
F3B3
F3B3_15J
F3B3_30J
F3B3_40J
F3B3_PEN
10000
8000
6000
4000
2000
0
F [N]
0
2
4
6
8
10
12
14
16
18
20
22
24
d [mm]

d)

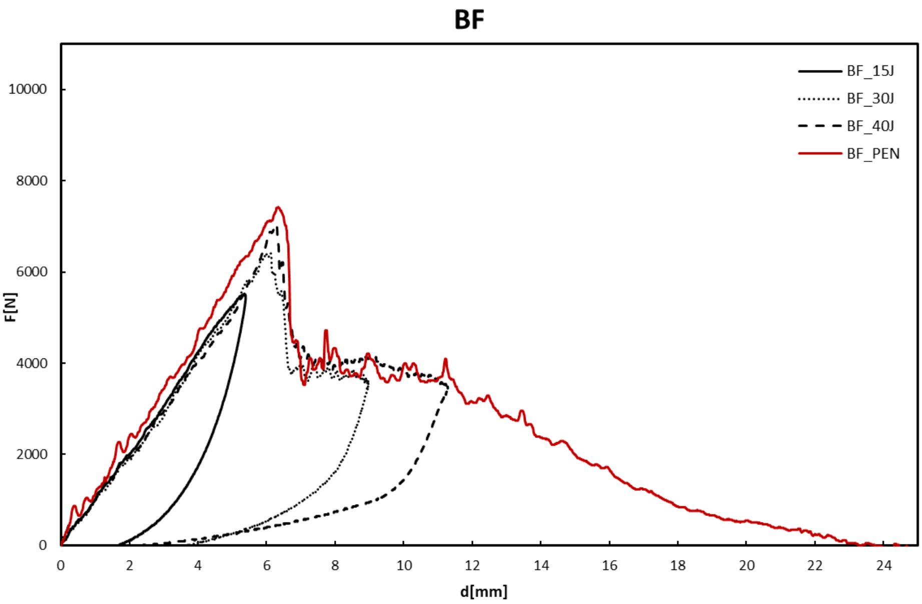
BF
BF_15J
BF_30J
BF_40J
BF_PEN
F[N]
d[mm]
0
2000
4000
6000
8000
10000
0
2
4
6
8
10
12
14
16
18
20
22
24

e)

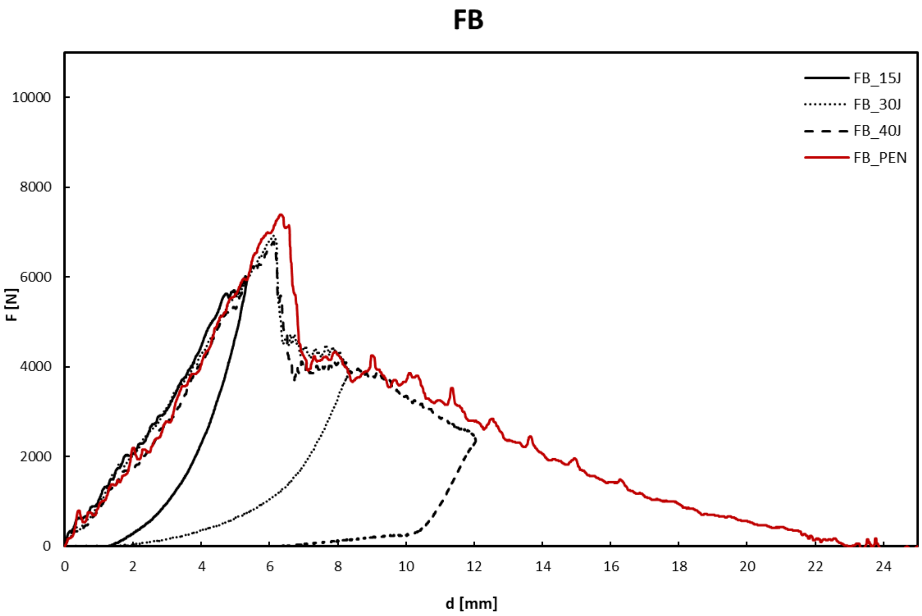
FB
FB_15J
FB_30J
FB_40J
FB_PEN
F [N]
d [mm]
0
2000
4000
6000
8000
10000
0
2
4
6
8
10
12
14
16
18
20
22
24

f)

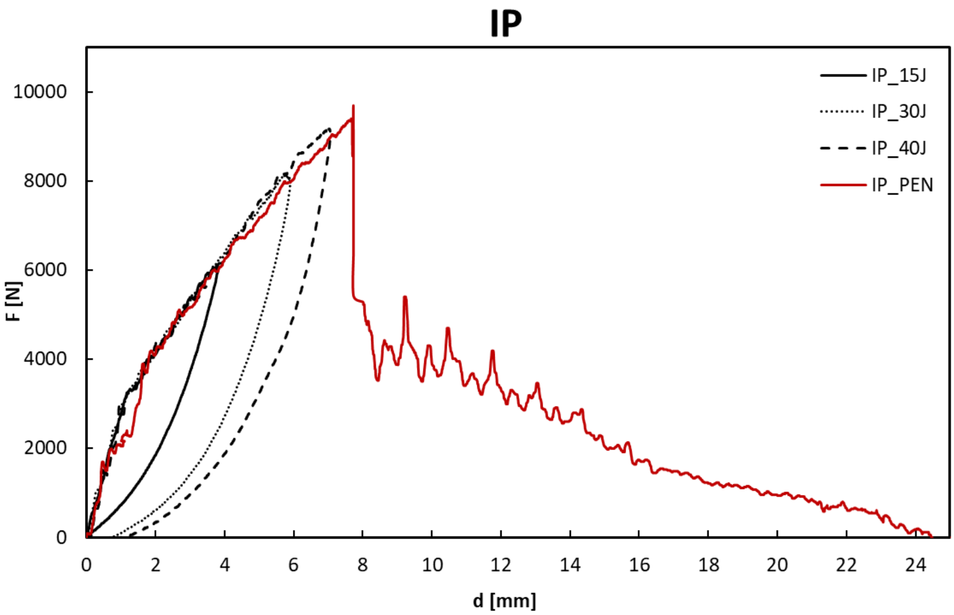


g)

**Figure 25** - Force-displacement curves for each laminate: a) Basalt; b) Flax; c) $B_3F_3$; d) $F_3B_3$; e) BF; f) FB; g) IP.

All the laminates, except for the flax laminate, show a similar behaviour, the force increases as the impact energy increases. At all the impact energy levels (15 J, 30J and 40J) these samples are not penetrated by the impactor that rebounds and the area under the curve represents the energy absorbed by the laminates to create damage. The flax reaches the same maximum load for each energy level and turns out perforated at 30J, a much lower energy than other laminates. At 15J the damage is already remarkable and close at the catastrophic penetration, it would be interesting investigate the behaviour at energies lower than 30J to evaluate the onset and the evolution of the damage. In this work we haven't focus on it because there weren't comparable reference but it would be interesting as future development.

The Figure 26 compares the curves of all laminates with the same energy level.

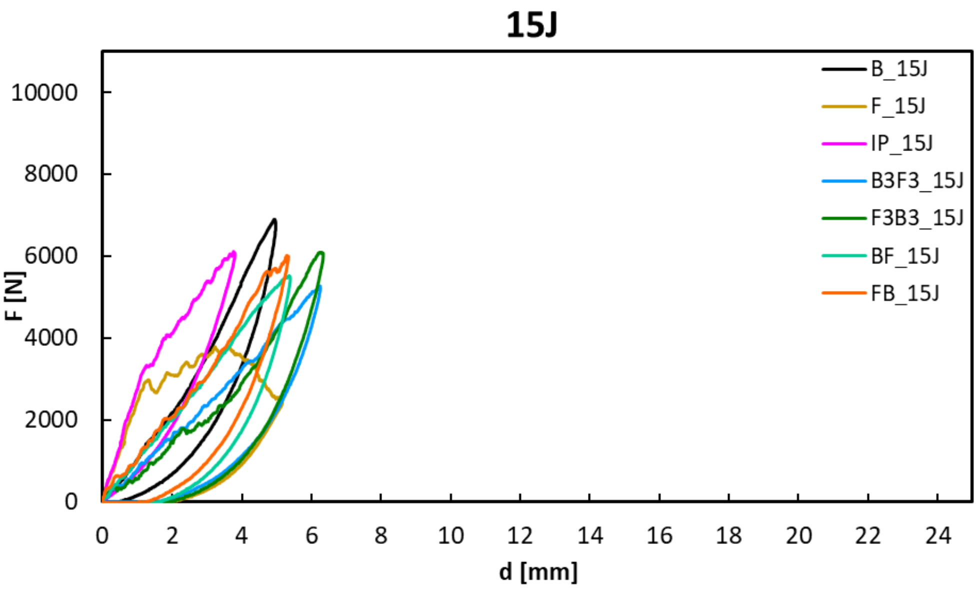


a)

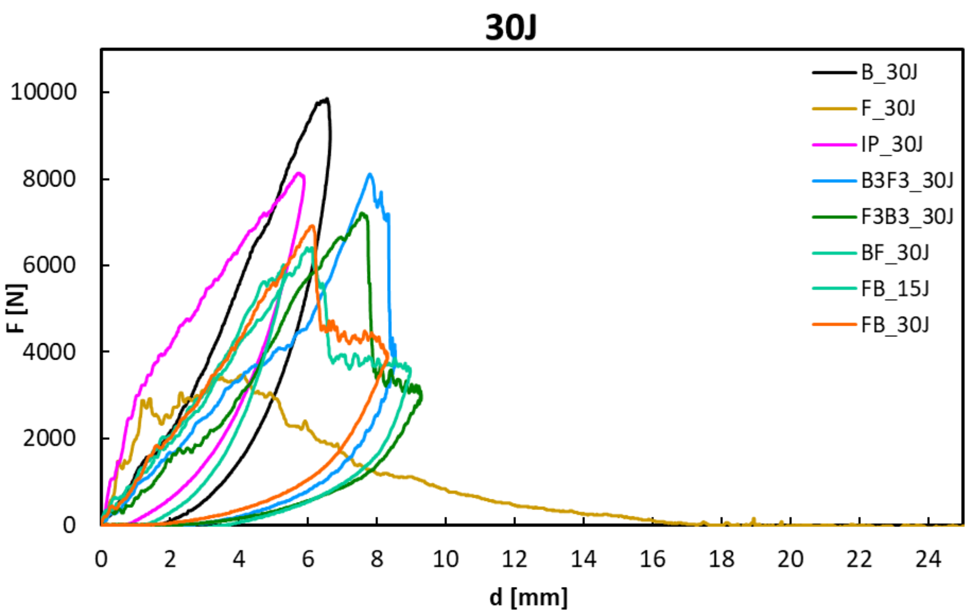


b)

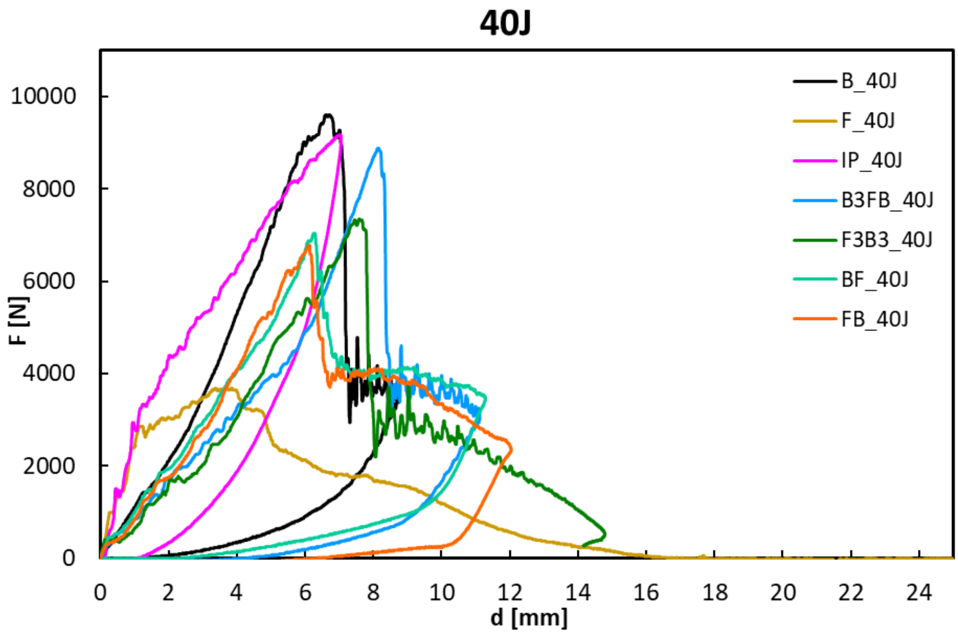


c)

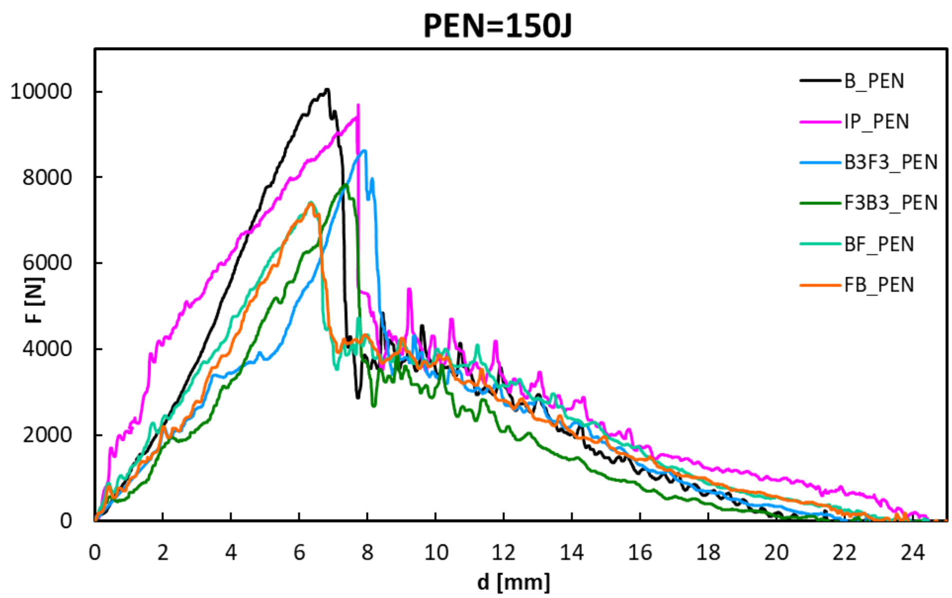


d)

**Figure 26** - Force-displacement curves of flax-basalt reinforced epoxy hybrid composite laminates at : a) 15J, b) 30J, c) 40J, d) penetration.

It is interesting to note that the curves relating to the hybrid laminates are placed in an intermediate position between the curves of pure flax and pure basalt, indicating an intermediate behaviour between the two no hybrid configurations. Several curve of the specimens impacted at energies higher than 15J shows a significant drop of the load before fiber breaking, but continues to bear the load after it. This phenomenon, already observed by Ricciardi et al.[59], increase with the increasing of the energy level, it is particularly evident at 40J, except for the intraply sample. It was already noted [77,78] that basalt fiber laminates in epoxy resin don’t show any sudden load drops or changing in slope on the first increasing part of the curve, denoting no delamination propagation confirmed by non-destructive analysis [79].

This is clearly confirmed in the present research where the basalt fibres are immersed in vinyl ester resin. Moreover, as it is simply noted in Figure 26, soon after the maximum peak, an important sudden load drop happens, followed by an increasing trend up to a second peak, lower than the first one, soon before the catastrophic final load drop. The explained trend denotes the aptitude to continue supporting the load even if the material is significantly damaged. The latter behaviour is very interesting in real applications like the naval ones during military expeditions where, following impacts from ice or projectiles, it is crucial that the ships are able to arrive safe at destination.

**Table 8** - Impact at indentation properties

| | INDENTATION | | | | | | | | |
|---|---|---|---|---|---|---|---|---|---|
| | 15J | | | 30J | | | 40J | | |
| | **Fmax [N]** | **Ua[J]** | **dmax [mm]** | **Fmax [N]** | **Ua[J]** | **dmax [mm]** | **Fmax [N]** | **Ua[J]** | **dmax [mm]** |
| **B** | 6848,3 | 6,49 | 4,97 | 9562,1 | 19,66 | 11,6 | 9490,3 | 33,15 | 8,81 |
| **F** | 3664,2 | 12,26 | 5,73 | 3638,1 | | 29,7 | 3357,2 | | 42,71 |
| **$B_3F_3$** | 5199,1 | 8,25 | 6,57 | 8092,5 | 23,89 | 8,4 | 8393,0 | 34,81 | 10,67 |
| **$F_3B_3$** | 6152,7 | 6,78 | 6,20 | 7504,7 | 25,02 | 9,5 | 6982,2 | 38,79 | 18,09 |
| **BF** | 5597,5 | 8,10 | 5,01 | 6590,3 | 24,35 | 2252,2 | 6799,3 | 33,29 | 11,10 |
| **FB** | 6067,8 | 6,34 | 5,35 | 7073,6 | 23,31 | 8,4 | 6858,1 | 35,76 | 11,82 |
| **IP** | 5793,4 | 6,88 | 3,85 | 7877,0 | 17,07 | 6,0 | 8099,1 | 25,17 | 7,31 |

Table 7 the impact properties and indentation measurements at three different energy levels are indicated and clearly shown in Figure 27.

From Figure 27, it is possible to observe that basalt sample show the best performance and the flax sample the worst performance at three different energy levels. All the hybrid configurations properties are located between the two pure laminates, displaying a intermediate behaviour. No significant differences regarding maximum load or total absorbed energy are recorded as clearly appear in Figure 27a.

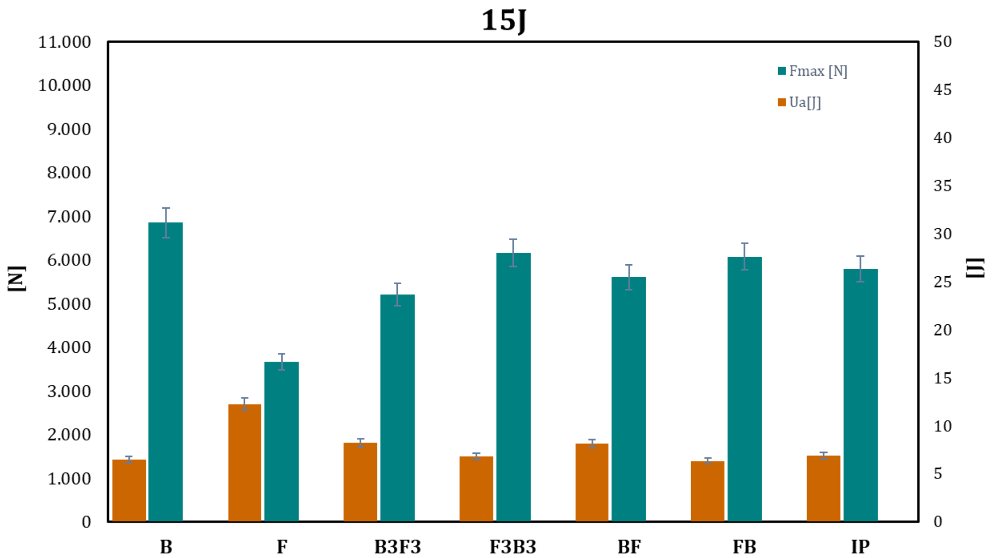
15J
11.000
10.000
9.000
8.000
7.000
6.000
5.000
4.000
3.000
2.000
1.000
0
[N]
50
45
40
35
30
25
20
15
10
5
0
[J]
Fmax [N]
Ua[J]
B
F
B3F3
F3B3
BF
FB
IP

a)

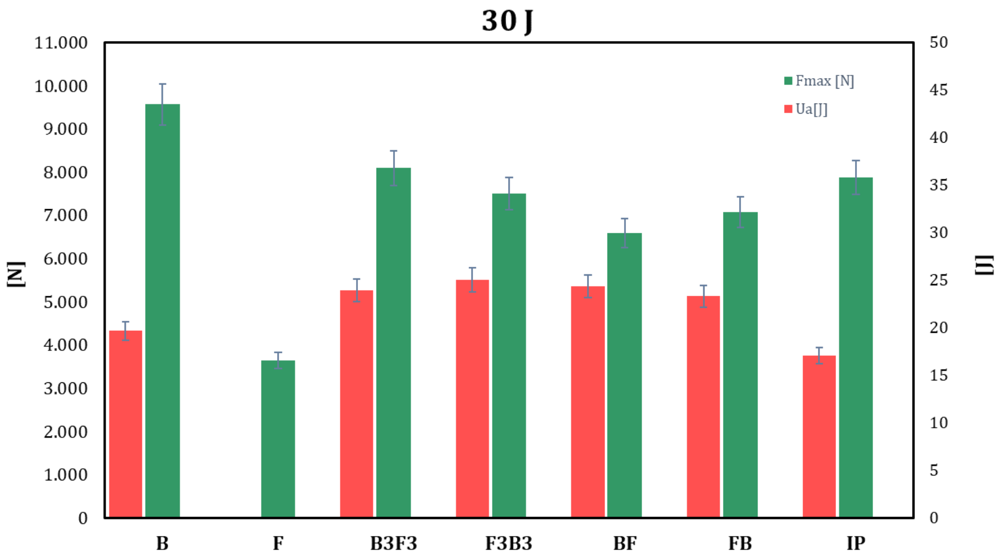
30 J
11.000
10.000
9.000
8.000
7.000
6.000
5.000
4.000
3.000
2.000
1.000
0
[N]
50
45
40
35
30
25
20
15
10
5
0
[J]
Fmax [N]
Ua[J]
B
F
B3F3
F3B3
BF
FB
IP

b)

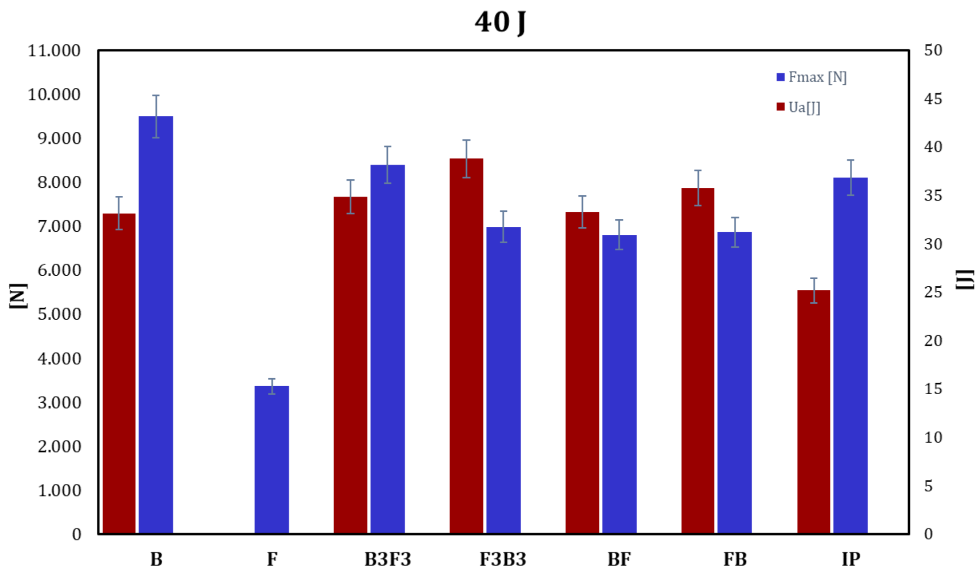


c)

**Figure 27** - Maximum load and Absorbed energy for each laminates at: a) 15J, b) 30J, c) 40J

With the increasing of the impact energy, the maximum force increases for all the configuration, it is interesting to see how passing by 30J to 40J the maximum load keeps on been constant meanwhile the adsorbed energy increases. It means that with the increasing of the energy levels, the basalt sample and all the hybrid configurations are able to adsorb higher amount of energy, damaging without reaching the catastrophic failure. This is probably due to the matrix because, as reported in literature, as the impact energy increases, the maximum load and the absorbed energy increase.

At 30J and 40J the intraply laminate and the laminate with the configuration characterised by basalt skins and the core of flax reinforcement show the best behaviour. In particular the intraply laminate is characterized by a good maximum load, the highest together with the B3F3 configuration, and a less adsorbed energy than the other hybrid configuration.

Table 9 summarizes the impact data at penetration, the maximum load, the maximum deformation and the energy at penetration, that is the energy in correspondence of which the force drop to zero and the samples result penetrated.

**Table 9** - Impact at penetration properties

| | PENETRATION | | |
|---|---|---|---|
| | **Fmax[kN]** | **Up[J]** | **dmax[mm]** |
| **B** | 10051,99 | 64,43 | 66,04 |
| **F** | 3638,05 | 24,97 | 29,67 |
| **B3F3** | 8993,89 | 61,73 | 66,65 |
| **F3B3** | 7485,11 | 46,49 | 71,56 |
| **BF** | 7034,44 | 57,59 | 67,99 |
| **FB** | 7387,14 | 55,60 | 68,93 |
| **IP** | 9693,89 | 63,78 | 58,91 |

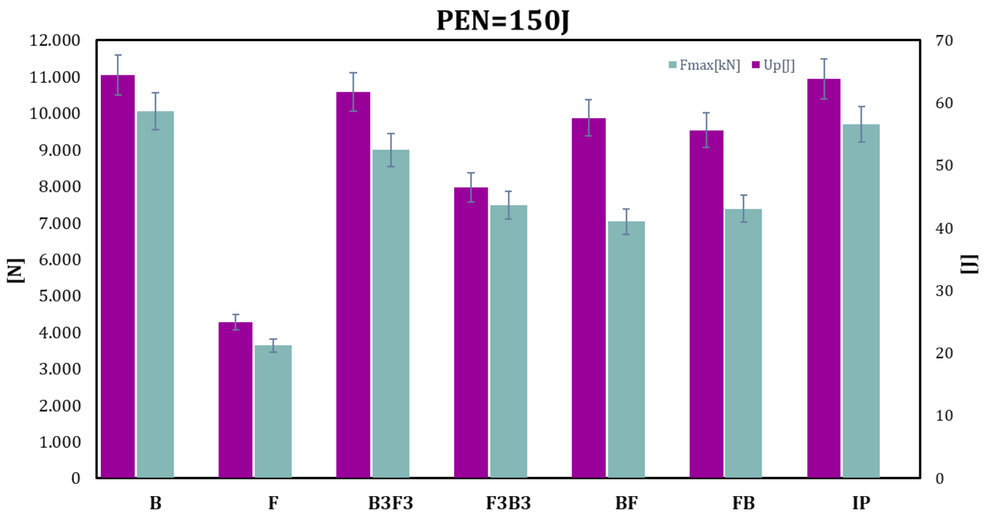


**Figure 28** - Maximum load and Absorbed energy for each laminates at penetration

Figure 28 compares the force and the energy at penetration for all the configurations. The intraply and the B3F3 laminates show a behaviour really close to the pure basalt laminate. This behaviour ensures an important reduction in term of weight and cost and it is surely characterized by different damage data that we will analyse in the next paragraph. The other laminates have a comparable penetration energy showing a lower impact resistance in terms of maximum load.

## 4. Damage Analysis

The strength of a laminate composite is strongly dependent on the interfacial load transfer capability, when laminated composites are exposed to dynamic or repeated loading, the interlaminar adhesive strength among plies tends to significantly deteriorate. After some time, the laminate reaches a point where it can no longer sustain the loading, causing separation of the plies. Studies have demonstrated that delamination is a considerably more complex phenomenon that involves brittle fiber fracture, progressive transverse matrix cracking, and debonding of the fiber-matrix interface. Impact behaviour of composite is strictly related both to the fibre matrix interfacial adhesion and to the properties of matrix and fibre. In Table 10, the indentation depth, I, and the damaged area, A, are listed in addition to impact energy, U, values. Indentation depth, the plastic deformation impressed on the surface of the material by the impactor during the loading phase at the contact point, was measured by an OLS5000 confocal microscope Olympus. The microscope was equipped with different magnifications (5-150 X), an x-y table and dedicated software. Electronic Speckle Pattern Interferometry, ESPI, to evaluate the influence of the stacking sequence on the delaminated area. ESPI technique was performed by means of 532nm laser source to illuminate the specimens. The object beam, scattered from the object and through the objective, arrives in the camera forming on the sensor's plane the speckle interferogram. Upon an external perturbation (mechanical or thermal), the specimen is deformed, i.e. the reflected wavefront is slightly changed, while the reference beam remains unperturbed. Thus, after the perturbation, the camera sensor records a new speckle pattern. The digital subtraction of the registered speckle patterns (deformed and non-deformed states) provides the correlation fringes that show the out of plane displacement of the specimen surface. Table 10 show the results of the damage analysis and Figure 29 highlights the correlation with the absorbed energy. During the impact test a certain amount of energy is absorbed by a material. This absorbed energy is a measure of a given material's toughness and acts as a tool to study the damage, matching it with the indentation analysis and the no-destructive techniques.  As we can see from table 10 he pure flax is perforated at 30J and the hybrid configuration made of three external layers of flax and 6 of basalt is perforated at 40J. For this reason they are not shown in the graphs. A multiplicative factor of 10 is applied to the absorbed energy in the graphs in order to make the correlation and comparison between the data easier.

**Table 10** - Damage Indentation I, damaged area A  and absorbed energy Ua

| | 15J | | | 30J | | | 40J | | |
|---|---|---|---|---|---|---|---|---|---|
| | **I [µm]** | **A [mm2]** | **Ua [J]** | **I [µm]** | **A [mm2]** | **Ua [J]** | **I [µm]** | **A [mm2]** | **Ua [J]** |
| **B** | 118,39 | 30,00 | 6,49 | 116,42 | 81,00 | 19,66 | 2409,94 | 145,00 | 33,15 |
| **F** | 1796,36 | 230,00 | 12,26 | | | | | | |
| **B3F3** | 443,092 | 47,00 | 8,25 | 851,33 | 60,00 | 23,89 | 2467,95 | 158,00 | 34,81 |
| **F3B3** | 155,31 | 60,00 | 6,78 | 3095,53 | 355,00 | 25,02 | | | 38,79 |
| **BF** | 349,89 | 90,00 | 8,10 | 1918,45 | 201,00 | 24,35 | 2506,83 | 469,00 | 33,29 |
| **FB** | 312,28 | 24,00 | 6,34 | 1440,82 | 250,00 | 23,31 | 3971,59 | 520,00 | 35,76 |
| **IP** | 355,73 | 9,00 | 6,88 | 588,54 | 34,00 | 17,07 | 941,73 | 58,00 | 25,17 |

From Figure 29 it is possible to observe a similar behaviour in terms of absorbed energy but a different failure modes occurring through the composites. At 15J all the laminates, except the flax one, shows a similar absorbed energy, the F3FB3 configuration has the indentation more similar to the basalt laminate, that is the lowest. The IP laminate shows the lower delamination area. With the increasing of the impact energy level the different failure mode becomes more evident. The hybrid F3B3 configuration F3B3 appears susceptible at damage at 30J and fails at 40J, on the contrary the B3F3 configuration shows the best performance among the hybrid configuration. This means that the configurations with a lower interfaces layers ensure a better behaviour under dynamic load. The BF and FB configurations show the same delaminated area but a different indentation at 40J, that's because the external basalt side  increases the surface stiffness of the structure and the plastic deformation is lower. The innovation of this study is the intraply configuration. With the increasing of the impact energy level the IP laminate maintains the lower values of indentation and the delaminated area. The hybrid woven fabric minimizes the issues related to the staking sequence and provides performance closer to the pure basalt.

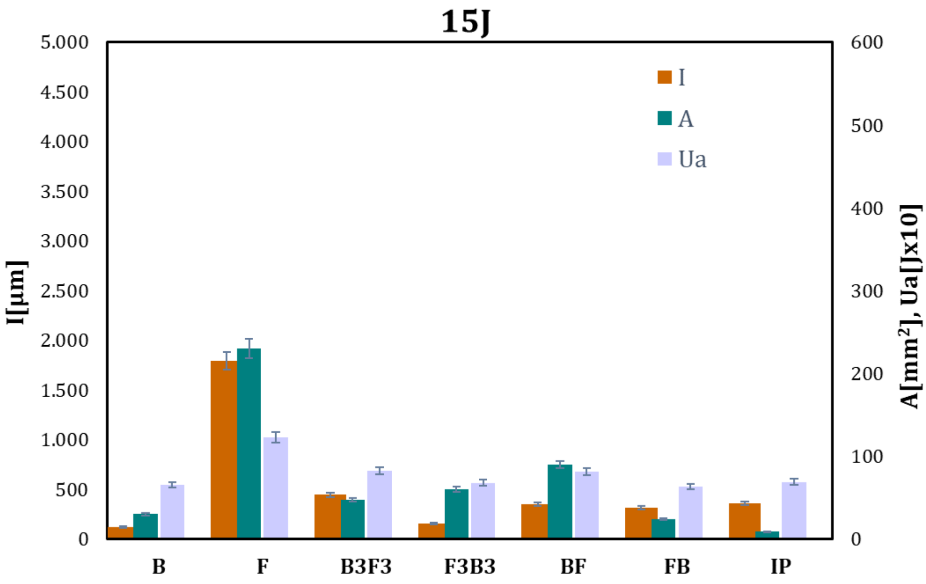


a)

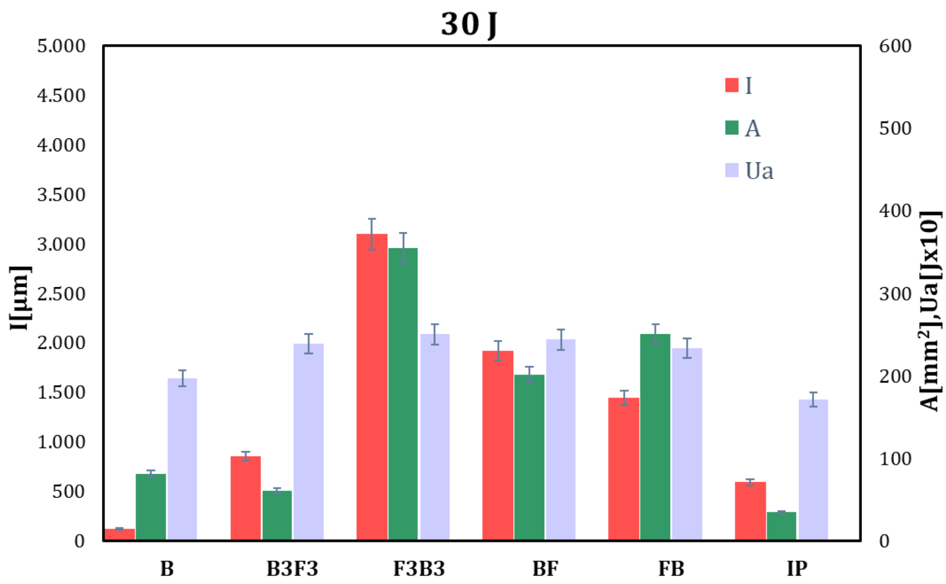


b)

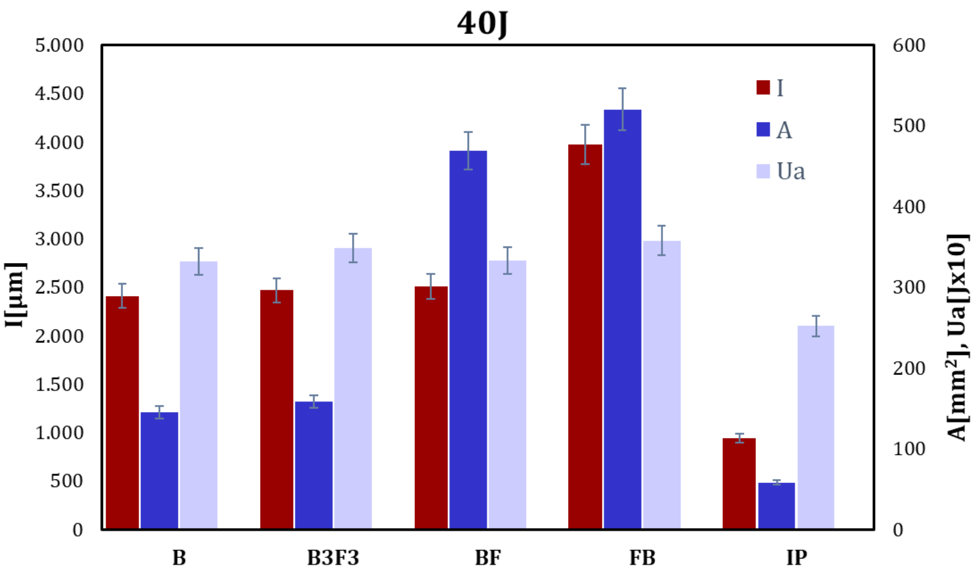


c)

**Figure 29** - Indentation depth, damaged area absorbed energy at: a) 15J, b) 30J, c) 40J

In Figure 30 are reported the pictures of all samples, in the upper row, and the correspondent ESPI analysis in the bottom row.

At visual inspection the damage aspect changes from pure materials to hybrids, among the latter, the ones which have flax on surface show greater indentation extension and circular apsect instead, the ones which have basalt on surface show concentrated damage with cross aspect. It can be deduce that hybrid samples having flax surface are able to absorb the energy without delamination, those with basalt surface are more rigid and the damage activates the delamination. Another peculiar behaviour is reported by intraply samples, after the lower energy impacts, 15J and 30J, the shape of the superficial damage is thin and oriented in one direction; after the 40J impact, the damage appears to became thicker by enlarging in the perpendicular direction.

As concerns the unwrapped phase-contrast ESPI maps of all impacted samples, focusing on the visual inspection of the laminates it can be noticed that the presence of more interfaces between layers including different fibres induces complex modes of failure and, hence, different kinds of damaged areas. The observations show a sign of the presence of subsurface damage invisible to the visual inspection. Looking at the specimens impacted at 15J, it is possible to recognize the shape of the impactor (red circle), a sign that the damage is concentrated below the point of contact. At higher impact energy levels it is possible to note a less defined area and blurred edges. It is possible to assume that, at this energy levels, in addition to the damage caused by the impactor, the gradual growth of the delaminated area is clearly visible.

We know that this don't match with the delaminated area data and the no-destructive analysis turns out to be indispensable.

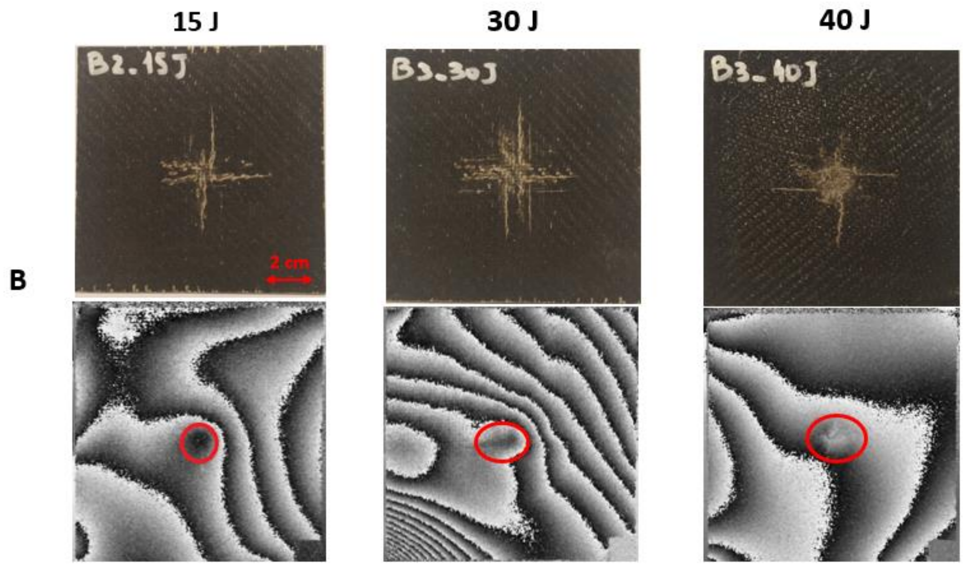


a)

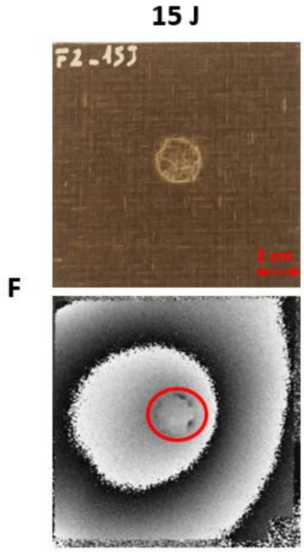


b)

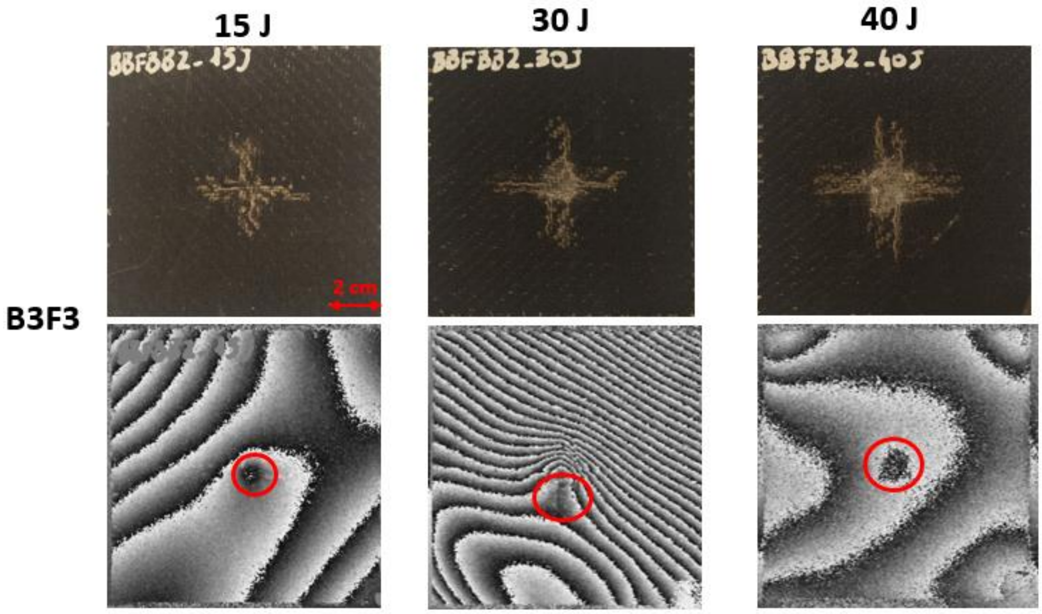


c)

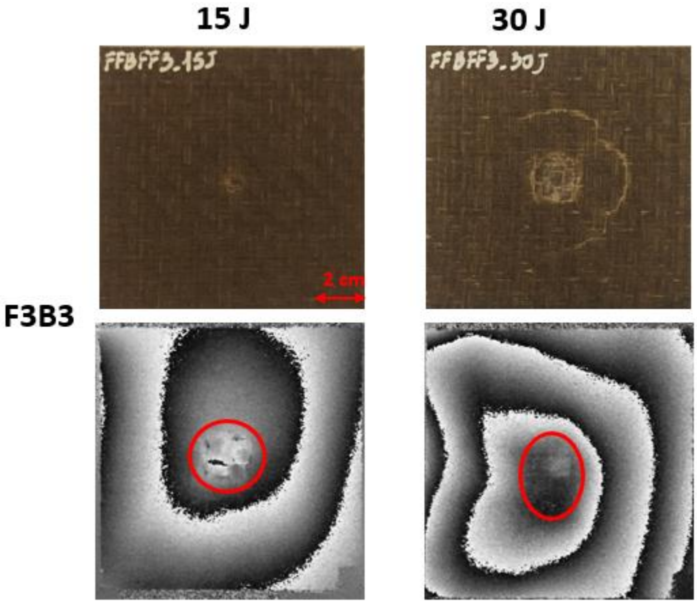
15 J
30 J
FFBFF3_15J
FFBFF3_30J
2 cm
F3B3

d)

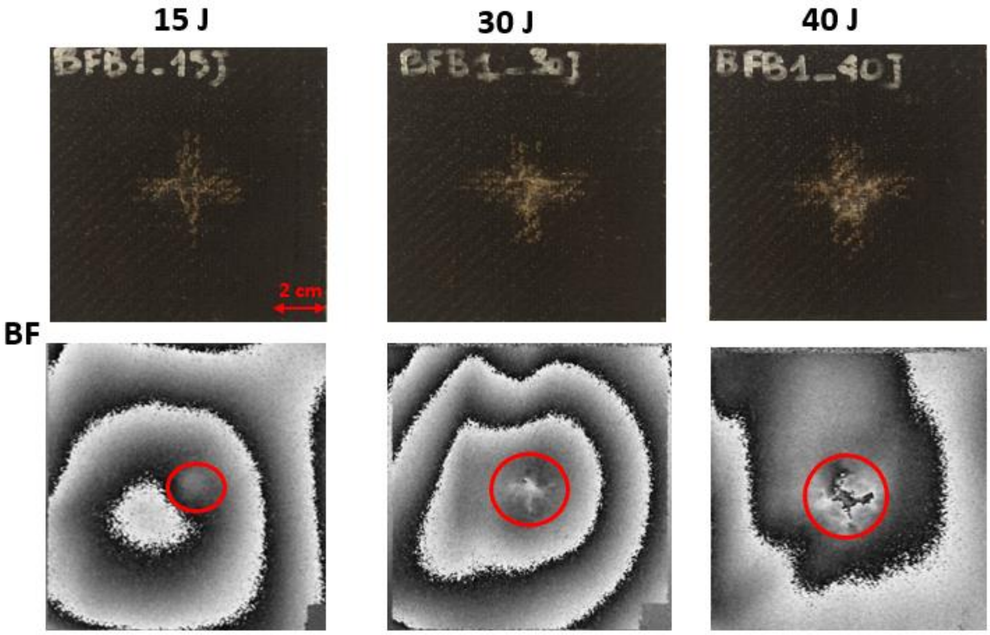
15 J
30 J
40 J
BFB1_15J
BFB1_30J
BFB1_40J
2 cm
BF

e)

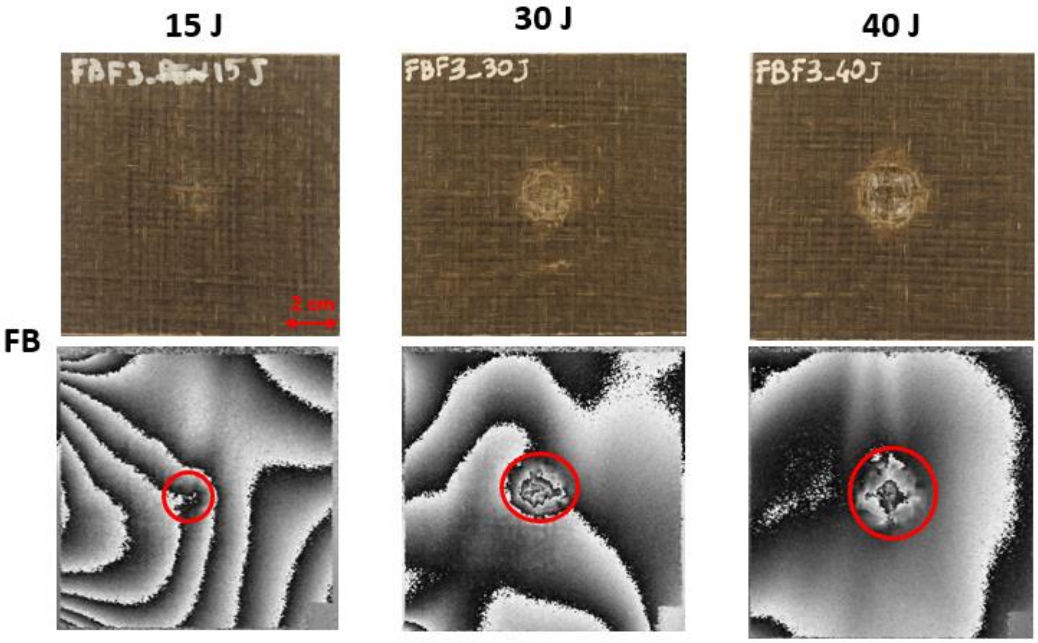


f)

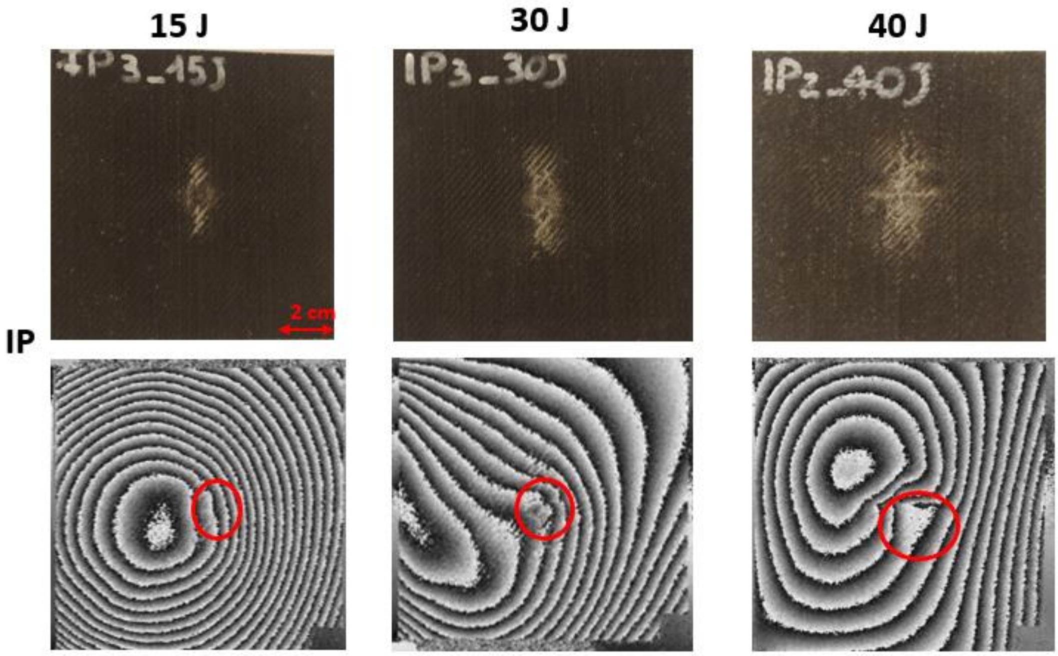


g)

**Figure 30** - ESPI and Visual inspection of the seven different laminates at three energy levels: a) Basalt, b) Flax, c) B3F3, d)F3B3, e) BF, f) FB, g) Intraply

# Section IV: Multi-hits: standard hybrid composites subjected to repeated low velocity impacts

## 1. Framework

Fibre-reinforced laminated composite materials are extensively used in several engineering fields such as naval industries, wind turbines, automotive, aerospace due to their in-plane properties. Thanks to the high stiffness and specific resistance, the high elastic modulus and the possibility of being customized for multiple applications, these materials offer undoubted advantages over more traditional structural ones. However, despite the many advantages, composite materials are highly susceptible to low-velocity impacts[80]. Their behaviour under impact is very worrying because these events induce internal damages undetectable with a simple visual inspection but capable of significantly reducing the strength characteristics of the material. Composite structures can be exposed to impact damage during both lifetime service, e.g bird strikes, hailstorms or lightning strikes, and common maintenance or manufacturing operations where they could be accidentally hit[81]. Small and insignificant defects generated by a single impact can easily extend to determine critical situations in the case of repeated collisions which, therefore, deserve particular attention.

Several studies regarding the effects of repeated impacts on the mechanical properties of composite structures can be found in the literature[5,27,82]. Among these studies, Liao et al.[83]investigated the mechanical response of carbon fibre reinforced laminates subjected to repeated low-velocity impacts at an energy of 15 J, and varying the diameter of the impactor. Moreover, a new damage index (DI-B), based on the reduction of bending stiffness and expressed by the ratio between the maximum displacement recorded during the repeated impact tests and the maximum displacement as the penetration happens, allowed to evaluate the bending stiffness reduction rate, to characterize the damage accumulation and to distinguish the occurrence of penetration simultaneously. Sugun and Rao[28] reported a numerical relationship between the impact energy and the impact numbers to failure in glass, carbon and Kevlar composites. Found et al.[84] conducted single and multiple impact tests on a CFRP laminate using a drop weight impactor. The impact test results at the energies of 0.54 J and 0.73 J show no significant changes in the peak force but only a small increase in contact duration.

In comparison, repeated impacts at 0.93 J show a significant drop in the peak force along with an increase in impact duration. Shah et al.[40] compared the performance of thermoplastic and thermoset 3D composites under recurrent low speed impacts at an energy of 50 J. Both composites show a reduction in peak force and an increase in contact duration as the number of impacts increased. Finally, Sadaghi et al.[85] investigated the response of Glare 5 and Glare 3, hybrid laminates containing composite and metal layers to repeated impacts due to a tool drop. They observed that due to Glare's high-energy absorption, the rebound impacts in the event of a tool fall do not further deform or propagate the damage created by the first impact.

Hosur et al.[41] performed an experimental investigation on the response of woven glass/epoxy laminates subjected to single and repeated low-speed impacts. The study shows the results of the damaged area, peak force and absorbed energy for samples subjected up to 40 repeated impacts at different energy levels from 10 to 50 J. Significant changes in the peak force were observed only at high energy levels, 40 and 50 J, where a sudden drop in peak force was found. Furthermore, the tests showed a growth of the damaged area with the number of impacts. Still, after a certain number of events, it does not increase significantly according to the energy.

In this regard, several approaches have been successfully exploited to enhance the impact damage resistance of composite laminates. A possible one is the development of composite laminates stacking different fibres layers in the same matrix[74].Hybridisation offers similar or better properties with respect to the primary constituents by taking advantage of the different properties of different stacked fibres, leading to a composite with more tailored behaviour[86]. In this regard, glass fibres are the best option from cost, availability and ease of processing. For example, Papa et al.[81,87] reported about hybrid composite samples with different carbon and glass fiber layers planned to observe the low temperature influence on their flexural and low velocity impact behaviour to improve the damage. Sevkat et al.[42] studied the multi-impacts effect on the responses of different hybrid composite laminates made by S2 glass fibre, and IM7 graphite fibre toughened epoxy varying the lay-up sequence. The results show a significant effect of the lay-up sequence on the repeated impact performance indeed, the hybrid glass/graphite/glass laminate withstood twice the number of impacts compared to the graphite/glass/graphite one. Ferrante et al.[43]focused on the influence of operating temperature, -40 °C, room temperature and 80 °C, and the number of repeated impacts on the damage response of polypropylene laminates reinforced with interplay flax/basalt hybrid fabric layers on the impact energy range 5-30J. Effects related to the presence of a coupling agent to enhance the fibre-matric interfacial adhesion were also considered, Briefly, the results showed that as the operating temperature decreases below the glass transition of the PP matrix, there is a significant reduction in the plasticity of the matrix and, regardless of interfacial adhesion, the composite laminates show a higher localization of the damage. Conversely, at high temperatures (80 ° C), a marked softening of the matrix and a greater extension of the damaged area in the composite laminates occur. Furthermore, the greater interfacial adhesion determines a greater sensitivity to repeated impacts with failures triggered by a smaller number of impacts in the case of compatibilized composite structures.

Ultimately, although this topic is the subject of several research already available in the literature, further investigations are deemed necessary, especially for hybrid systems since, as well known, the response of these materials depends, among others, on nature, architecture as well as mutual content and arrangement of the reinforcements included. This study investigated the damage response of hybrid composite laminates, reinforced with layers of carbon and glass woven into vinyl ester resin and subject to multiple impacts. To detect the damage initiation and evolution in composite laminates, several NDT methods are accessible as ultrasonic technique (US)[88,89], Electronic Speckle Pattern Interferometry (ESPI) technique[90,91], Pulsed Thermography (PT)[92,93], tomography[94] etc.

Nowadays, numerous authors have evaluated the different NDT abilities and their capability for process quality control and damage assessment in composite structures[95–97]. This work aims to gain further insights on the damage due to the dynamic behaviour of composite hybrid components. In particular, innovative composite structures multi low velocity impact response will be studied. The consequent damage will be identified and analysed using three different non-destructive techniques to suggest the most suitable and reliable, mainly through on-site inspection. The reference material was subject to drop tests performed up to 10 times with an impact energy of 5, 10 and 20 J, systematically recording key parameters such as maximum force, deflection, and absorbed energy and evaluating the damaged area's evolution with non-destructive techniques. Electronic speckle pattern interferometry, pulsed thermography and ultrasonic technique were used to detect damage shape and extension since the first impact event correlating it to impact parameters.

## 2. Materials and experimental setup

Hybrid composite laminates manufactured by vacuum bag infusion were examined in this work. Two kinds of reinforcement were utilized, carbon woven fabrics with fibre areal weight of 320 $\frac{g}{m^2}$ by Mike Composite and glass weaved fabrics with fibre areal weight of 300 $\frac{g}{m^2}$ by Castro Composites. The laminates were fabricated with a vinyl ester resin, Crystic VE 679PA, according to the RTM technique at IMDEA Materials Institute of Madrid, within the SMP financially supported by Office of Naval Research (ONR). The lay-up configurations of the panels were obtained by alternating two layers of glass to one of the carbon fibers $[GCG]_5$ (Figure 31) with a nominal thickness of t=3.5 ± 0.25 mm, and a fibre volume fraction of $V_f$=58%.

**CG**

**Figure 31** - Lay-up configurations

Low velocity impact tests were performed using an Instron/Ceast Drop Tower Impact System equipped with a digital acquisition system. The specimens (150mm x100mm x 3.5mm) cut from the original panels, were clamped between two metal fixtures, according to the ASTM D7137 standard, and centrally impacted by an impactor with a hemispherical nose 19.8 mm in diameter.

Three different non-destructive techniques systematically analysed the impacted specimens: Electronic Speckle Pattern Interferometry (ESPI), Pulsed Thermography (PT), and Ultrasounds (US).

ESPI is a well-known non-invasive optical technique that allows measuring the out-of-plane displacements of the specimen after a stress event to identify cracks, strain, and flaws without direct contact with the object through surface illumination by coherent light. The equipment needed to perform the ESPI tests was installed on a vibration isolation table to rule out environmental disturbances. The coherent beam generated from a laser source is split into a reference beam (RB) and an object beam (OB). The reference beam is guided via an optical fibre to reach a device (CCD camera), while mirrors guide the object beam to reach the object's surface under analysis where it is reflected the camera. Therefore, an electronic device (CCD camera) records a speckled image of the object's surface, resulting from the interference between the reference beam and the beam scattered from the object. Following the action of an external perturbation (i.e. thermal or mechanical), the specimen under analysis deforms, and the reflected wavefront is slightly modified, while the reference wavefront (i.e. RB) remains undisturbed. Thus, the camera’s sensor records a new speckle pattern, and the subtraction of the registered speckle patterns (deformed and non-deformed states) provides the correlation fringes. The technique is called Electronic Speckle Pattern Interferometry because this speckle pattern is recorded and electronically stored. The speckled fringes pattern results from the subtraction between the intensity of the calm and perturbed state, and it represents the out-of-plane surface displacement. Analytically the governing equations are given as follow:

$$\boldsymbol{I_1 = I_0 + I_r + 2\sqrt{I_0 I_r}\, cos(\theta)} \tag{1}$$

$$\boldsymbol{I_2 = I_0 + I_r + 2\sqrt{I_0 I_r}\, cos(\theta + \phi)} \tag{2}$$

$$\boldsymbol{I_{1-2} = 2\sqrt{I_0 I_r}[cos\,\theta - cos(\theta + \phi)]} \tag{3}$$

Where $I_0$, $I_1$ and $I_2$are the intensity scattered from the object, the intensity of the unperturbed state, and the intensity of perturbed speckle, respectively, $I_r$ is the intensity of the reference beam, $\boldsymbol{\theta}$ is the phase angle, and $\boldsymbol{\phi}$ is related to the displacement, i.e. the deformation. The maps, from correlation fringes, are digitally acquired and treated for contrast enhancement and noise removal, allowing obtaining the phase contrast, which is possible, by means an external bespoke software, to measure the displacement field with high accuracy.

Further analysis of the damage evolution on and inside the specimens was performed by means of  PT. These measurements were aimed to detect the presence of the defects within the composite specimens investigated. Two halogen lamps with tuneable power were used as heat sources to apply a thermal pulse of 10 s on the front surface of the specimens. The thermal response achieved during and after heating was recorded with a frame rate of 5 Hz using the infrared camera FLIR X6580sc with a cooled indium antimonide (InSb) detector (FPA 640 × 512 pixels and NETD ~ 20 mK at 25 °C) mounting a 50 mm focal lens with spectral band 3.5–5 μm and IFOV 0.3 mrad. The software ResearchIR (FLIR Systems), was used for monitoring the temperature in real-time and for basic operations. A Matlab code (R2019b, Math-Works) was used to calculate thermal recovery images analysing the movie recording. The emissivity considered for all composite specimens was 0.94. The measurements were done in the laboratory with 25 °C of ambient temperature and 55 % of relative humidity.

Finally, ultrasound (US) measurements were carried out by means of Multi2000 Pocket 16x64 system by M2M: the inspection was performed with a Linear phased array Probe, 5 MHz, 64 Elements[98]. The system works in the form of reflection: the probe is used for the emission and the reception of the ultrasonic waves, and the pulse Echo technique was adopted during the acquisition.

The depth of a reflective structure is inferred from the delay between pulse transmission and echo reception[99]. In this way, using a whole sample, the correct thickness plate is obtained, and the acquisition system is calibrated. The ultrasound analysis has been carried out only on the impact side to prevent the reflections and attenuation signals problems correlated to the contact technique used. Finally, the propagation velocity, equal to 3000 $\frac{mm}{s}$, is registered.

The specimens were subjected to ultrasonic analysis before and after the impact to evaluate possible damage due to the fabrication process. By appropriately setting the Gate (threshold of the signal detection), a relatively clear picture of the area characterised by delamination in the thickness (B-scan) and in the plane (C-scan) was obtained. Using the Echo Max (abs) procedure as detection mode, the Gate recorded only the peak that overcomes it. Depending on the height of the overrun Gate (and therefore the amplitude of the signal) a different colour was evidenced on the recorded image. The latter is analysed by a cad software to measure the damage detected.

# 3. Results and discussion

## 3.1. Damage characterization

Figure 32 shows the damage progression of the composite specimens after impact events (single, five and ten repeated impacts) for the three different energy levels U=5 J, 10 J and 20 J.

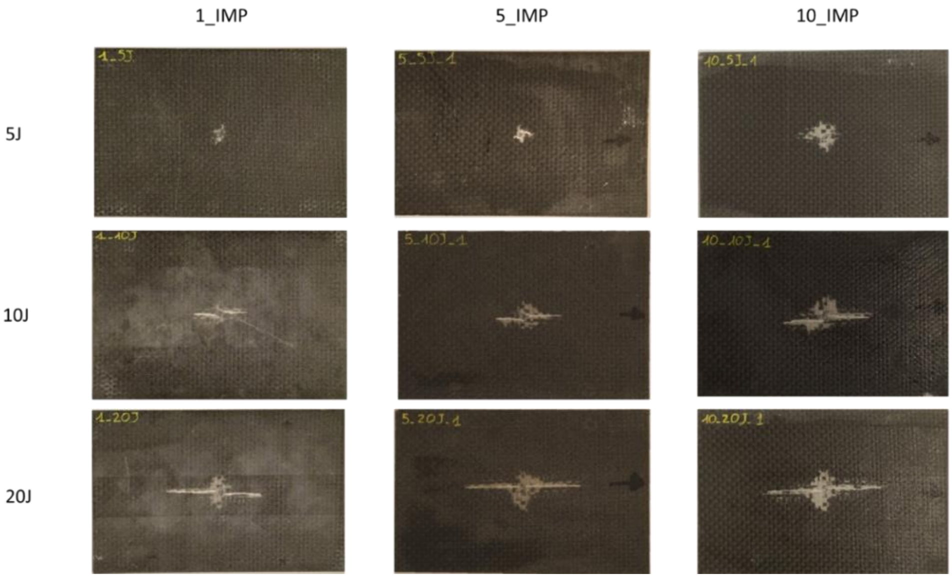


**Figure 32** - The appearance of the specimens subjected at single impact (first column), five repeated impacts (second column) and ten repeated impacts (third column) for impacted energy of U = 5 J (first row), 10 J (second row) and 20 J (third row).

From a first visual inspection (VI), it is evident that the damages increase continuously with the increase of the impact energy and for each impact condition. In the case of impact 5 J, first row of Figure 32, the damage is confined below the contact point of the impactor, but it extends slightly as the number of repeated collisions increases. For impacts at 10 J and 20 J (second and third row of Figure 32), instead, the damage, evident already after the first impact, extends more along the sample's longitudinal direction. As expected, also in this case the size of the damaged area increases with the increase in the number of impacts. However, this growth is less noticeable as energy increases. Finally, it should be noted that no perforation of the specimens occurred for all impact events.

Figure 33 shows the damages detected with the ESPI technique on a representative specimen after an impact event. Thanks to the ESPI, it is possible to clearly distinguish the different damage mechanisms induced on the impacted specimen by observing the variation in the grey scale. The presence of superficial or sub-superficial damages is highlighted by white areas (e.g longitudinal cracking), while the damage that extends deeper (e.g delamination) appears black.

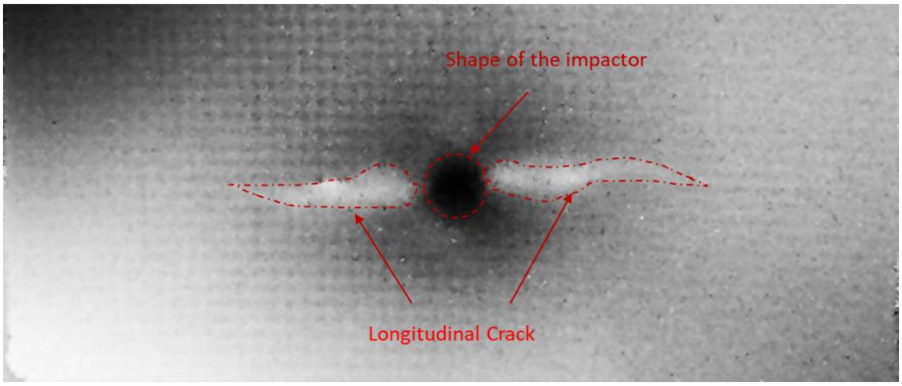


**Figure 33** - Damage mechanism detected by ESPI technique on a representative specimen

.

Figure 34 shows the unwrapped phase-contrast ESPI maps of all impacted samples. These observations, in line with the visual inspections, show that in reality, the damaged area is more extensive than what has already been found, as a sign of the presence of subsurface damage. Looking at the specimens impacted at 5 J, it is possible to recognize the shape of the impactor (black areas), a sign that the damage is concentrated below the point of contact. Only in the case of ten-repeated impacts it is possible to note a light presence of a longitudinal crack. Therefore, it is possible to assume that, at this energy level, indentation and delamination are the prevailing failure modes. For all other cases, in addition to the damage caused by the impactor (black areas), the gradual growth of the longitudinal crack (white areas) is clearly visible.

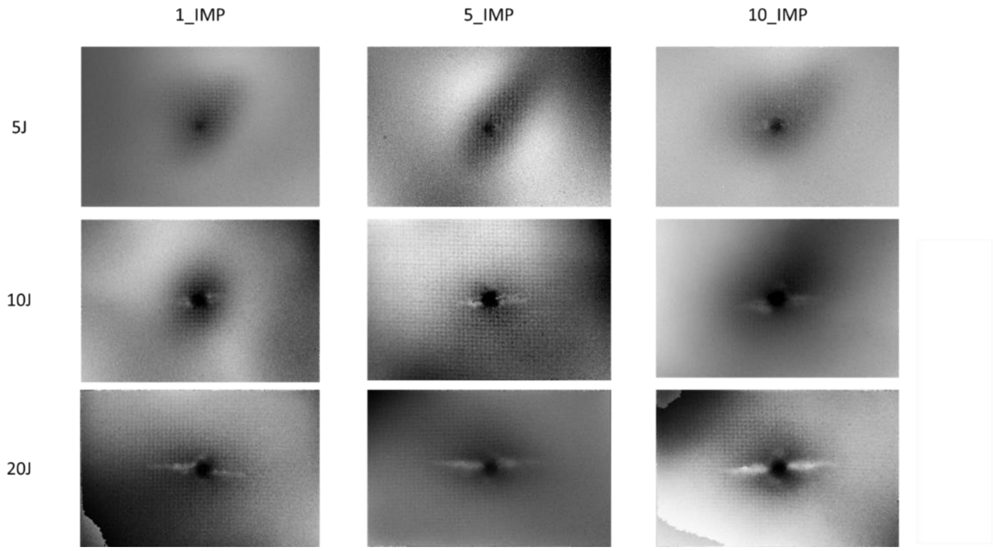


**Figure 34** - The unwrapped phase-contrast maps of the specimens after a single impact (first column), five repeated impacts (second column) and ten repeated impacts (third column) for impacted energy of U = 5 J (first row), 10 J (second row) and 20 J (third row)

.

Figure 35 shows the thermal recovery images calculated from the movies achieved by PT measurements. In particular, the different grey tones in the images represent the time (TRt) that each pixel spent to recover 50% of the induced thermal gap. As visible, in all experimental situations investigated, the presence of defective areas is characterized by low TRt (black areas). This is due to the lower value of the specific heat that characterizes the damaged areas where impacts have removed the cover material. As in the case of the ESPI analysis, delamination damages are clearly visible in the case of U=5 J, while both delamination and longitudinal cracks are well visible at U=10 J and U= 20 J. Qualitatively, as expected, the extensions of the damages are greater for higher impact numbers and it affects deeper layers of the samples as the impact energy increases.

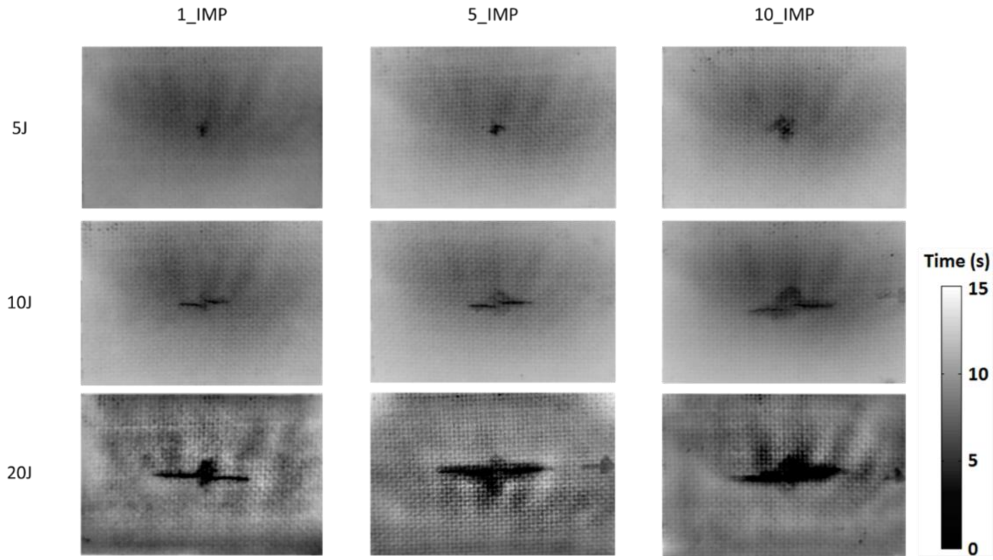


**Figure 35** - Thermal recovery images calculated by PT analysis for specimens subjected to a single impact (first column), five impacts (second column) and ten impacts (third column) for impacted energy of U = 5 J (first row), 10 J (second row) and 20 J (third row)

.

It should be noted that the black area in the images represents the convolution of the damages induced on the various layers of the sample, both superficial and sub-superficial.

Ultrasonic C-scanning provides an in plain view of the damage in specimens after impact. By properly setting the Gate (threshold of the signal detection), a fairly clear picture of the area characterized by delamination was obtained. Then, the US device provides the correct sizing of the defect. Once the Gate is set, only the peak that overcomes will be recorded on the implementation of the scan. Depending on the height of the overrun Gate (and therefore on the signal's amplitude), a different colour is evidenced on the C-scan. It could indicate a higher sample homogeneity or several damage types. The more the signal is not attenuated, the more red the image. On the contrary, when the signal is attenuated and, therefore, in the presence of discontinuity of the material (defect or non-homogeneity), the signal tends to be blue and becomes black if it is completely attenuated.

Ultrasonic C-scan images of all tested specimens are given in Figure 36. For every impact energy, the damaged area increases gradually as the number of the impacts. As the impact energy increases, the damaged area increases and the shape of the damage changes. The acquisitions on samples impacted at U=5 J show a circular damaged area. At the tenth impact, the area extends on the length of the sample, and it tends to a diamond pattern. For higher energy levels, the shape of the projected damaged area is a diamond already from the first impact.

Moreover, from Figure 36 it is possible to highlight that the impact energy influences the evolution damage. For the 20 J energy, the damaged area is already of considerable importance at the first impact: further impacts to this energy do not determine significant increases in the extension of the delamination. This trend changes at 5 J and 10 J energy levels, and the damaged area have a regular steady increase. It is possible to observe an interesting change in the impact behaviour between 10 J and 20 J energy levels.

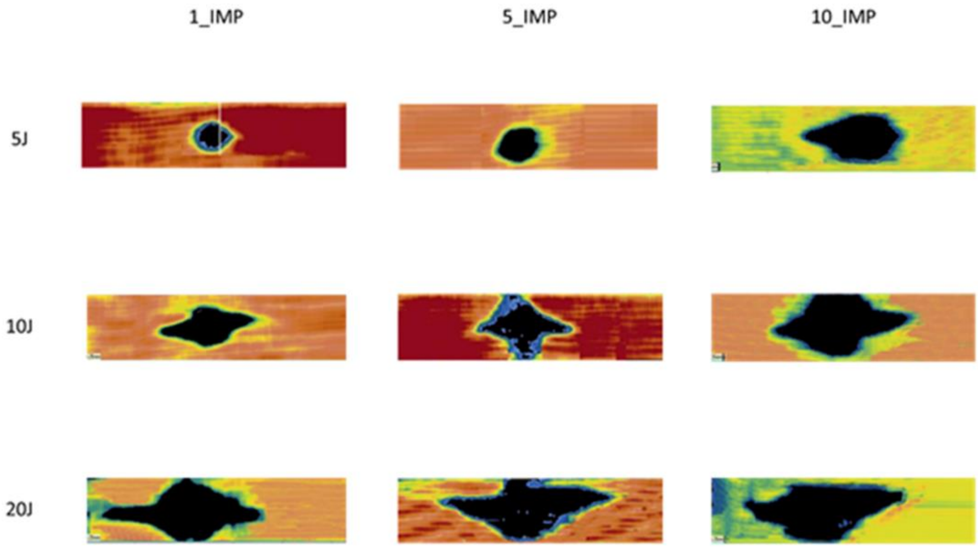


**Figure 36** - Ultrasonic C-Scan image of the specimens after single impact (first column), five repeated impacts (second column) and ten repeated impacts (third column) for impacted energy of U = 5 J (first row), 10 J (second row) and 20 J (third row)

.

The extent of damaged areas, registered by the different NDT techniques under repeated impacts for the three energy levels, are summarized in Table 11.

Of course, to obtain reliable results from the US, it was essential to set the system precisely to consider the signal absorption coefficient depending on the fibre and matrix type, fibre orientation, thickness and composite stacking sequence. Both ESPI and PT techniques, being a full-field imaging technique, didn't require additional measurements even if, in the case of the ESPI, to obtain information about the impact damage through the thickness of the laminates, it was used to analyse both the front side and the back side of the plates. The damaged areas recorded by US appear to be higher than those evaluated by both the ESPI and PT techniques. This result can be explained taking into account the characteristics of the investigated laminates or rather their low deformability that makes it difficult the damage detection by these last two methods, especially on the edge of the impacted area. The cross-ply composites are characterised not only by fibre breaking but also by matrix cracking on the impacted surface that is more complicated to be identified by both PT and ESPI technique, while the US technique can identify the visible impact damage such as matrix cracking and subsurface delamination. The measurements with the three different techniques are better highlighted in Figure 37 and Figure 38.

Figure 37 shows the bar graphs of damaged areas versus the impact number. It is evident that the damage caused by low velocity impacts is well detected by all the non-destructive investigation techniques considered. Still, the use of ultrasound seems to be more sensitive to capture the response of the impacted material at 20 J.

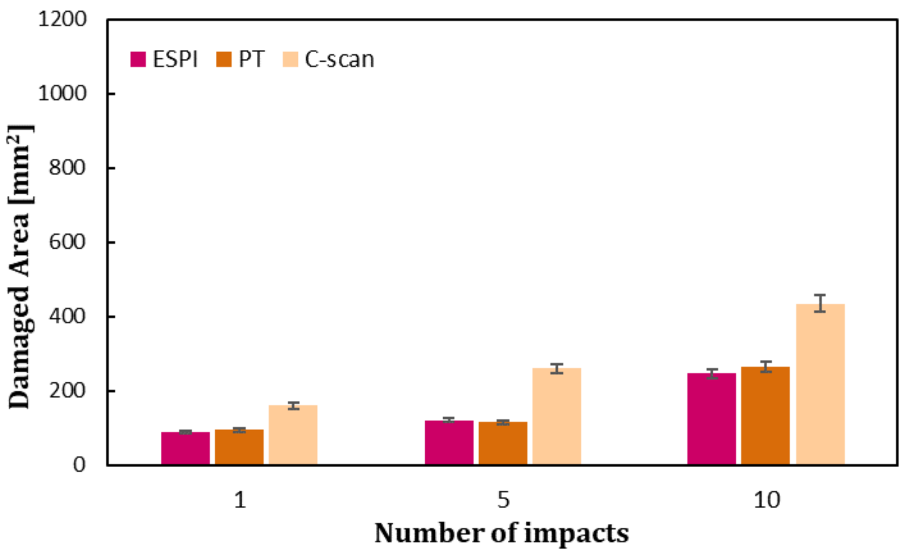


a)

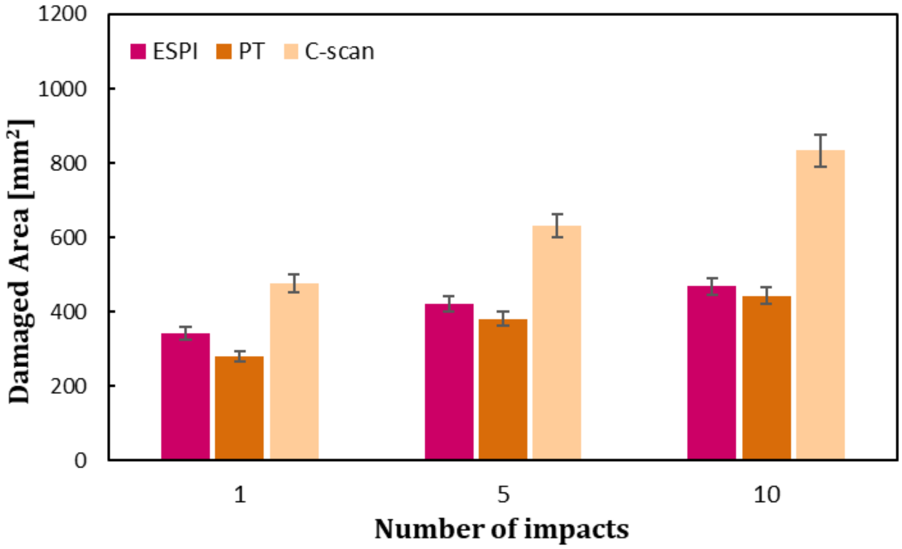


b)

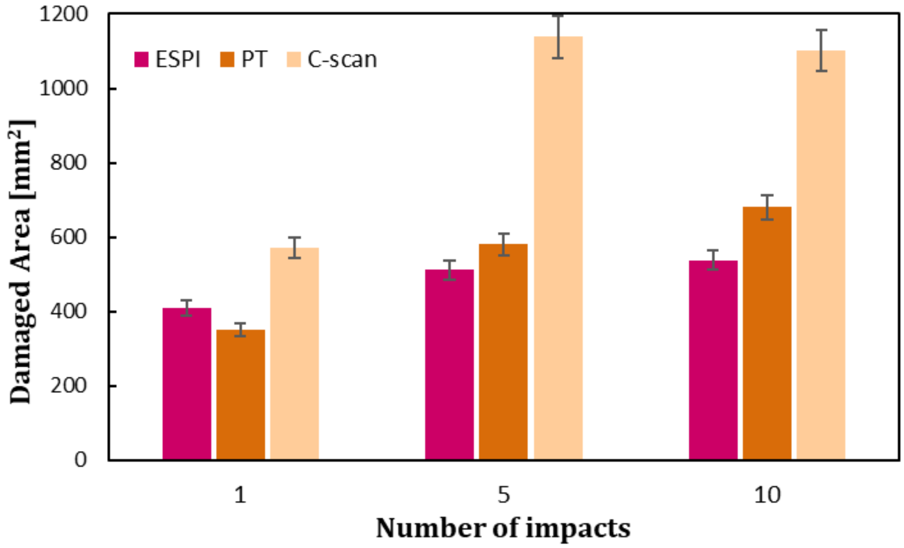


c)

**Figure 37** - The damaged area registered by different techniques as a function of the number of impacts at (a)5 J, (b)10 J and (c)20 J

Figure 38 shows the damaged area as a function of the impact energy for the samples that have undergone 1, 5 and 10 collisions as detected with the three non-destructive techniques. The graphs evidence how the ultrasound analysis detects a larger damaged area at any impact for high energy level as numerically reported in Table 11.

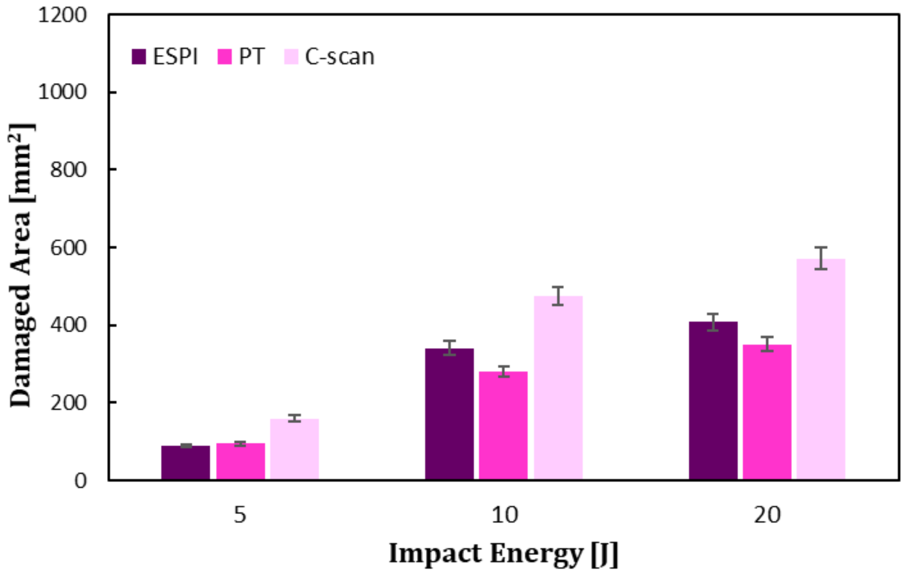


a)

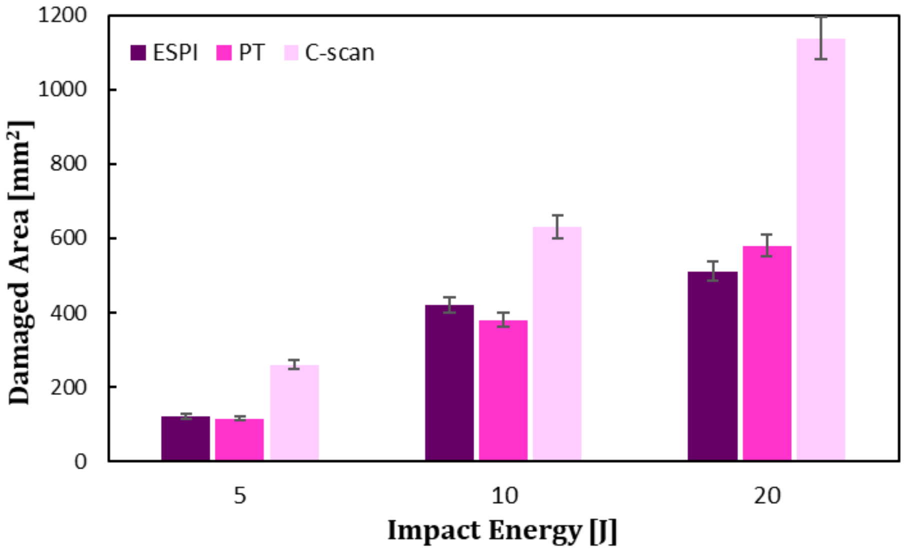


b)

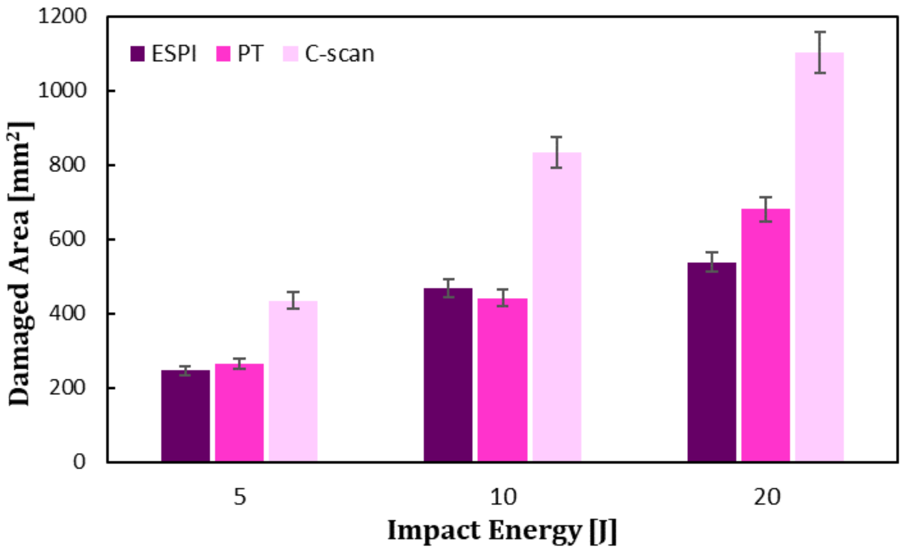


c)

**Figure 38** - The damaged area registered by different techniques as a function of the impact energy at (a) first impact, (b)fifth repeated impact and (c)tenth repeated impact

**Table 11** - Damaged areas measured by non-destructive techniques

| **Energy** | **N° Impact** | **Area [mm²]** | | |
|---|---|---|---|---|
| | | ESPI | PT | C-scan |
| 5 J | 1 | 89,01±5 | 95,00±4 | 159,91±10 |
| | 5 | 121,10±10 | 115,00±8 | 259,60±8 |
| | 10 | 246,75±10 | 265,00±7 | 434,77±5 |
| 10 J | 1 | 341,33±12 | 280,00±10 | 476,10±10 |
| | 5 | 419,70±7 | 380,00±10 | 630,74±10 |
| | 10 | 467,65±6 | 442,00±8 | 832,99±10 |
| 20 J | 1 | 408,20±5 | 351,00±10 | 571,44±10 |
| | 5 | 511,67±5 | 580,00±6 | 1138,73±15 |
| | 10 | 538,01±6 | 680,00±4 | 1102,44±42 |

However, in the case of impact tests performed at 5 J and 10 J, and in particular for single impact and five impact events, it is possible to note the good agreement between the different techniques. This evidence confirms that the damage is limited to the layers below the impacted side of the specimens under these test conditions. Conversely, in the case of 20 J impact events, the area detected by the C-scan differs significantly from the other two techniques. This is due to the extent of the damage, which extends deeper in the case of high-impact energy.

In this regard, for impacts at 20 J, the C Scan inspection seems to detect an unexpected trend in the extension of the damaged area as the number of impacts increases. However, this effect is not reliable since the relative mean value of the damaged area at 5 impacts has a smaller standard deviation than the mean value of the same parameter detected at 10 impacts. Therefore, it can reasonably be assumed that the extension of the damaged area detected by ultrasonic analysis is almost constant for impacts subsequent to the fifth. By the way, it is also known that repeated impact may induces a compaction and relaxation of each single delaminated sheet. Therefore, small variations in the damaged area could also be attributed to variations in the original configuration following subsequent impacts.

To understand the extent to which the damage has spread in-depth, B-scan and microscopic analyses have been carried out on the cross-sections of the central points of the laminates. B-Scan ultrasonic analysis displays a cross-section of the sample perpendicular to the scanning surface and parallels to a reference direction. In Figure 39, the cross-sectional view of the specimens after a single impact, five repeated impacts and ten repeated impacts at U= 10 J are shown. In all the sections analysed the damage extends within about 1 mm in depth. This is because the damaged area starts just below the impact surface and, increasing the number of impacts, it becomes larger. The images show how, for impacts at 10 J, passing from 1 to 5 and then to 10 repeated impacts, the distance between the blue signals on the pink band, which represents the amplitude of the delamination, increases.

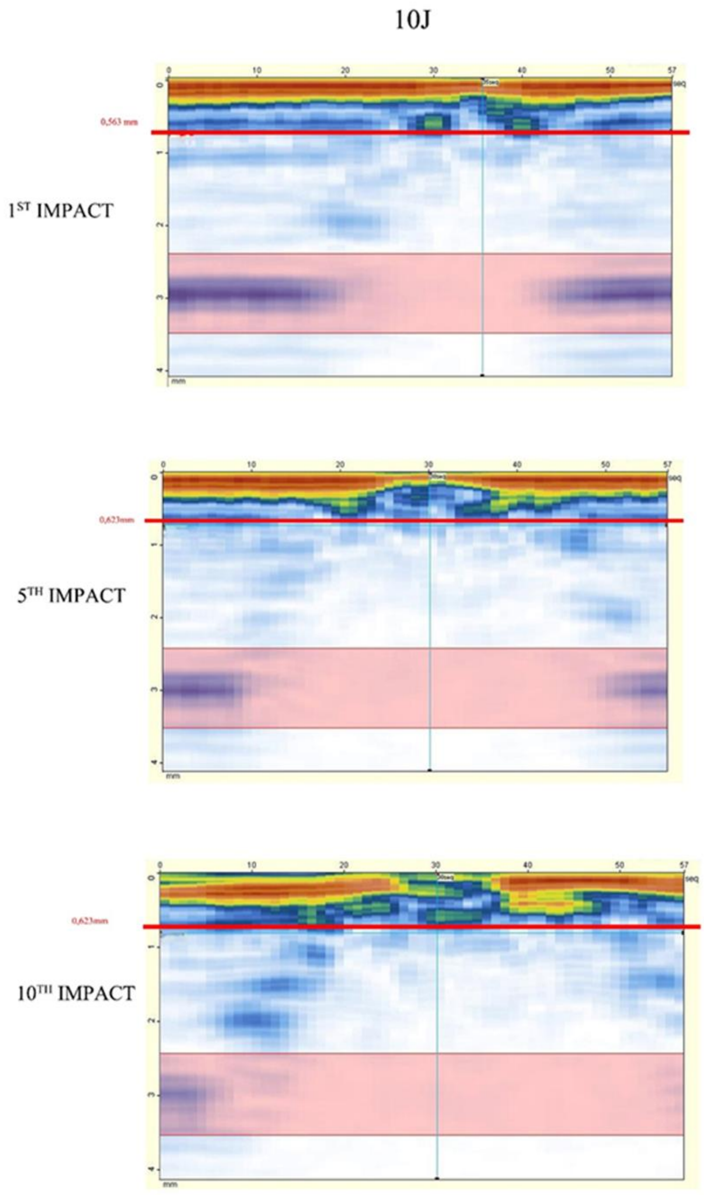


**Figure 39** - Ultrasonic B-Scan image of the specimens after single impact, five repeated impacts and ten repeated impacts for impacted energy of U = 10 J

.

Figure 40 shows the confocal microscope acquisition of the cross-sectional slice along the short side of the specimens impacted after one (a) and five (b) repeated impact tests at 10 J, right at the location under the zone directly struck by the impactor. Although the impact energy was relatively low, it caused damage under the impacted region already visible at the first impact. The first impact caused delamination of the first interface between carbon and glass layers and several matrix cracks visible in the bottom-most plies (Figure 40a). After five repeated impacts, the damage proceeded to extend downward, drawing a sort of pyramid (Figure 40b). The delamination affects almost the entire specimen section at the interface zone between different materials. From Figure 41b, it is evident how the repeated impacts induce the propagation and the growth of the delamination, causing the separation of the carbon and glass plies.

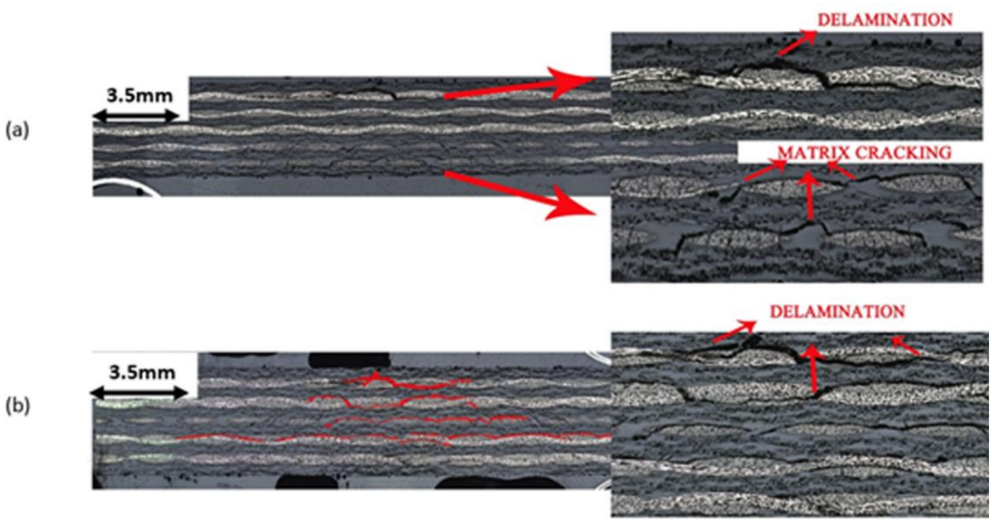


**Figure 40** - Confocal acquisition of the cross-section after one (a) and five (b) repeated impacts for the 10 J impact energy level

.

### *3.2. Impact force*

The variation of the impact force under repeated impacts is shown in Figure 41. The peak force supported by the composite specimens increases after the first impact until reaching a maximum for the 5th impact and then stabilizes at values almost constant. Several works regarding this behaviour are available in the literature[42,83,100]. The studies conducted by Wyrick and Adams [101] on a carbon/epoxy laminate suggest the first explanation of this phenomenon. They attributed the initial increase in peak force to the thin layer of unreinforced matrix on the impacted surface. This compaction effect occurs at low energy levels, so damage to the fibres near the contact surface is minimal, thus providing a more rigid surface for the subsequent impact. A second explanation for the phenomenon was proposed by Liu[102]. He conducted a series of impact tests on glass/epoxy laminates and observed that although the delamination occurs very early in an impact event, for energies up to 70 J indentation and local matrix cracking were the principal damages modes up to reach the maximum in the peak force. Thus, the maximum of the peak force is affected by the change in the dominant damage mode.

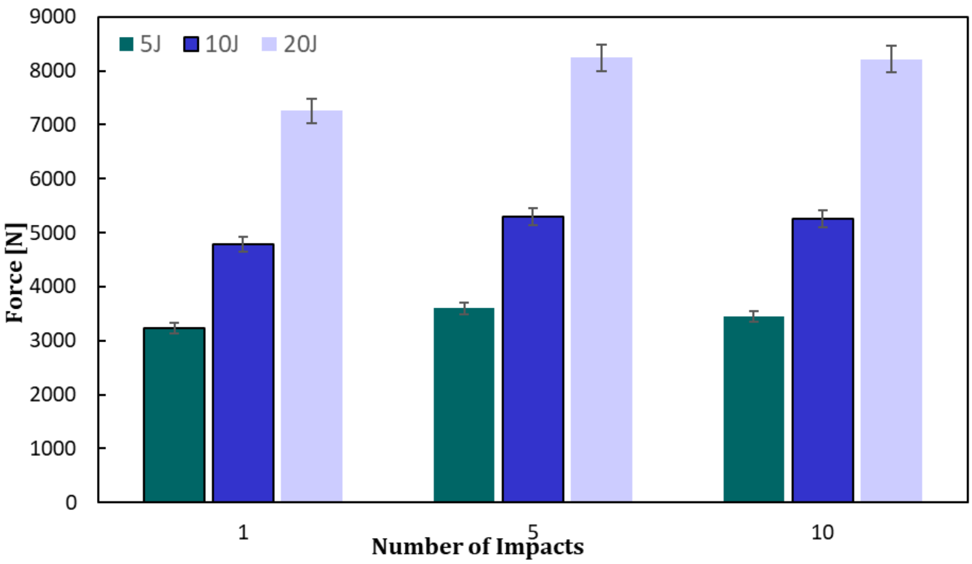


**Figure 41** - Variation of impact force versus repeat number of impacts subjected to impact energies of 5 J, 10 J and 20 J

.

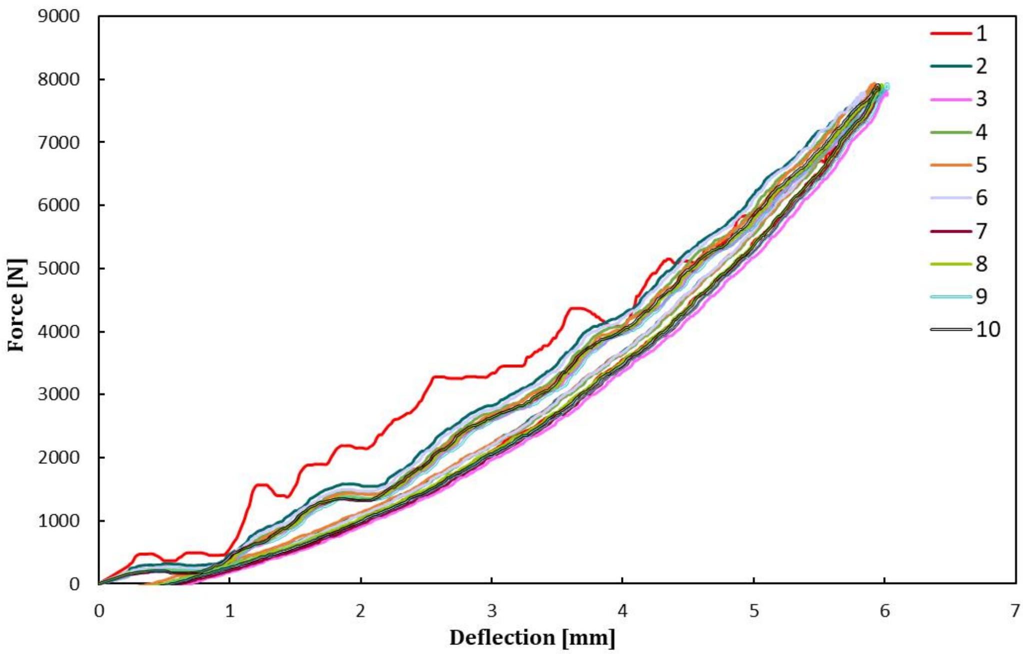


**Figure 42** - Force-displacement curves for all impact tests at 20 J

The force curves versus the displacement recorded in all the impact tests at 20 J are shown in Figure 42. Only the curves at the highest energy are reported because these considerations are more evident as the impact energy increases. Still, the following comment can also be applied to the other cases. The first impact causes the greatest force fluctuations to occur. It is represented by a force-deflection loop curve that extends over a larger area than similar loop curves representative of subsequent impacts. This result is due to the generation of the first cracks in the matrix accompanied by the beginning of the fracture of the reinforcing fibers with more pronounced effects following the initial impact. The closed-form of each curve became thinner and higher with the number of impacts, without showing significant reductions in stiffness (initial slope) but indicating a progressive decrease in the absorbed energy as the number of impacts increased.

Figure 43 shows the impact force histories of the hybrid composite for the one, the second, the fifth and the tenth repeated impacts.

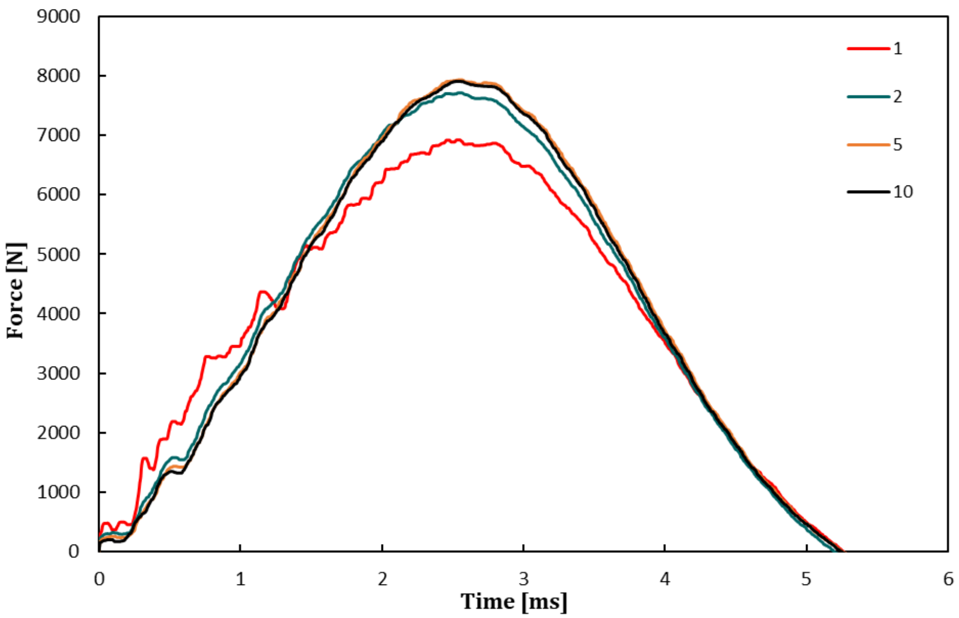


**Figure 43** - The impact force histories for all impact tests at 20 J

Also in this case, focusing the attention on the tests performed at 20 J for which the effects are more pronounced, it is clear that the peak impact force increases from the first subsequent impacts. Furthermore, in line with the previous considerations, the characteristic curve of the first impact appears more jagged than those of subsequent impacts, which occur smoother due to initial matrix cracking and the fibers fracture dissipative phenomena.

### *3.3. Absorbed energy*

During the low-velocity impact tests, the energy absorbed by the laminate was quite little, and the impactor rebounded without causing any perforation. Therefore, the absorbed energy detected is the energy absorbed by the laminate as a consequence of the formation of internal damage in terms of delamination, matrix cracking, and fiber breakage.

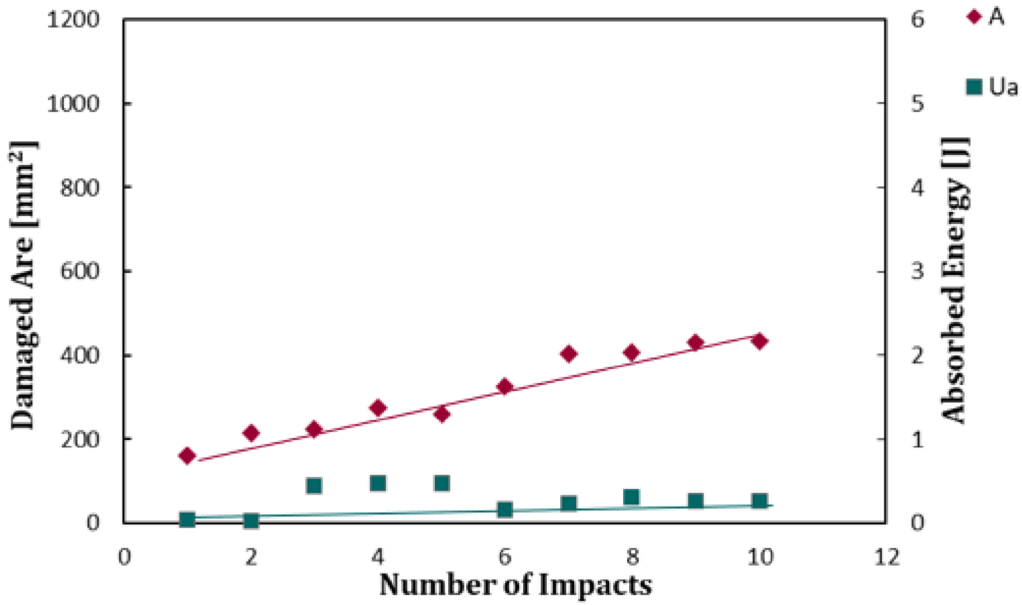
Damaged Are [mm$^2$]
Absorbed Energy [J]
Number of Impacts
A
Ua
0
200
400
600
800
1000
1200
0
1
2
3
4
5
6
0
2
4
6
8
10
12

a)

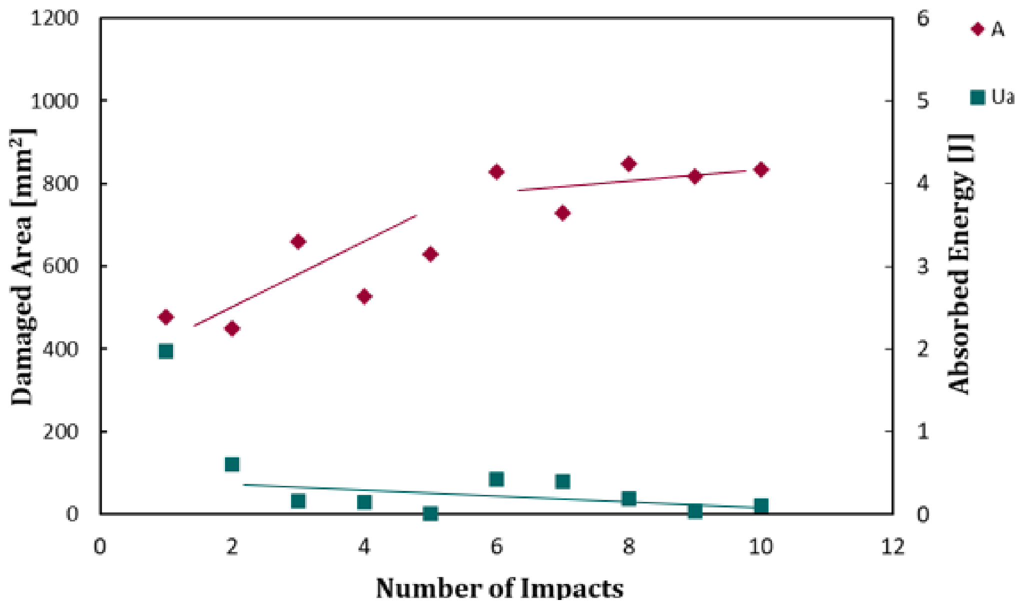
Damaged Area [mm$^2$]
Absorbed Energy [J]
Number of Impacts
A
Ua
0
200
400
600
800
1000
1200
0
1
2
3
4
5
6
0
2
4
6
8
10
12

b)

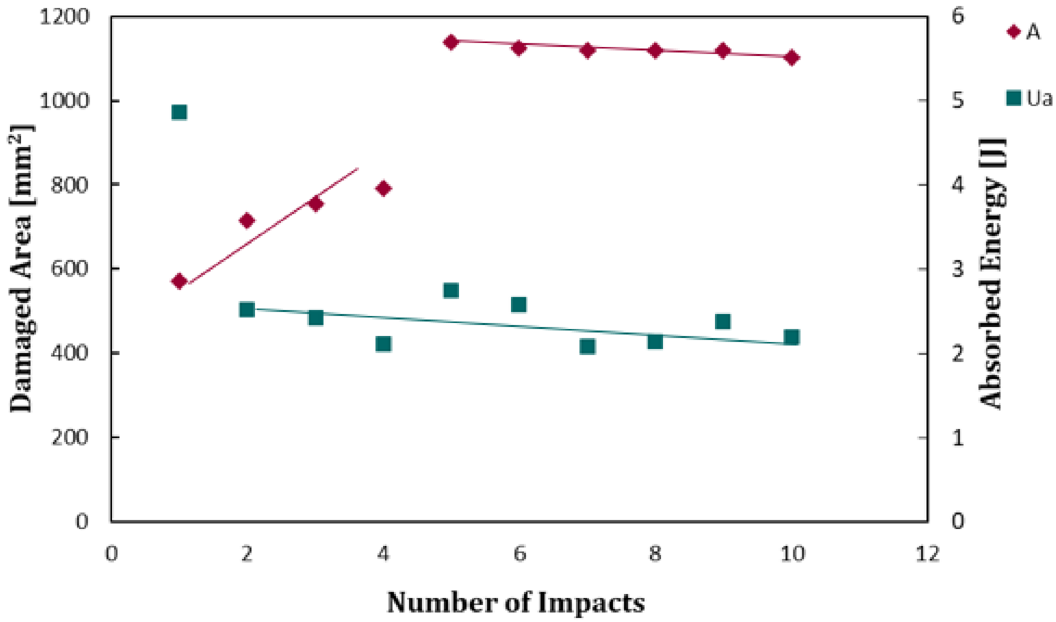


c)

**Figure 44** - Damaged area (A) and absorbed energy (Ua) vs the number of impacts for impacted energy of U = 5 J (a), 10 J (b) and 20 J (c)

.

Figure 44 shows the damaged area (detected by the C-scan) and the absorbed energy as functions of the number of impacts for all impact energy levels studied.

At 5 J the damaged area seems to grow monotonously with the number of impacts from 159 mm$^2$ to 434 mm$^2$. At the same time, the absorbed energy always appears relatively low and, net of standard deviations, almost constant around 0.3 J.

On the other hand, by applying higher impact energies, it is always clear that the initially growing damaged area reaches a plateau value after a certain number of impacts. In contrast, the absorbed energy, particularly high at the first impact, is reduced suddenly for subsequent impacts, reaching values approximately equal to 0.2 J after only two impacts at 10 J and settling around 2.5 J from the second impact onwards for events occurring at 20 J.

This behaviour can be explained by assuming that for collisions made below a certain energy threshold the damaged area extends slowly and will probably tend to a plateau not visible in the impact number range considered and in any case such as not to cause a catastrophic failure of the material.

For higher impact energy levels and especially at 20 J, however, the accumulation of absorbed energy is not likely to be reflected in the extension of the damaged area, detectable with the C-scan technique, but induce dissipative phenomena such as to generate a prevalently volumetric propagation of the damage up to the failure of the material.

# Section V: Summary of results

The first study has had two objectives. First of all, we investigated the high and low speed impact performance of hybrid composite configurations made of glass/carbon and basalt fibres.

It is so exciting to compare the ballistic limit of the hybrid composites at different temperatures ($T_{room}$ and $T_{low}$) and also their low velocity impact behaviour in terms of maximum load and penetration energy needs to penetrate the material. By comparing the experimental ballistic limits at different temperatures has been observed that the temperatures at which usually navy ship is exposed in the Arctic ocean do not affect the ballistic limit of the composite material under attention. However, the residual velocity of the projectile is lower for the BC samples for both temperatures tested, denoting a higher resistance of the material configuration used. By the results obtained in this work is possible to conclude that when the impact velocity is near to the ballistic limit, each laminate tested shows a very large delamination area.

As regards the low velocity impact behaviour, comparing the maximum load and the penetration energy detected at both room and low temperatures, the BC sample shows a better performance. Interestingly, BC laminates don't reach the complete penetration showing the same behaviour in both cases, and it was not possible to penetrate the panels.

In general, the proposed hybridization seems to be an excellent alternative to laminates made up of only single elements (basalt, fibre or glass) offering a new composite material to be used in Navy industry for its lightness, recyclability, efficiency and strength to the high and low speed impact at different temperatures and costs more moderate than the existing materials. We can say that the basalt fibres are an eco-friendly solution to provide excellent high and low impact properties at low costs. The cost of the used S2-glass woven fabric is $11\frac{e}{m^2}$ and one of the used carbon woven fabric is $40\frac{e}{m^2}$ higher than the costs of basalt woven fabric that are a little bit lower than glass depending on the specific fibre. All the hybrids configurations tested are very interesting because, at fixed dimensions and thickness, they are lighter than the homogeneous materials.

The investigation of different biocomposite configurations could be extremely summarized by stating that basalt contributes to highly improve the stiffness whereas flax increases the renewable content. The configuration with high flax content should be avoided because, after impact tests, it was perforated at 30J which is much lower than 150J that is the energy used for the other laminates.

By considering the maximum load and the adsorbed energy, the laminates reinforced with basalt have the best performance, the laminates reinforced with the flax have the worst performance, in the middle are all the hybrid laminates which prove the importance to use both fibers to obtain a compromise situation between cost, performance and recyclability.

Since the strength of a laminate composite is strongly dependent on the interfacial load transfer capability, lower number of interfaces layers ensure a better behavior under dynamic load. So the hybrid configuration F3B3 fails at 40J, instead B3F3 configuration shows the best performance among the hybrids. The stiffness of the basalt reinforcement contributes to increase the laminate surface resistance and to reduce the indentation, as a matter of fact, for the configuration BF and FB the delaminated areas are the same but the indentation is lower in the first one.

Important mention has to be done for intraply reinforcement, it has outstanding resistance under dynamic loads, very close to the basalt performance; this is also due to its fabric woven structure.

ESPI and visual inspection could help to deepen the investigation procedure, but the typical laminated structure and the damages that have to be analyzed make the ultrasonic inspection mandatory.

In the fourth section, glass/carbon hybrid composite laminates were subjected to repeated low velocity impacts at three different energy levels 5, 10 and 20 J. Mechanical responses to multiple impacts were recorded in terms of impact force, deflection, energy absorbed during the tests. In addition, a thorough analysis on the evolution of damage was conducted by combining both non-destructive and optical microscopy inspections.

The examined results highlighted the start of the damage and illustrated its evolution with the impact repetition. An interesting difference was found in the impact behaviour and the damage development among the first and the subsequent impacts. Under the same impact energy, the first collision initiates a sort of compaction of the first layers of material at the point of application of the impulse load as evidenced by the increasing value of the maximum contact force in subsequent impacts and is responsible for more pronounced dissipative phenomena of fracture of the matrix and of the reinforcing fibers. However, as the impacts proceed, the damage does not seem to worsen (almost zero energy absorbed) unless a certain impact energy threshold is exceeded, beyond which the detection of a significant, constant and non-zero absorbed energy is recorded. The extent of this parameter can be attributed to a propagation of the effects in the volume of the material rather than in the enlargement of the area evaluated with the inspection techniques adopted.

All the non-destructive inspections used the result to be able to detect the start of the damage and highlight in different ways its evolution. More specifically, the results showed that the damaged area grows less and less with the repetition of the events. Below a certain threshold of the impact energy, the damaged area expands slowly and does not cause catastrophic failure of the material.

For the highest impact energy level explored so far (20 J), the accumulation of absorbed energy is not reflected in an expansion of the damaged area, visible with the C-scan technique, but generates dissipative phenomena such as to produce a volumetric increase of the damaged area to the point of causing failure of the material.

# Section VI: Conclusion and Future developments

The present work was focused on the optimization of hybrid composite structures for applications under dynamic loading conditions.

The study of the impact behaviour of hybrid composites made of standard material like carbon, glass and basalt suggested that the hybridization improves the impact response. Basalt fiber could be a potential replacement for glass fibers and other synthetic fibers in a wide range of applications thanks its cost effective and eco-friendly nature.

As second goal bio-composites with high renewable contents were successfully produced from natural fibers and biobased thermosets. Hybrid composites with varying fibre ply with different combination of flax fiber has been studied. In particular, this combination reduces the stiffness and brittleness of basalt, demonstrated by a plastic behaviour after yielding, confirmed also from the results of falling weight impact testing, which provides greater flexibility to the material. Conversely, hybridization considerably increases impact performance of flax fibre composites with a non-excessive increase in weight. The results evidenced the role of fibre hybridization with natural fibres on the performance of a composite material.

A new hybrid composite using an intraply flax-basalt woven fabric has been tested. This material shows a notable behaviour at impact, in particular it is characterized by a good damage resistance.

Finally, the repeated low-velocity impact responses of hybrid composite panels were studied by drop-weight tests to study the capability of energy absorption in a more realistic test. The results showed that the damaged area grows less and less with the repetition of the events.

These considerations suggest that hybridization is able to offer a flexible behaviour,a large number of configurations in different dynamic condition test will must be investigate for the purpose to offer performance tailored on the requirement of the specific application and context of use selected.

This research leads to useful results, in terms of bio-based composites application and development. Also the testing methodology allows to obtain a satisfying assessment of these materials in the perspective of aerospace components integration. However, after this PhD research, the following future developments are suggested:

- To implement a numerical model to forecast the impact behavior of composite materials with specific stacking sequence.
- To improve the interaction between different plies of natural fibers, by using other manufacturing technologies (f.i. autoclave), with the aim to produce high-performance laminate.
- To study new combinations resins-hardeners to increase the quantity of biobased material in each composite.
- To enhance the design of new intraply fiber reinforcement, in order to obtain new opportunities for sustainability and mechanical performance.
- To study the integration of intraply and biobased fibers in the perspective of environmental impact reduction.
- To apply this testing methodology, comprehending low-velocity and high-velocity impacts to all the specimens that have to be used in the aerospace sector.

# References


[1] Campbell, F. C., 2010, “Structural Composite Materials,” Struct. Compos. Mater.

[2] Rajak, D. K., Pagar, D. D., Menezes, P. L., and Linul, E., 2019, “Fiber-Reinforced Polymer Composites: Manufacturing, Properties, and Applications,” Polymers (Basel)., **11**(10).

[3] Grand View Research, 2021, *Composites Market Size, Share & Trends Analysis Report By Product (Carbon, Glass), By Manufacturing Process (Layup, Filament, RTM), By End Use, By Region, And Segment Forecasts, 2021 - 2028*.

[4] Grand View Research, 2018, *Natural Fiber Composites (NFC) Market Size, Share & Trends Analysis Report By Raw Material, By Matrix, By Technology, By Application, And Segment Forecasts, 2018 - 2024*.

[5] Atas, C., and Dogan, A., 2015, “An Experimental Investigation on the Repeated Impact Response of Glass/Epoxy Composites Subjected to Thermal Ageing,” Compos. Part B Eng., **75**, pp. 127–134.

[6] Taylor, R., 2008, *Fibre Composite Aircraft: Capability and Safety*.

[7] Petrucci, R., Santulli, C., Puglia, D., Sarasini, F., Torre, L., and Kenny, J. M., 2013, “Mechanical Characterisation of Hybrid Composite Laminates Based on Basalt Fibres in Combination with Flax, Hemp and Glass Fibres Manufactured by Vacuum Infusion,” Mater. Des., **49**, pp. 728–735.

[8] Papa, I., Boccarusso, L., Langella, A., and Lopresto, V., 2020, “Carbon/Glass Hybrid Composite Laminates in Vinylester Resin: Bending and Low Velocity Impact Tests,” Compos. Struct., **232**, p. 111571.

[9] Ahmad, F., Choi, H. S., and Park, M. K., 2015, “A Review: Natural Fiber Composites Selection in View of Mechanical, Light Weight, and Economic Properties,” Macromol. Mater. Eng., **300**(1), pp. 10–24.

[10] Brebu, M., 2020, “Environmental Degradation of Plastic Composites with Natural Fillers—A Review,” Polymers (Basel)., **12**(1), p. 166.

[11] Lotfi, A., Li, H., Dao, D. V., and Prusty, G., 2021, “Natural Fiber–Reinforced Composites: A Review on Material, Manufacturing, and

Machinability," J. Thermoplast. Compos. Mater., **34**(2), pp. 238–284.

[12] Hapuarachchi, T. D., Ren, G., Fan, M., Hogg, P. J., and Peijs, T., 2007, "Fire Retardancy of Natural Fibre Reinforced Sheet Moulding Compound," Appl. Compos. Mater., **14**(4), pp. 251–264.

[13] Koronis, G., Silva, A., and Fontul, M., 2013, "Erratum: Green Composites: A Review of Adequate Materials for Automotive Applications (Composites Part B: Engineering (2013) 44 120-127) (Composites Part B: Engineering (2013) 47 391))," Compos. Part B Eng., **49**, p. 93.

[14] Sathishkumar, T. P., Naveen, J., and Satheeshkumar, S., 2014, "Hybrid Fiber Reinforced Polymer Composites - A Review," J. Reinf. Plast. Compos., **33**(5), pp. 454–471.

[15] Ashik, K. P., and Sharma, R. S., 2015, "A Review on Mechanical Properties of Natural Fiber Reinforced Hybrid Polymer Composites," J. Miner. Mater. Charact. Eng., **03**(05), pp. 420–426.

[16] Findlay, S. J., and Harrison, N. D., 2002, "Why Aircraft Fail," Mater. Today, **5**(11), pp. 18–25.

[17] Safri, S. N. A., Sultan, M. T. H., Yidris, N., and Mustapha, F., 2014, "Low Velocity and High Velocity Impact Test on Composite Materials – A Review," Int. J. Eng. Sci., **3**(9), pp. 50–60.

[18] Naik, N. K., and Shrirao, P., 2004, "Composite Structures under Ballistic Impact," Compos. Struct., **66**(1–4), pp. 579–590.

[19] Pandya, K. S., Pothnis, J. R., Ravikumar, G., and Naik, N. K., 2013, "Ballistic Impact Behavior of Hybrid Composites," Mater. Des., **44**, pp. 128–135.

[20] Delavari, K., and Safavi, A., 2022, "The Effect of Stacking Sequence on High-Velocity Impact Resistance of Hybrid Woven Reinforced Composites: Experimental Study and Numerical Simulation," Fibers Polym., **23**(1), pp. 184–195.

[21] Kazemi, M. E., Shanmugam, L., Dadashi, A., Shakouri, M., Lu, D., Du, Z., Hu, Y., Wang, J., Zhang, W., Yang, L., and Yang, J., 2021, "Investigating the Roles of Fiber, Resin, and Stacking Sequence on the Low-Velocity Impact Response of Novel Hybrid Thermoplastic Composites," Compos. Part B Eng., **207**(December 2020).

[22] Chamis, C. C., 1989, "Mechanics of Composite Materials: Past, Present, and Future," J. Compos. Technol. Res., **11**(1), pp. 3–14.

[23] Sánchez Gálvez, V., Gálvez, F., Cendón, D., Sancho, R., and González, C., 2020, "Effect of Temperature and Moisture on the High-Velocity Impact Performance of Glass/Carbon Hybrid Composites," ECCM 2018 - 18th Eur. Conf. Compos. Mater., (June), pp. 24–28.

[24] Meola, C., Boccardi, S., Boffa, N. D., Palma, M. D. I., Maio, L., and Carlomagno, G. M., 2014, "Impact Damaging of Carbon Fibre-Reinforced Composites : A Comparison between Infrared Thermography and Ultrasonics," Proc. 11th Eur. Conf. Non-Destructive Test., (Ecndt), pp. 1–10.

[25] Randjbaran, E., Zahari, R., Abdul Jalil, N. A., and Abang Abdul Majid, D. L., 2014, "Hybrid Composite Laminates Reinforced with Kevlar/Carbon/Glass Woven Fabrics for Ballistic Impact Testing," Sci. World J., **2014**.

[26] Summerscales, J., and Short, D., 1978, "Carbon Fibre and Glass Fibre Hybrid Reinforced Plastics," Composites, **9**(3).

[27] Icten, B. M., 2009, "Repeated Impact Behavior of Glass/Epoxy Laminates," Polym. Compos., **30**(11), pp. 1562–1569.

[28] Sugun, B. S., and Rao, R. M. V. G. K., 2016, "Low-Velocity Impact Characterization of Glass, Carbon and Kevlar Composites Using Repeated Drop Tests:," http://dx.doi.org/10.1177/0731684404039798, **23**(15), pp. 1583–1599.

[29] Swolfs, Y., Gorbatikh, L., and Verpoest, I., 2014, "Fibre Hybridisation in Polymer Composites: A Review," Compos. Part A Appl. Sci. Manuf., **67**, pp. 181–200.

[30] 1991, "Impact Properties of Sisal-Glass Hybrid Laminates," Composites, **22**(5), p. 408.

[31] Santulli, C., Janssen, M., and Jeronimidis, G., 2005, "Partial Replacement of E-Glass Fibers with Flax Fibers in Composites and Effect on Falling Weight Impact Performance," J. Mater. Sci., **40**(13), pp. 3581–3585.

[32] Almeida, J. H. S., Amico, S. C., Botelho, E. C., and Amado, F. D. R., 2013, "Hybridization Effect on the Mechanical Properties of Curaua/Glass Fiber Composites," Compos. Part B Eng., **55**, pp. 492–497.

[33] Uma Devi, L., Bhagawan, S. S., and Thomas, S., 2010, "Dynamic Mechanical Analysis of Pineapple Leaf/Glass Hybrid Fiber Reinforced

Polyester Composites," Polym. Compos., **31**(6).

[34] De Rosa, I. M., Santulli, C., Sarasini, F., and Valente, M., 2009, "Effect of Loading-Unloading Cycles on Impact-Damaged Jute/Glass Hybrid Laminates," Polym. Compos., **30**(12).

[35] Sunt, C. T., and Potti, S. V, 1996, "Velocities of Thick Composite Laminates Subjected To High Velocity Impact," Int. J. Impact Eng., **18**(3), pp. 339–353.

[36] Kretsis, G., 1987, "A Review of the Tensile, Compressive, Flexural and Shear Properties of Hybrid Fibre-Reinforced Plastics," Composites, **18**(1).

[37] Özben, T., 2016, "Impact Behavior of Hybrid Composite Plates Dependent on Curing and Different Stacking Sequences," Mater. Test., **58**(5), pp. 442–447.

[38] Sarasini, F., Tirillò, J., D'Altilia, S., Valente, T., Santulli, C., Touchard, F., Chocinski-Arnault, L., Mellier, D., Lampani, L., and Gaudenzi, P., 2016, "Damage Tolerance of Carbon/Flax Hybrid Composites Subjected to Low Velocity Impact," Compos. Part B Eng., **91**, pp. 144–153.

[39] Mansor, M. R., Sapuan, S. M., Zainudin, E. S., Nuraini, A. A., and Hambali, A., 2013, "Hybrid Natural and Glass Fibers Reinforced Polymer Composites Material Selection Using Analytical Hierarchy Process for Automotive Brake Lever Design," Mater. Des., **51**, pp. 484–492.

[40] Shah, S. Z. H., Megat-Yusoff, P. S. M., Karuppanan, S., Choudhry, R. S., Ahmad, F., Sajid, Z., Gerard, P., and Sharp, K., 2021, "Performance Comparison of Resin-Infused Thermoplastic and Thermoset 3D Fabric Composites under Impact Loading," Int. J. Mech. Sci., **189**, p. 105984.

[41] Hosur, M. V., Karim, M. R., and Jeelani, S., 2003, "Experimental Investigations on the Response of Stitched/Unstitched Woven S2-Glass/SC15 Epoxy Composites under Single and Repeated Low Velocity Impact Loading," Compos. Struct., **61**(1–2), pp. 89–102.

[42] Sevkat, E., Liaw, B., Delale, F., and Raju, B. B., 2010, "Effect of Repeated Impacts on the Response of Plain-Woven Hybrid Composites," Compos. Part B Eng., **41**(5), pp. 403–413.

[43] Ferrante, L., Sergi, C., Tirillò, J., … P. R.-P., and 2021, undefined,

2021, “Temperature Effect on the Single and Repeated Impact Responses of Intraply Flax/Basalt Hybrid Polypropylene Composites,” Wiley Online Libr., **42**(9), pp. 4397–4411.

[44] Ghasemnejad, H., Soroush, V. R., Mason, P. J., and Weager, B., 2012, “To Improve Impact Damage Response of Single and Multi-Delaminated FRP Composites Using Natural Flax Yarn,” Mater. Des., **36**, pp. 865–873.

[45] Pernas-Sánchez, J., Pedroche, D. A., Varas, D., López-Puente, J., and Zaera, R., 2012, “Numerical Modeling of Ice Behavior under High Velocity Impacts,” Int. J. Solids Struct., **49**(14), pp. 1919–1927.

[46] Rajesh Mathivanan, N., and Jerald, J., 2010, “Experimental Investigation of Low-Velocity Impact Characteristics of Woven Glass Fiber Epoxy Matrix Composite Laminates of EP3 Grade,” Mater. Des., **31**(9), pp. 4553–4560.

[47] Shyr, T. W., and Pan, Y. H., 2003, “Impact Resistance and Damage Characteristics of Composite Laminates,” Compos. Struct., **62**(2), pp. 193–203.

[48] NEMES, J. A., H., E., and RAKITCH, L., 1998, “22 1996; 1996),” Engineering, (97), pp. 97–112.

[49] Chib, A., 2006, “Parametric Study of Low Velocity Impact Analysis on Composite Tubes,” … Compos. Conf. …, (August).

[50] Kim, E. H., Rim, M. S., Lee, I., and Hwang, T. K., 2013, “Composite Damage Model Based on Continuum Damage Mechanics and Low Velocity Impact Analysis of Composite Plates,” Compos. Struct., **95**, pp. 123–134.

[51] Nisini, E., Santulli, C., and Liverani, A., 2017, “Mechanical and Impact Characterization of Hybrid Composite Laminates with Carbon, Basalt and Flax Fibres,” Compos. Part B Eng., **127**, pp. 92–99.

[52] de Rosa, I. M., Marra, F., Pulci, G., Santulli, C., Sarasini, F., Tirillò, J., and Valente, M., 2011, “Post-Impact Mechanical Characterisation of E-Glass/Basalt Woven Fabric Interply Hybrid Laminates,” Express Polym. Lett., **5**(5), pp. 449–459.

[53] Sánchez-Gálvez, V., Paradela, L. S., and Gálvez, F., 2014, “Analytical Simulation of High-Speed Impact onto Hybrid Glass/Carbon Epoxy Composites Targets,” *Procedia Engineering*.

[54] Naik, N. K., Ramasimha, R., Arya, H., Prabhu, S. V., and ShamaRao,

N., 2001, “Impact Response and Damage Tolerance Characteristics of Glass-Carbon/Epoxy Hybrid Composite Plates,” Compos. Part BEngineering, **32**(7).

[55] Papa, I., Langella, A., and Lopresto, V., 2019, “Dynamic Performances of Basalt Fibre Laminates at Room and Low Temperatures,” Compos. Struct., **220**.

[56] Liu, Q., Shaw, M. T., Parnas, R. S., and McDonnell, A. M., 2006, “Investigation of Basalt Fiber Composite Mechanical Properties for Applications in Transportation,” Polym. Compos., **27**(1).

[57] Papa, I., Ricciardi, M. R., Antonucci, V., Pagliarulo, V., and Lopresto, V., 2018, “Impact Behaviour of Hybrid Basalt/Flax Twill Laminates,” Compos. Part B Eng., **153**.

[58] Carmisciano, S., Rosa, I. M. De, Sarasini, F., Tamburrano, A., and Valente, M., 2011, “Basalt Woven Fiber Reinforced Vinylester Composites: Flexural and Electrical Properties,” Mater. Des., **32**(1).

[59] Ricciardi, M. R., Papa, I., Lopresto, V., Langella, A., and Antonucci, V., 2019, “Effect of Hybridization on the Impact Properties of Flax/Basalt Epoxy Composites: Influence of the Stacking Sequence,” Compos. Struct., **214**(January), pp. 476–485.

[60] grandviewresearch, 2017, “Fiber Reinforced Polymer (FRP) Composites Market Report, 2014-2025,” www.grandviewresearch.com.

[61] Hariharan, A. B. A., and Khalil, H. P. S. A., 2005, “Lignocellulose-Based Hybrid Bilayer Laminate Composite: Part I - Studies on Tensile and Impact Behavior of Oil Palm Fiber-Glass Fiber-Reinforced Epoxy Resin,” J. Compos. Mater., **39**(8), pp. 663–684.

[62] Jawaid, M., and Abdul Khalil, H. P. S., 2011, “Cellulosic/Synthetic Fibre Reinforced Polymer Hybrid Composites: A Review,” Carbohydr. Polym., **86**(1), pp. 1–18.

[63] Faruk, O., Bledzki, A. K., Fink, H. P., and Sain, M., 2014, “Progress Report on Natural Fiber Reinforced Composites,” Macromol. Mater. Eng., **299**(1), pp. 9–26.

[64] Wambua, P., Ivens, J., and Verpoest, I., 2003, “Natural Fibres: Can They Replace Glass in Fibre Reinforced Plastics?,” Compos. Sci. Technol., **63**(9), pp. 1259–1264.

[65] Rwawiire, S., Tomkova, B., Militky, J., Jabbar, A., and Kale, B. M.,

2015, “Development of a Biocomposite Based on Green Epoxy Polymer and Natural Cellulose Fabric (Bark Cloth) for Automotive Instrument Panel Applications,” Compos. Part B Eng., **81**, pp. 149–157.

[66] Research and Markets, 2022, *Natural Fiber Reinforced Composites Market - Growth, Trends, COVID-19 Impact, and Forecasts (2022 - 2027)*.

[67] Alagesan, P. K., 2020, “Recent Advances of Hybrid Fiber Composites for Various Applications,” Hybrid Fiber Compos., pp. 381–404.

[68] Jawaid, M., Sapuan, S. M., and Alotman, O. Y., 2017, “Green Biocomposites Manufacturing and Properties,” p. 409.

[69] Selver, E., Ucar, N., and Gulmez, T., 2018, “Effect of Stacking Sequence on Tensile, Flexural and Thermomechanical Properties of Hybrid Flax/Glass and Jute/Glass Thermoset Composites,” J. Ind. Text., **48**(2), pp. 494–520.

[70] Audibert, C., Andreani, A. S., Lainé, É., and Grandidier, J. C., 2018, “Mechanical Characterization and Damage Mechanism of a New Flax-Kevlar Hybrid/Epoxy Composite,” Compos. Struct., **195**(September 2017), pp. 126–135.

[71] Karthi, N., Kumaresan, K., Sathish, S., Prabhu, L., Gokulkumar, S., Balaji, D., Vigneshkumar, N., Rohinth, S., Rafiq, S., Muniyaraj, S., and Pavithran, S., 2021, “Effect of Weight Fraction on the Mechanical Properties of Flax and Jute Fibers Reinforced Epoxy Hybrid Composites,” Mater. Today Proc., **45**, pp. 8006–8010.

[72] Cihan, M., Sobey, A. J., and Blake, J. I. R., 2019, “Mechanical and Dynamic Performance of Woven Flax/E-Glass Hybrid Composites,” Compos. Sci. Technol., **172**(November 2018), pp. 36–42.

[73] Chaudhary, V., Sahu, R., Manral, A., and Ahmad, F., 2019, “Comparative Study of Mechanical Properties of Dry and Water Aged Jute/Flax/Epoxy Hybrid Composite,” Mater. Today Proc., **25**, pp. 857–861.

[74] Petrucci, R., Santulli, C., Puglia, D., Sarasini, F., Design, L. T.-M. &, and 2013, undefined, “Mechanical Characterisation of Hybrid Composite Laminates Based on Basalt Fibres in Combination with Flax, Hemp and Glass Fibres Manufactured by Vacuum,” Elsevier.

[75] Petrucci, R., Santulli, C., Puglia, D., Nisini, E., Sarasini, F., Tirillò, J.,

Torre, L., Minak, G., and Kenny, J. M., 2015, “Impact and Post-Impact Damage Characterisation of Hybrid Composite Laminates Based on Basalt Fibres in Combination with Flax, Hemp and Glass Fibres Manufactured by Vacuum Infusion,” Compos. Part B Eng., **69**, pp. 507–515.

[76] Roy, A., Naskar, A., Ghosh, A., Adhikari, J., Saha, P., and Ghosh, M., 2022, *Hybrid Plastics and Natural Materials*.

[77] Lopresto, V., Caprino, G., Langella, A., and Leone, C., 2012, “PENETRATION AND INDENTATION ON BASALT FIBRE REINFORCED PLASTIC LAMINATES UNDER LOW VELOCITY IMPACTS,” (June), pp. 24–28.

[78] Langella, V. L. I. P. A., 2018, “Basalt Fibres in Vinyl Ester Resin Laminates Under Low Velocity Impact Conditions,” J. Dyn. Behav. Mater., **4**(3), pp. 328–335.

[79] Papa, I., Lopresto, V., Simeoli, G., Langella, A., and Russo, P., 2017, “Ultrasonic Damage Investigation on Woven Jute/Poly (Lactic Acid) Composites Subjected to Low Velocity Impact,” Compos. Part B Eng., **115**, pp. 282–288.

[80] Belingardi, G., and Vadori, R., 2002, “Low Velocity Impact Tests of Laminate Glass-Fiber-Epoxy Matrix Composite Material Plates,” Int. J. Impact Eng., **27**(2), pp. 213–229.

[81] Papa, I., Boccarusso, L., Langella, A., and Lopresto, V., 2020, “Carbon/Glass Hybrid Composite Laminates in Vinylester Resin: Bending and Low Velocity Impact Tests,” Compos. Struct., **232**, p. 111571.

[82] Wang, C., Chen, Z., Silberschmidt, V. V., and Roy, A., 2018, “Damage Accumulation in Braided Textiles-Reinforced Composites under Repeated Impacts: Experimental and Numerical Studies,” Compos. Struct., **204**, pp. 256–267.

[83] Liao, B., Zhou, J., Li, Y., Wang, P., Xi, L., Gao, R., Bo, K., and Fang, D., 2020, “Damage Accumulation Mechanism of Composite Laminates Subjected to Repeated Low Velocity Impacts,” Int. J. Mech. Sci., **182**, p. 105783.

[84] Found, M. S., and Howard, I. C., 1995, “Single and Multiple Impact Behaviour of a CFRP Laminate,” Compos. Struct., **32**(1–4), pp. 159–163.

[85] Sadighi, M., Yarmohammad Tooski, M., and Alderliesten, R. C., 2017, “An Experimental Study on the Low Velocity Impact Resistance of Fibre Metal Laminates under Successive Impacts with Reduced Energies,” Aerosp. Sci. Technol., **67**, pp. 54–61.

[86] Safri, S. N. A., Sultan, M. T. H., Jawaid, M., and Jayakrishna, K., 2018, “Impact Behaviour of Hybrid Composites for Structural Applications: A Review,” Compos. Part B Eng., **133**, pp. 112–121.

[87] Papa, I., Ricciardi, M. R., Calzolari, A., Langella, A., Tirillò, J., Sarasini, F., and Lopresto, V., 2021, “Mechanical Behavior and Damage Degree of Hybrid Glass/Carbon Composites at Low Temperature,” Polym. Compos., **42**(5), pp. 2432–2444.

[88] Drinkwater, B., International, P. W.-N. & e, and 2006, undefined, “Ultrasonic Arrays for Non-Destructive Evaluation: A Review,” Elsevier.

[89] Gardiner, G., 2011, “Primary Structure Repair: The Quest for Quality,” High-Performance Compos., **19**(6), pp. 48–54.

[90] Pagliarulo, V., Bianco, V., Memmolo, P., Distante, C., Ruggiero, B., and Ferraro, P., 2018, “Leaks Detection in Stainless Steel Kegs via ESPI,” Opt. Lasers Eng., **110**, pp. 220–227.

[91] Russo, P., Pagliarulo, V., Bianco, V., Simeoli, G., Cimino, F., and Ferraro, P., 2020, “Characterization of ‘Green’ Composite Laminates after Flexural Tests by Speckle Interferometry,” Opt. Eng., **59**(10), p. 1.

[92] Rippa, M., Pagliarulo, V., Lanzillo, A., Grilli, M., Fatigati, G., Rossi, P., Cennamo, P., Trojsi, G., Ferraro, P., and Mormile, P., 2021, “Active Thermography for Non-Invasive Inspection of an Artwork on Poplar Panel: Novel Approach Using Principal Component Thermography and Absolute Thermal Contrast,” J. Nondestruct. Eval., **40**(1).

[93] Papa, I., Mocerino, D., Pagliarulo, V., Rippa, M., and Langella, A., 2021, “Damage Evolution in Sandwich Components at Different Extreme Temperatures,” J. Compos. Mater.

[94] Militello, C., Bongiorno, F., Epasto, G., and Zuccarello, B., 2020, “Low-Velocity Impact Behaviour of Green Epoxy Biocomposite Laminates Reinforced by Sisal Fibers,” Compos. Struct., **253**.

[95] Ibrahim, M., Smith, R., International, C. W.-N. & E., and 2017,

undefined, "Ultrasonic Detection and Sizing of Compressed Cracks in Glass-and Carbon-Fibre Reinforced Plastic Composites," Elsevier.

[96] Papa, I., Ricciardi, M. R., Antonucci, V., Langella, A., Tirillò, J., Sarasini, F., Pagliarulo, V., Ferraro, P., and Lopresto, V., 2020, "Comparison between Different Non-Destructive Techniques Methods to Detect and Characterize Impact Damage on Composite Laminates," J. Compos. Mater., **54**(5), pp. 617–631.

[97] Caprino, G., Lopresto, V., Leone, C., and Papa, I., 2011, "Acoustic Emission Source Location in Unidirectional Carbon-Fiber-Reinforced Plastic Plates with Virtually Trained Artificial Neural Networks," J. Appl. Polym. Sci., **122**(6), pp. 3506–3513.

[98] Fischer, B., Sarasini, F., Tirillò, J., Touchard, F., Chocinski-Arnault, L., Mellier, D., Panzer, N., Sommerhuber, R., Russo, P., Papa, I., Lopresto, V., and Ecault, R., 2019, "Impact Damage Assessment in Biocomposites by Micro-CT and Innovative Air-Coupled Detection of Laser-Generated Ultrasound," Compos. Struct., **210**(October 2018), pp. 922–931.

[99] Busse, G., 1979, "Optoacoustic Phase Angle Measurement for Probing a Metal," Appl. Phys. Lett., **35**(10), pp. 759–760.

[100] Belingardi, G., Cavatorta, M. P., and Salvatore Paolino, D., 2008, "Repeated Impact Response of Hand Lay-up and Vacuum Infusion Thick Glass Reinforced Laminates," Int. J. Impact Eng., **35**(7), pp. 609–619.

[101] Wyrick, D. A., and Adams, D. F., 2016, "Residual Strength of a Carbon/Epoxy Composite Material Subjected to Repeated Impact:," http://dx.doi.org/10.1177/002199838802200804, **22**(8), pp. 749–765.

[102] Liu, D., 2016, "Characterization of Impact Properties and Damage Process of Glass/Epoxy Composite Laminates:," http://dx.doi.org/10.1177/0021998304042741, **38**(16), pp. 1425–1442.